

# Structure-function analysis of the *Arabidopsis* EDS1 immune regulatory complex

Inaugural-Dissertation

zur

Erlangung des Doktorgrades

der Mathematisch-Naturwissenschaftlichen Fakultät der Universität  
zu Köln

vorgelegt von

**Deepak Bhandari**

aus Chennai

**Köln 2015**



Diese Arbeit wurde durchgeführt am Max-Planck-Institut für Pflanzenzüchtungsforschung in Köln in der Abteilung für Pflanze-Mikroben Interaktionen (Direktor: Prof. Dr. P. Schulze-Lefert), Arbeitsgruppe Prof. Dr. Jane Parker, angefertigt.

The work described in this thesis was conducted under the supervision of Prof. Dr. Jane Parker at the Max Planck Institute for Plant Breeding Research (Department of Plant-microbe interactions, Director: Prof. Dr. P. Schulze-Lefert)



MAX-PLANCK-GESELLSCHAFT



Max Planck Institute for  
Plant Breeding Research

Berichterstatter: Prof. Dr. Jane E. Parker  
Prof. Dr. Alga Zuccaro  
Prof. Dr. Mark Banfield

Prüfungsvorsitzender: Prof. Dr. Ulf-Ingo Flügge

Tag der Disputation: 26.01.2016



असतो माँ सद गमया

तमसो माँ ज्योतिर गमया

Asato Ma Sad Gamaya

Tamaso Ma Jyotir Gamaya

-Bṛhadāraṇyaka Upaniṣad

**From unreal lead me to real,**

**From darkness lead me to light**



# Contents

<b>Acknowledgements .....</b>	<b>A-1</b>
<b>Abbreviations .....</b>	<b>A-3</b>
<b>Summary.....</b>	<b>1</b>
<b>Zusammenfassung.....</b>	<b>3</b>
<b>1. Introduction.....</b>	<b>5</b>
1.1 The plant immune system .....	5
1.2 NLR triggered immunity .....	6
1.3 Hormonal signalling in plant immunity .....	9
1.4 NLR signalling .....	10
1.5 The EDS1 resistance signalling node .....	12
1.5.1 Molecular insights into Arabidopsis EDS1 signalling .....	13
1.5.2 Potential significance of the EDS1-family EP domain .....	13
1.6 Insights from the EDS1-SAG101 crystal structure .....	14
1.7 Thesis aims .....	19
<b>2. Results .....</b>	<b>21</b>
2.1 Architecture of the EP domain .....	21
2.2 Selection of EDS1 residues for targeted mutagenesis.....	22
2.3 Disease resistance phenotypes of T <sub>1</sub> transgenic mutant plants .....	25
2.4 The EP domain of EDS1 is critical for immune functions.....	26
2.4.1 EDS1 EP domain variants disrupt TNL mediated-ETI .....	26
2.4.2 EDS1 EP domain variants cause a complete loss of basal resistance to virulent pathogens .....	31
2.5 EP domain mutations do not alter EDS1 nucleocytoplasmic localization .....	32
2.6 Interaction with PAD4 and SAG101 is maintained in EDS1 EP domain variants .....	35
2.7 Disease susceptibility of EDS1 EP domain mutants cannot be explained by low protein accumulation .....	37
2.7.1 EDS1 variant proteins accumulate upon pathogen infection.....	37
2.7.2 Disease susceptibility does not correlate with low initial EDS1 protein levels .....	38
2.8 EDS1 EP domain mutants accumulate salicylic acid after TNL activation.....	39
2.8.1 Exogenous SA induces <i>PR1</i> in EDS1 R493A EP variant .....	42
2.8.2 Plants expressing EDS1 EP variant R493A display full CNL ( <i>RPS2</i> ) immunity .....	43

2.9 Effect of R493A variant on EDS1-mediated SA-JA pathway crosstalk .....	44
2.10 R493A delays SA accumulation upon infection with <i>Pst</i> /AvrRps4 .....	49
2.10.1 EDS1 R493A but not other EP domain mutations cause delayed SA accumulation .	50
2.11 A positive charge at R493 is essential for EDS1-mediated TNL resistance .....	51
2.12 Transcriptome analysis of the R493A defence response .....	53
<b>3. Structure-guided analysis of EDS1 self-association</b> .....	65
3.1 Introduction .....	65
3.2 Results and discussion .....	67
<b>4. Discussion</b> .....	71
4.1 The EDS1 EP domain represents a key immunity signalling module .....	73
4.1.1 EDS1 EP domain mutants are compromised in TNL resistance .....	74
4.1.2 EDS1 EP domain mutants cause a complete loss of basal resistance .....	76
4.2 EDS1 R493A delays immune signalling and SA accumulation .....	77
4.2.1 SA accumulation is delayed only in R493A but not in other EP domain mutants .....	80
4.3 The EP domain mutant R493A fails to counteract bacterial coronatine-induced susceptibility .....	81
4.3.1 EP domain mutants are resistant to <i>P. syringae</i> lacking coronatine .....	82
4.3.2 Delayed SA accumulation is an inherent feature of R493A .....	84
4.4 A positive charge at R493 is essential for EDS1-mediated TNL resistance .....	86
4.5 Conclusions and future perspectives .....	88
<b>5. Materials and Methods</b> .....	91
5.1 Materials .....	91
5.1.1 Plant materials .....	91
5.1.2 Pathogens .....	92
5.1.3 Bacterial strains .....	93
5.1.4 Oligonucleotides .....	94
5.1.5 Enzymes .....	96
5.1.6 Chemicals .....	96
5.1.7 Antibiotics (stock solutions) .....	96
5.1.8 Media .....	97
5.1.9 Antibodies .....	97
5.2 Methods .....	100
5.2.1 Maintenance and cultivation of <i>Arabidopsis</i> plants .....	100



---

5.2.2 <i>Agrobacterium</i> -mediated stable transformation of <i>Arabidopsis</i> (floral dip) .....	100
5.2.3 Maintenance of <i>P. syringae</i> pv. <i>tomato</i> cultures .....	101
5.2.4 Transient protein expression in tobacco .....	103
5.2.5 <i>Arabidopsis</i> seed surface sterilization .....	103
5.2.6 Exogenous application of salicylic acid .....	103
5.2.7 Biochemical methods .....	104
5.2.8 Molecular biological methods .....	106
<b>Appendix</b> .....	113
<b>References</b> .....	117
<b>Erklärung</b> .....	133
<b>Curriculum Vitae</b> .....	135



## Acknowledgements

Foremost, I want to express my deep gratitude to Prof. Dr. Jane Parker, for all your faith and support, for nurturing and moulding my scientific temper, for showing me that even my best work had scope for improvement. If not for the “gamble” you had taken, this thesis would not have been possible. THANK YOU!!

I would also like to thank Prof. Dr. Karsten Niefind, for always being available and for the encouragement and advice in exploring the structural aspects of this thesis.

Thanks to Prof. Alga Zuccaro and Prof. Mark Banfield, for kindly agreed to examine my thesis and Prof. Ulf-Ingo Flügge for chairing my examination committee. Thanks for your time, comments and scientific inputs.

A special thanks Johannes Stuttmann and Stephan Wagner for guiding me in my initial phase, helping with adaptation and teaching essential techniques- I wish it would have been longer. Johannes, you were right, “if one works hard for 3 years, one invariably finds something worthy”.

Special thanks to all the **JPies**, past and present, for a great working environment and scientific discussions. Jaqueline, you deserve a special mention for the endless hardwork and the support you provide in the background for all our work, not to mention the chocolates that you shower upon us. Am sure not only mine, but most projects would have been nowhere, if not for your presence- DANKE. Thomas and Haitao, thanks for always being available for my smallest queries and advices, not necessarily limited to EDS1/EDS1. Dmitry, thanks for being constantly critical, not asking me to slowdown/repeat what I said, the energy you transfer to all of us - I absolutely enjoy working with you. Friederike, for all the help with ‘R’ and stats. Marcel, the *G. maximus* – you are special! Jingde, the other G, thanks for just being there and making the lab fun. Anne, for disciplining me and all the Deutsch translations. Christine, for all the support at the university and for discussions on EDS1 structure. Aleksandra, for agreeing to be supervised and trained by me, who in turn made me learn. Shachi, for the daily dose of sanity over a cup of ‘kappi’ and the endless trivia of “did you know...”

I should also thank Prof. Dr. P. Schluze-Lefert and the PSL department for unhindered use of all the facilities and always willing to share resources, especially Dr. Kenichi Tsuda and Dr. Eric Kemen for always being available for discussion and sparing their time

DHANYAWAD, to the Indian diaspora in the institute and in Köln for making this time memorable. Thanks to Sush, Geo, Vivek and Vimal for providing a home, away from home.

A very special thanks to Lakshmi and Divya for dragging me into science, some friends truly change the direction of your life....

The biggest thanks, I reserve for my family. I wouldn't have been able to reach this far without their constant support and confidence, am truly grateful to have them.

## Abbreviations

### Amino acids

Amino acid	3-letter code	1-letter code
Alanine	Ala	A
Arginine	Arg	R
Asparagine	Asn	N
Aspartic acid	Asp	D
Cysteine	Cys	C
Glutamine	Gln	Q
Glutamic acid	Glu	E
Glycine	Gly	G
Histidine	His	H
Isoleucine	Ile	I
Leucine	Leu	L
Methionine	Met	M
Phenylalanine	Phe	F
Proline	Pro	P
Serine	Ser	S
Threonine	Thr	T
Tryptophan	Trp	W
Tyrosine	Tyr	Y
Valine	Val	V

### Further abbreviations

Å	Ångström (1Å= 0.1 nm)
°C	degree Celsius
aa	amino acid
AMP/ADP/ATP	Adenosine mono/di/triphosphate
Avr	Avirulence
bp	base pair
C-terminal	Carboxy-terminal
CC	Coiled-coil
cDNA	complementary DNA
cfu	colony forming unit

---

CLSM	confocal laser scanning microscopy
d	day(s)
Dex	dexamethasone
dH <sub>2</sub> O	deionised water
ddH <sub>2</sub> O	distilled, deionized water
DMF	dimethylformamide
DMSO	dimethylsulfoxide
DNA	deoxyribonucleic acid
DNase	deoxyribonuclease
dNTP	deoxynucleosidetriphosphate
dpi	days post inoculation
EDTA	ethylenediaminetetraacetic acid
ET	ethylene
ETI	effector triggered immunity
GFP	green fluorescent protein
h	hour(s)
HA	hemagglutinin
hpi	hours post inoculation
HR	hypersensitive response
HRP	horseradish peroxidase
JA	jasmonic acid
kb	kilo base(s)
kDa	kilo Dalton
l	litre
LRR	leucine-rich repeat
M	molar (mole/l)

---

---

$\mu$	micro
MAMP	microbe-associated molecular pattern
MAPK	mitogen activated protein kinase
mg	milligram
min	minute(s)
mM	millimolar
MPIPZ	Max-Planck-Institute for Plant Breeding Research
mRNA	messenger RNA
MW	molecular weight
NB	nucleotide-binding
ng	nanogram
NLR	nucleotide-binding leucine-rich repeat
nM	nanomolar
NOD	nucleotide-binding-oligomerization domain
N-terminal	Amino-terminal
OD	optical density
p35S	35S promoter of Cauliflower Mosaic Virus
PAGE	polyacrylamide gel electrophoresis
PAMP	pathogen-associated molecular pattern
PCR	polymerase chain reaction
pH	negative decimal logarithm of the $H^+$ concentration
PR	pathogenesis related
PRR	PAMP/ pattern recognition receptor
<i>Pst</i>	<i>Pseudomonas syringae</i> pv. <i>tomato</i>
PTI	PAMP/ pattern-triggered immunity
pv.	pathovar

---

---

pRT-PCR	quantitative real-time PCR
R	resistance
RNA	ribonucleic acid
RNAi	RNA interference
ROS	reactive oxygen species
rpm	revolutions per minute
RT	room temperature
RT-PCR	reverse transcription -PCR
SA	salicylic acid
SAR	systemic acquired resistance
SDS	sodium dodecyl sulphate
T3SS	type III secretion system
TBS	Tris buffered saline
T-DNA	transfer-DNA
TIR	<i>Drosophila</i> Toll- and mammalian interleukin-1 receptor
TLR	Toll-like receptor
TNL	TIR-NB-LRR
Tris	Tris- (hydroxymethyl-) aminomethane
V	Volt(s)
v/v	volume per volume
WT	wild type
w/v	weight/volume
Y2H	Yeast two-hybrid
Rmsd	root-mean-square deviation

---



## Summary

Activation of plant innate immune responses by intracellular receptors involves dynamic changes in the subcellular localisations, assemblies and activities of signalling complexes. The *A. thaliana* nucleo-cytoplasmic protein EDS1, together with its signalling partners PAD4 and SAG101, coordinates basal and TNL receptor-triggered cell defence reprogramming in response to pathogens. *EDS1*, *PAD4* and *SAG101* genes exist in all seed plants and form a plant-specific family with a N-terminal lipase-like domain and a unique C-terminal EP (EDS1-PAD4) domain. Functional analysis of the crystal structure of an *A. thaliana* EDS1-SAG101 heterodimer showed that EDS1 forms molecularly distinct heterodimers with its partners through a large conserved interface. EDS1 heterodimer formation is chiefly driven by the juxtaposed lipase-like domains and is essential for EDS1 disease resistance signalling. The EDS1 lipase-like domain without its EP domain is stable but insufficient for immunity. These features suggested a key role of the EP domain.

To gain functional insights to EP domain function, the EDS1-SAG101 heterodimer crystal structure was used to generate EP domain mutants that were defective in resistance signalling but retained a nucleo-cytoplasmic distribution and direct partner interactions. Functional analysis of the EDS1 EP domain variants revealed two conserved residues (K478 and R493) that are important for *A. thaliana* basal and TNL immunity. Mutation of K478 to arginine (K478R) or R493 to alanine (R493A) led to a partial and complete loss of TNL resistance, respectively. These mutants were completely compromised in EDS1-mediated basal resistance. Disease susceptibility of K478R and R493A in TNL resistance to bacterial pathogen strains is due to their failure to counteract virulence activity of the phytotoxin coronatine (a jasmonic acid-isoleucine conjugate mimic).

EDS1-dependent transcriptional defence reprogramming over a 24 h time course after TNL activation is delayed in R493A and this causes delayed accumulation of the important stress hormone, salicylic acid (SA). Coronatine does not affect the SA accumulation profile of this mutant, although it suppresses SA accumulation in wild-type plants. By contrast, wild-type like SA accumulation in the K478R mutant in TNL resistance suggests two distinct activities of EDS1 EP domain: one is to promote the SA pathway (intact in K478R and defective in R493A), the second is to antagonize coronatine-promoted JA outputs (defective in both mutants) in disease

resistance signalling. Further targeted mutational analysis shows that a positively charged residue at R493 is vital for EDS1 immunity functions and correlates with an ability of EDS1 to bind to nucleic acid *in situ*.

Results presented here identify amino acids in the EP domain that are important for two different EDS1 signalling outputs and suggest that EDS1 chromatin association is integral to EDS1 immune function. This protein structure-function study provides tools to dissect the molecular function and interactions of this central plant immune regulatory node.

## Zusammenfassung

Die Aktivierung der pflanzlichen Immunantwort durch intrazelluläre Rezeptoren unterliegt dynamischen Änderungen der subzellulären Lokalisation, der Zusammensetzung und der Funktionen signaltransduzierender Komplexe. In *A.thaliana* wird die basale und die TNL Rezeptor-vermittelte Reprogrammierung zellautonomer Pathogenabwehr durch das nukleozytoplasmische Protein EDS1, zusammen mit seinen signalgebenden Partnern PAD4 und SAG101, übertragen. *EDS1*, *PAD4* und *SAG101* existieren in allen Samenpflanzen und bilden eine pflanzenspezifische Genfamilie, welche für eine lipaseähnliche Domäne am C-Terminus und eine einzigartige C-terminale EP (EDS1-PAD4) Domäne kodieren. Die funktionelle Analyse der Kristallstruktur eines *A.thaliana* EDS1-SAG101 Heterodimers zeigte, dass EDS1 mit seinen Signalpartnern individuelle Komplexe über eine große, konservierte molekulare Oberfläche bildet. Die Formierung des EDS1 Heterodimers ist hauptsächlich durch die nebeneinandergestellten lipaseähnlichen Domänen bedingt und ist für die EDS1-vermittelte Immunantwort unverzichtbar. Die lipaseähnliche EDS1-Domäne ist auch ohne EP-Domäne stabil, jedoch in ihrer Funktionalität ungenügend für eine Immunantwort. Diese Eigenschaften suggerieren eine Schlüsselfunktion der EP-Domäne für die EDS1-vermittelte Immunantwort.

Um weitere Erkenntnisse über die Funktion der EP-Domäne zu gewinnen, wurde die EDS1-SAG101 Kristallstruktur zur Entwicklung neuer Mutationen innerhalb der EP-Domäne genutzt. Ziel war dabei die Entwicklung von Varianten, welche in der Signalweiterführung zur Resistenzausbildung beeinträchtigt sind, jedoch nicht in der nukleozytoplasmatischen Verteilung des Proteins oder bekannten, direkten Protein-Protein Interaktionen.

Die funktionelle Untersuchung dieser Varianten der EDS1 EP-Domäne entschlüsselte zwei konservierte Aminosäuren (K478 und R493), welche in der basalen und der TNL Immunantwort in *A.thaliana* eine wichtige Rolle spielen. Mutationen der Aminosäure K478 zu Arginin (K478R) oder R493 zu Alanin (R493A) führten entsprechend zu einem partiellen oder völligen Verlust der TNL Resistenz. Beide Mutationen verursachten zudem einen kompletten Ausfall der EDS1-abhängigen basalen Resistenz. Die resultierende erhöhte Anfälligkeit der K478R- und R493A-Varianten gegenüber bakteriellen Pathogenen konnte im Weiteren auf den Verlust der Fähigkeit

zurückgeführt werden, der virulenten Aktivität des Phytotoxins Coronatin (Ein Imitator des Jasmonsäure[JA]-Isoleucin Konjugats) entgegen zu wirken.

Die EDS1-abhängige transkriptionelle Reprogrammierung während der Pathogenabwehr ist über einen Zeitraum von 24 Stunden nach TNL-Aktivierung in R493A verzögert und führt zu einer Verzögerung in der Akkumulation des wichtigen Stresshormons Salizylsäure (SA). Coronatin beeinflusst die SA-Akkumulation in dieser Mutante nicht, wenngleich es die SA-Akkumulation im Wildtyp unterdrückt. Im Gegensatz dazu konnte eine Wildtyp-ähnliche SA-Akkumulation in der K478R-Mutante in der TNL Immunantwort beobachtet werden. Dies legt zwei unterschiedliche Funktionen der EDS1 EP-Domäne nahe: Eine in der Verstärkung der SA Biosynthese und Signalwege (Intakt in K478R und defekt in R493A), die andere Funktion liegt im Entgegenwirken Coronatin-verstärkter JA signale (Defekt in beiden Mutanten). Die Analyse weiterer gezielter Mutationen zeigt, dass ein positiv geladener Aminosäurerest an R493 wichtig für die Funktion von EDS1 in der Immunantwort ist und mit der Fähigkeit von EDS1 korreliert *in situ* an Nukleinsäuren zu binden.

Die hier präsentierten Ergebnisse führen zur Identifikation von Aminosäuren in der EP-Domäne, die für die Funktion von EDS1 in zwei unterschiedlichen Signalwegen von Bedeutung sind. Zudem legen sie nahe, dass die physische Assoziation von EDS1 mit Chromatin von wesentlicher Bedeutung für die Funktion von EDS1 in der pflanzlichen Immunantwort ist. Diese Proteinstruktur- und Proteinfunktionsstudie liefert zudem die nötigen Werkzeuge zur Entschlüsselung der molekularen Funktion und der Interaktionen für diesen zentralen Knotenpunkt in der pflanzlichen Immunantwort.

# 1. Introduction

## 1.1 The plant immune system

Land plants lack an adaptive immune system and are not able to physically escape microbes in the environment. Constant exposure of plants to pathogens has, however, led to the building of a sophisticated, multi-layered innate immune system (Jones & Dangl, 2006). Co-evolving plant-pathogen interactions have created genetic variations of disease resistance and susceptibility leading to race-specific immunity (Nurnberger et al., 2004; Thomma et al., 2011). The plant innate immune system is tightly controlled eliciting a measured response, subject to the potency and mode of pathogen perception (Dodds & Rathjen, 2010). Surface structures such as a waxy cuticle and preformed anti-microbial compounds act as constitutive barrier against entry and colonisation by non-specialised pathogens (Spoel & Dong, 2012).

The first line of plant induced defence is activated upon perception of conserved pathogen associated molecular patterns (PAMPs) by surface bound pattern recognition receptors (PRRs) resulting in pattern triggered immunity (PTI) (Böhm et al., 2014; Macho & Zipfel, 2014). Activation of PTI is associated with reactive oxygen species (ROS) burst, induction of mitogen-activated protein kinases (MAPKs), expression of immune-related genes leading to resistance which halts non-adapted pathogens from infecting (Boller & Felix, 2009). Pathogens that have adapted to a particular host plant secrete virulence factors (effectors) into the host cell cytoplasm or the apoplast. Effectors can be delivered by the type III secretion systems (T3SS) in the case of bacterial strains or elaborate infection structures (haustoria) in the case of fungal and oomycete pathogens (Kemen et al., 2005; Kemen & Jones, 2012). Evidence exists that different effectors interfere with PTI defence pathways to allow pathogen colonization, producing a state known as effector-triggered susceptibility (ETS) (Jones & Dangl, 2006). Pathogen effector molecules or their activity are in-turn specifically recognized by plant intracellular nucleotide binding/leucine rich repeat (NLR) receptors which leads to effector-triggered immunity (ETI) (Cui et al., 2015; Dodds & Rathjen, 2010; Jacob et al., 2013). ETI is considered as an amplified version of PTI and is characterized by sustained transcriptional reprogramming, localized plant cell death known as hypersensitive response (HR) (Cui et al., 2015; Tsuda et al., 2008; Tsuda et al., 2009). Though

ETI is often associated with HR, resistance triggered by pathogen effectors and host programmed cell death (pcd) can be uncoupled in certain cases (Birker et al., 2009). ETI also leads to priming of adjacent cells via salicylic acid (SA) – dependent signalling upregulation (Vlot, Dempsey, & Klessig, 2009; Yan & Dong, 2014).

In this study, basal resistance is defined as the basal immune response against a virulent pathogen which is not obviously recognized by a NLR in ETI. Basal resistance, which slows virulent pathogen growth in susceptible plants, is likely to be the sum of ETS and residual PTI (Jones & Dangl, 2006). Importantly, plant basal and ETI responses differ mainly quantitatively in the transcriptional reprogramming of overlapping sets of induced or repressed host genes (Cui et al., 2015; Tao et al., 2003). It is proposed that the underlying immune network is similar for PTI, basal and ETI, and that a sustained and higher amplitude reprogramming defines the strength of plant resistance (Tsuda et al., 2013).

## **1.2 NLR triggered immunity**

The seminal genetic work by H. Flor in the 1940s and 1950s on gene-for-gene relationships between plant host disease resistant genotypes and ‘avirulent’ resistance-triggering pathogenic strains first suggested that resistance activation is based on specific recognition between a plant receptor and a cognate pathogen effector (Flor, 1971). It was not until the 1990s that plant receptor genes were cloned and a molecular underpinning for intracellular pathogen effector recognition by large panels of NLR receptors was developed (Johal & Briggs, 1992; Martin et al., 1993; Mindrinos et al., 1994; Staskawicz et al., 1992; Xiao et al., 2001). NLRs are highly diverse components of plant immune system that scout for effector perturbations by invading pathogens (Chisholm et al., 2006). The diversity of NLRs and their evolution is likely driven by evolutionary pressure to recognise new pathogen/receptor (Karasov et al., 2014; Yue et al., 2012).

Plant and animal NLRs belong to the STAND (signal transduction ATPases with numerous domains) superfamily of proteins (Danot et al., 2009). Both plant and animal NLRs exhibit a capacity for self-association as well as formation of NLR heterocomplexes (Griebel et al., 2014). NLR activation occurs in the form of a molecular switch which operates between an auto inhibited

ADP-bound (off) form to an activated ATP-bound (on) form (Takken & Govere, 2012). Plant and animal NLRs are modular proteins that are organized into three distinct domains consisting of a variable N-terminal domain, a central nucleotide binding domain (NB-ARC), a C-terminal leucine rich repeat (LRR) domain (Maekawa, Kufer, & Schulze-Lefert, 2011). Plant NLRs can be subdivided based on the structural diversity at their N-terminal regions into TNLs (Toll-interleukin-1 receptor, TIR) or CNLs (coiled-coil, CC) (Jacob et al., 2013; Maekawa et al., 2011; Takken & Govere, 2012). Also, phylogenetic analysis of *NLR* genes across plant lineages including early land plants such as mosses and liverworts revealed additional functionally uncharacterised classes of *NLRs*, such as *PNLs* (protein kinase) and *HNLs* ( $\alpha/\beta$  hydrolase) (Xue et al., 2012). The sites of NLR activation by pathogen effectors are not the same, with some NLRs being activated at and signalling from the plasma membrane (Boyce et al., 1998), some in the cytoplasm, and others binding cognate effectors in the nucleus (Bhattacharjee et al., 2011; Fenyk et al., 2015; Heidrich et al., 2011). For several nucleo-cytoplasmic NLRs, nuclear accumulation is necessary to activate immune signalling (Bai et al., 2012; Cui et al., 2015; Tasset et al., 2010; Wirthmueller et al., 2007). Association of certain NLRs with transcription factors in the nucleus or cytoplasm not only enables them to raise a quick and robust immune response but also to fine-tune responses (Chang et al., 2013; Iii et al., 2002; Le Roux et al., 2015; Sarris et al., 2015). Association of NLRs with transcription factors and functional relevance of the association has been demonstrated in some cases, for example in barley HvWRKY1 and HvMLA1, but how general this concept is, needs further elucidation (Chang et al., 2013).

Intracellular recognition of pathogen effectors by NLRs occurs either, 1) directly – such as the recognition of ATR1 (*Arabidopsis thaliana* recognized 1) oomycete effector, by RPP1 (*Resistance to peronospora parasitica 1*) (Steinbrenner et al., 2015) or 2) indirectly through modification of host target or associated molecular decoy (mimic) of the host target (van der Hoorn & Kamoun, 2008). The NLRs RPM1 (resistance to *pseudomonas syringae* pv. *Maculicola* 1) and RPS2 (resistance to *pseudomonas syringae* 2) recognize their respective cognate effectors AvrRpm1 and AvrRpt2, indirectly by the effector mediated degradation of RIN4 (RPM1-interacting protein 4) (Axtell & Staskawicz, 2003; M. G. Kim et al., 2005; M. Li et al., 2014). Though there are a few examples of direct effector recognition, most effectors are recognized by decoy NLRs.

Several plant and animal NLRs co-function as a pair, for instance the *Arabidopsis* TNL receptors RPS4-RRS1 (Resistance to *Pseudomonas syringae* 4 – Resistance to *Ralstonia solanacearum* 1), rice CNL receptor RGA4-RGA5 (R Gene Analog) and the mouse NLRC4-NAIP (NLR family CARD domain-containing protein 4) (NLR family of apoptosis inhibitory proteins) inflammasome (Cesari et al., 2014; Griebel et al., 2014; Narusaka et al., 2009; Vance, 2015) where each protein plays a distinct function. Our current knowledge indicates that the NLR proteins interact physically to form a hetero-complex, in which one component acts as an integrated decoy sensing effectors and activating the second protein, probably through conformational changes within the NLR complex, which then executes the signalling response (Cesari et al., 2013; Williams et al., 2014). The nucleo-cytoplasmic TNL pair of *Arabidopsis* RPS4-RRS1 is a well-studied example of an integrated decoy. *RPS4-RRS1* are genetically linked in a head-to-head orientation in *Arabidopsis* and are required for resistance to diverse pathogens (Birker et al., 2009; Heidrich et al., 2011; Narusaka et al., 2009). The RRS1 protein contains a WRKY domain in its C-terminus (Deslandes et al., 2002). The WRKY domain of RRS1 senses the bacterial effectors PopP2 (from *Ralstonia solanacearum*) and AvrRps4 (from *Pseudomonas syringae* pv. *pisi*) (Le Roux et al., 2015; Sarris et al., 2015), effector sensing leads to conformational changes and domain reorganization resulting in activated immune signalling (Williams et al., 2014). PopP2 is an acetyl transferase belonging to the Yop-J family of acetyltransferases (Tasset et al., 2010). PopP2 binds to and acetylates the WRKY domain of RRS1 leading to dislodging of RPS4-RRS1 from DNA (Le Roux et al., 2015). Dislodging of RRS1 from DNA activates the RPS4-dependent TNL pair which then signals via EDS1. Thus, the WRKY domain of RRS1 is proposed to act as a decoy to bind pathogen effectors. AvrRps4 is unrelated to PopP2, but associates with WRKY domain of RRS1 (Sarris et al., 2015) suggesting that bacterial effectors target WRKY TFs (transcription factors) to modulate host immunity. A similar functional pair of NLRs, is the CNL pair of RGA4 and RGA5 in rice, wherein the RGA5 is predicted to act as the effector binding partner similar to RRS1 (Cesari et al., 2013).

Major advances have been made recently in understanding fundamental NLR dynamics and functions using structural biology (Fenyk et al., 2015; Takken & Goverse, 2012; Wirthmueller et al., 2013). Structural analysis of TIR domains of *Arabidopsis* RPS4-RRS1 (Williams et al., 2014), Rice NLR Pikp-HMA and its cognate effector AVR-PikD (Maqbool et al., 2015), and the mouse NLRC4 (Hu et al., 2013, 2015) have revealed interesting facets on self-association, auto inhibition



and effector recognition. Structure-guided mutational analysis of the TIR domains of RPS4-RRS1 crystal identified critical amino acids responsible for homo- and hetero-dimerization of the RPS4-RRS1 TIR domains (Williams et al., 2014). The crystal structure of AVR-PikD/Pikp-HMA domain revealed details of effector recognition which enabled mutational analysis to perturb effector responses (Maqbool et al., 2015). Structural analysis on mouse NLRC4 revealed ADP mediated stabilization of the closed conformation of NLRC4, disruption of ADP-mediated interactions led to constitutive activation of NLRC4 (Hu et al., 2013).

### 1.3 Hormonal signalling in plant immunity

Activation of NLRs results in immune reprogramming enabled by phytohormones, MAPKs and TFs (Moore et al., 2011; Pieterse et al., 2009). The strength and dynamics of immune response is a result of synergistic/antagonistic interplay between phytohormones such as salicylic acid (SA), jasmonic acid (JA), ethylene (ET) and abscisic acid (ABA) (Rivas-San Vicente & Plasencia, 2011). Optimum expression and control of these hormones is crucial to maintain the balance between growth and defence (Eichmann & Schäfer, 2015; Huot et al., 2014; Naseem et al., 2015)

SA is a small phenolic compound with an important role in defence against biotrophic pathogens (Loake & Grant, 2007; Vlot et al., 2009). SA mediated transcriptional reprogramming has been implicated in PTI, basal resistance and ETI (Tsuda et al., 2009). Extensive network analysis points towards PTI and ETI using a common signalling network with different intensities (Tsuda & Katagiri, 2010). Unregulated SA production and SA mediated signalling negatively regulates plant growth and exhibits an auto immune phenotype (Li et al., 2001; Y. Li et al., 2010). Unregulated SA signalling is controlled by hormonal networks, wherein SA levels are regulated negatively by JA/ET pathways (Gimenez-ibanez et al., 2015; Pieterse et al., 2009). As a counter measure SA can also downregulate JA when plants are attacked by biotrophic pathogens (Caarls et al., 2015). In addition to its role in local resistance, SA plays an important role in systemic acquired resistance (SAR) (Durrant & Dong, 2004; Vlot et al., 2009).

The complex network formed by phytohormones is regulated at multiple levels to elicit a robust immune response against an array of pathogens (Pieterse et al., 2009). JA is upregulated in

response to necrotrophic pathogens. The bioactive form of JA, JA-Isoleucine (JA-Ile) binds to the complex of F-box protein COI1 (coronatine insensitive 1) and JAZ (jasmonate ZIM domain) to release the JAZ-repressed bHLH TF MYC2. Upon de-repression MYC2 binds to MED25 (mediator complex) leading to transcriptional regulation of genes involved in JA signalling (R. Chen et al., 2012; Kazan & Manners, 2013; Sasaki-Sekimoto et al., 2013). MYC2 was also found to suppress SA biosynthesis by binding to NAC TF such as *ANAC019*, *ANAC055* and *ANAC072* (X.-Y. Zheng et al., 2012).

Hormonal cross talk used for fine-tuning plant defences is hijacked by pathogens to downregulate SA and proliferate (X.-Y. Zheng et al., 2012). Coronatine (COR) is a phytotoxin produced by various strains of *P. syringae*, which is structurally and functionally similar to JA-Ile and upregulates JA-signalling (Mittal & Davis, 1995; X.-Y. Zheng et al., 2012). The complex formation of COI1-JAZ can also be facilitated by coronatine resulting in degradation of JAZ and release of MYC2. In addition, COR can reopen stomata, which were closed after bacterial infection (Melotto et al., & He, 2006). Other pathogenic effectors also target SA signalling like the *Hyaloperonospora arabidopsidis* (*Hpa*) effector HaRxL44 (Caillaud et al., 2013; Uppalapati et al., 2007). Reconstructing the network of hormonal pathways of SA, JA and ET revealed compensatory interactions that underlie a robust immune response (Tsuda et al., 2009).

#### 1.4 NLR signalling

Network analysis of large-scale yeast 2-hybrid and protein-protein interactions, indicate that effectors from diverse pathogens converge on a limited set of plant targets with major immune related functions (Mukhtar et al., 2011; Weßling et al., 2014). Accumulating evidence also points towards modification of host target as a widespread form of NLR activation (Le Roux et al., 2015). A missing piece in our understanding of plant intracellular immunity, are events immediately after NLR activation leading to defence reprogramming. Mechanisms by which NLR activation leads to resistance remain obscure. Also, how different NLRs activated in different parts of the cell converge on a broadly conserved basal resistance signalling network is unclear (Cui et al., 2015; Tsuda & Katagiri, 2010). In *Arabidopsis*, activated NLRs trigger an array of immune responses that converge on two major hubs; EDS1 (Enhanced Disease Susceptibility 1) for TNL triggered

immunity and NDR1 (Non race specific Disease Resistance 1) for CNL triggered immunity (Aarts et al., 1998). Both EDS1 and NDR1 signal chiefly via SA pathway to provide a robust immune response against biotrophic pathogens (Feys et al., 2001; Shapiro et al., 2001; Zhou et al., 1998).

*Arabidopsis* immune signalling upon activation of TNLs is completely EDS1-dependent. Wirthmüller et al., (2007) showed that EDS1 functions downstream of RPS4 activation but upstream of transcriptional reprogramming. Association of EDS1 with TNLs such as RPS4, RPS6 (Resistance to *Pseudomonas syringae* 6), VICTR (Variation In Compound Triggered Root growth response) and effectors like AvrRPS4, PopP2 (Bhattacharjee et al., 2011; Heidrich et al., 2011; Kim et al., 2012; Le Roux et al., 2015; Sarris et al., 2015), suggests that EDS1 acts as a bridge between effector activated TNLs and downstream defence signalling including pcd (programmed cell death) pathways and systemic resistance. (Figure 1.1).

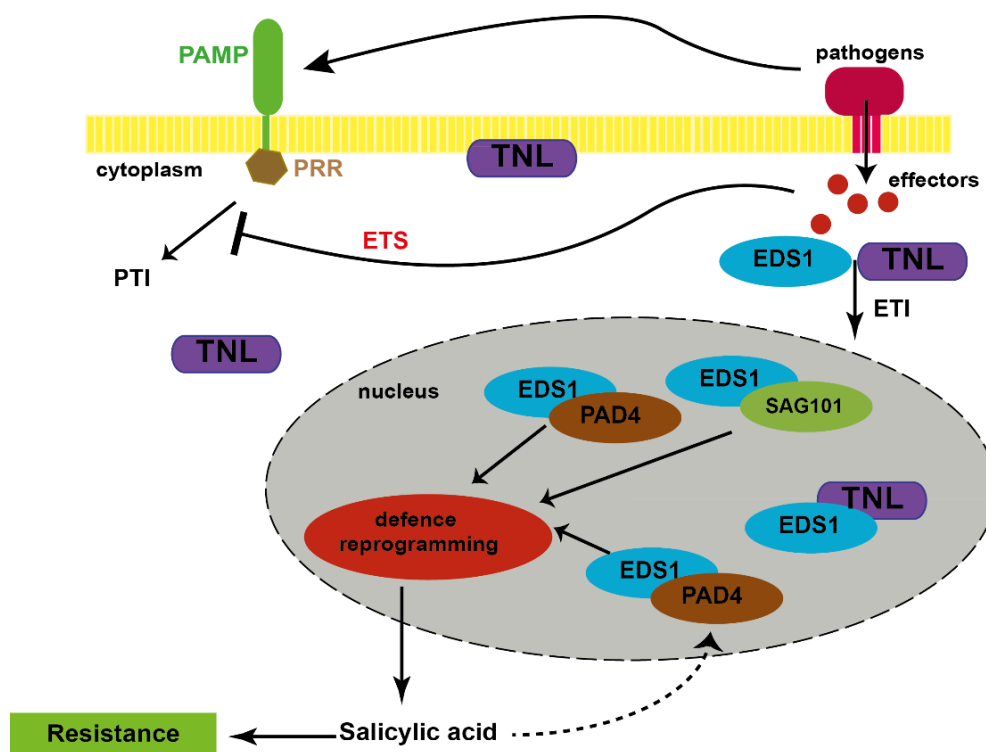


**Figure 1.1: EDS1 complexes in TNL-triggered immunity:** Dynamics of the plant immune system (PTI, ETI and ETS) are depicted in a simplified form. Nuclear and cytosolic complexes of EDS1 are represented as illustrated. The nuclear pool of EDS1 is chiefly involved in transcriptional defence reprogramming leading to salicylic acid (SA) upregulation and resistance. Upregulated SA forms a feedback loop that upregulates EDS1 and PAD4. The interaction of EDS1 with effector/s (AvrRps4) and TNLs (RPS4) is also depicted in a simplified form.

### 1.5 The EDS1 resistance signalling node

*Arabidopsis* EDS1, a nucleo-cytoplasmic protein, is an indispensable component of basal and TNL-triggered defence responses (Figure 1.1) (Falk et al., 1999; Feys et al., 2005; Wiermer et al., 2005). Nevertheless, several CNL receptors have also been reported to mediate immunity via EDS1 (Eckardt, 2009; Venugopal et al., 2009). For example, *Arabidopsis* CNL protein HRT (HR to TCV), confers resistance to Turnip Crinkle Virus (TCV) and is dependent on both EDS1 and SA for resistance (Venugopal et al., 2009). Single mutations in *EDS1* and *ICS1* (*Isochorismate synthase 1*), respectively in an *eds1-22* and *sid2-1* background were resistant to TCV. Combining these mutations in an *eds1-22/sid2-1* double mutant resulted in susceptibility to TCV (Venugopal et al., 2009). Similarly, *eds1-22/sid2-1* double mutant exhibited enhanced susceptibility compared to the single mutants (Venugopal et al., 2009).

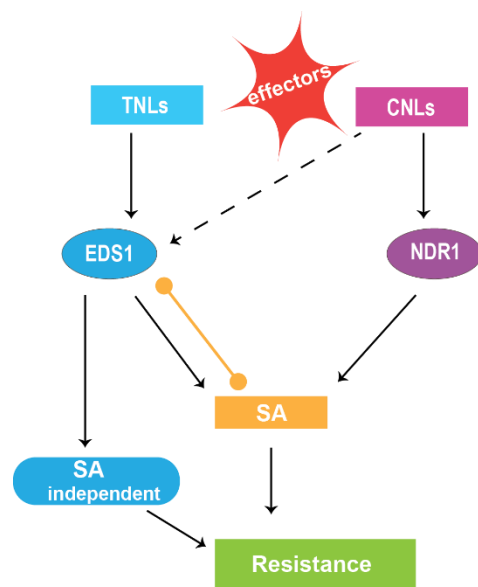


**Figure 1.2: Simplified illustration of EDS1 signalling in NLR-triggered immunity.** In *Arabidopsis*, pathogen effectors are recognized by TNLs and CNLs, which activate signalling chiefly via EDS1 and NDR1, respectively. A CNL (RPS2) also signals through EDS1 (dashed arrow). Both EDS1 and NDR1 upregulate SA (salicylic acid) leading to robust defence. EDS1 also signals in an SA-independent branch leading to plant resistance. EDS1 and SA are functionally redundant (orange dumbbell) against effectors such as AvrRpt2. For clarity, EDS1 partners (essential for immune signalling) – PAD4 and SAG101 are not depicted.

Other examples of CNLs recruiting EDS1 in resistance signalling include RPW8 (Resistance to powdery mildew 8), a CC-domain containing membrane associated protein which confers broad spectrum resistance to powdery mildew (Xiao et al., 2005). Thus, EDS1 is involved in basal, CNL- and TNL-triggered immunity making it an important hub in plant resistance (Figure 1.2).

### 1.5.1 Molecular insights into *Arabidopsis* EDS1 signalling

*Arabidopsis* EDS1 interacts with its sequence-related partners PAD4 (Phytoalexin deficient 4) and SAG101 (Senescence-associated gene 101), in nucleo-cytoplasmic and nuclear complexes, respectively (Feys et al., 2001; Feys et al., 2005; Wiermer et al., 2005). The three proteins constitute a plant-specific family with an N-terminal lipase-like domain that has homology to  $\alpha/\beta$  hydrolases and a highly conserved unique C-terminal 'EP' (initially derived from being unique in 'EDS1-PAD4') domain with no known homologies to other proteins (Feys et al., 2005) (Figure 1.3). EDS1 and PAD4 are conserved across diverse seed plants (Wagner et al., 2013). The  $\alpha/\beta$  hydrolase fold is one of the most versatile protein family consisting of eight  $\beta$ -sheets connected by  $\alpha$ -helices which provide a framework for diverse catalytic enzymes (Lenfant et al., 2013; Ollis et al., 1992). Various studies have shown, however, that the  $\alpha/\beta$  hydrolase fold also provides a structural scaffold for non-catalytic but functionally important plant receptors (Janssen & Snowden, 2012). The EDS1 and PAD4 lipase-like domains possess the characteristic Ser-His-Asp catalytic triad (Figure 1.3) but no catalytic activity has been detected in EDS1 tested *in vitro* against different substrates (Rietz et al., 2011; Wagner et al., 2013). Targeted mutational analysis of *Arabidopsis* EDS1 and PAD4 catalytic triad residues showed that these are dispensable for basal and TNL-triggered immunity against the *Arabidopsis*-adapted oomycete pathogen *Hyaloperonospora arabidopsidis* (*Hpa*) (Wagner et al., 2013). Thus, EDS1 and PAD4 immune signalling functions do not appear to be catalysis-related. Notably, SAG101 is found only in dicotyledenous plant lineages and does not possess the catalytic triad (Feys et al., 2005) but was reported to have low acyl hydrolase activity *in vitro* (He & Gan, 2002). Lower accumulation of YFP-cEDS1<sup>SDHFV</sup> (catalytic triad mutant) was immunocompetent against pathogens tested, suggesting that a low amount of basal protein is sufficient for EDS1 immune functions (Wagner et al., 2013).

### 1.5.2 Potential significance of the EDS1-family EP domain

The C-terminal EP domain (amino acids 385-623 in *At* EDS1) is exclusively made up of  $\alpha$ -helical sheets. This arrangement provides an extended surface area and potential flexibility which might enable interaction with diverse protein partners (Groves & Barford, 1999). These helical repeats can be modified by lengthening or shortening, thereby presenting different surfaces to interacting

partners whilst retaining a stable fold. These properties make  $\alpha$ -helical repeats ideal for assembling multi-protein complexes and fulfilling multiple functions depending on the proteins they interact with and the site of interaction (Groves & Barford, 1999). Major repeat families that are made up of  $\alpha$ -helices are armadillo-, TPR1-like-, Ankyrin- and leucine rich- repeats (Andrade et al., 2001; D'Andrea, 2003; Ellisdon & Stewart, 2012). The functional significance of repeat motifs has been attributed to an ability to acquire diverse molecular conformations and functions with different partners during evolution. The evolution of repeat proteins is hypothesized to have started from a single repeat which formed an oligomeric complex, resulting in a structure resembling the repeats (Ponting & Russell, 2000). It might be postulated from this structural framework that EDS1-PAD4 or EDS1-SAG101 EP domains are able to form multi-protein complexes with various binding partners.

The closest structural homologues to the EDS1 EP domain include Tom70 (tetratricopeptide repeat protein) and Rpn6 (regulatory subunit of 26s proteasome) (Pathare et al., 2012; Yunkun Wu & Sha, 2006). *Arabidopsis* EDS1 also interacts with SRFR1 (suppressor of rps4-RLD1) which is a negative regulator of TNL-mediated ETI (Bhattacharjee et al., 2011; Y. Li et al., 2010). SRFR1 contains an  $\alpha$ -helical tetratricopeptide repeat domain (Kwon et al., 2009). It has been proposed that SRFR1 mediated negative regulation of intracellular immunity is lost upon bacterial effector interaction with EDS1 (Bhattacharjee et al., 2011). These data together with the association of EDS1 with TNLs (Bhattacharjee et al., 2011) suggest that the EDS1 EP domain might act as a potential site for interaction with effector proteins, TNLs and other interactors essential for downstream signalling.

### **1.6 Insights from the EDS1-SAG101 crystal structure**

Structural biology has provided key insights to molecular mechanisms underlying the functions of immune-related proteins (Bai et al., 2012; Bernoux et al., 2011; Gao et al., 2012; Wirthmueller et al., 2013). Structural information is being utilized to understand and engineer plant immunity components, including NLR receptors, for robust resistance (Maqbool et al., 2015; L. Zhang et al., 2015). While intensive structural studies have been done for NLRs in both plants and mammals (Lechtenberg et al., 2014; Williams et al., 2014; Wirthmueller et al., 2013) only few studies have

focused on the signalling components downstream of NLR activation (Shimada et al., 2008; Wagner et al., 2013; F. Zhang et al., 2015). The COI1-MYC3-JAZ structure (F. Zhang et al., 2015) has provided an important insight into how transcriptional repression is switched to transcriptional activation upon perception of the stress and developmental hormone, JA. Similarly, the GID1-DELLA protein structure showed how conformational changes in a lipase-like protein upon gibberellin perception, is important for its signal transduction leading to growth changes (Murase et al., 2008; Shimada et al., 2008).

Resolving the crystal structure of *Arabidopsis* EDS1-SAG101 heterodimer (Wagner et al., 2011) and its structure-function analysis (Wagner et al., 2013) have provided first insights into the structural organization and function of the lipase-like domain of the EDS1 protein family. The instability of recombinantly expressed PAD4 protein has rendered a EDS1-PAD4 structure elusive. Nevertheless, the EDS1-SAG101 crystal structure was used as a template to model a EDS1-PAD4 structure. Key interfaces in the EDS1-SAG101 heterodimer structure and EDS1-PAD4 heterodimer model were validated in Y2H and plant co-expression assays (Wagner et al., 2013).

EDS1, PAD4 and SAG101 form separate protein groups across flowering plants (Wagner et al., 2013), suggesting there is a selection from pathogens and/or signalling partners to retain distinct protein attributes and functions. It is noteworthy that SAG101 is maintained only in plant lineages in which *TNL* genes are present (Yue et al., 2012), hinting towards a functional relationship between SAG101 and TNLs. EDS1 and PAD4 occur in all examined seed plant genomes and likely represent an ancestral immune regulatory complex because EDS1-PAD4 interaction is necessary for *Arabidopsis* basal immunity (Rietz et al., 2011). Overexpression of EDS1 in the absence of PAD4 or SAG101 failed to signal in TNL-conditioned ETI (Feys et al., 2005; Wagner et al., 2013). However, *Arabidopsis* EDS1 functions in absence of both PAD4 and SAG101 in the case for basal immunity have not been extensively studied. Nuclear accumulation of EDS1 is necessary for TNL and basal immunity and transcriptional defence reprogramming (García et al., 2010).

Association of EDS1 with SAG101 or PAD4 in separate complexes *in vitro* and *in vivo* suggests that co-ordination between different EDS1-PAD4 and EDS1-SAG101 complexes and the intricate

balance between these heterodimers might underlie immune regulation (Feys et al., 2005; Rietz et al., 2011; Wagner et al., 2013). EDS1 along with PAD4 forms a major protein hub acting upstream of SA in defence responses against virulent and avirulent biotrophic pathogens (Feys et al., 2001; Rietz et al., 2011; Zhou et al., 1998). EDS1-PAD4 complexes alone are sufficient for basal resistance which is in part mediated via SA (Feys et al., 2001; Jirage et al., 1999; Rietz et al., 2011). EDS1 and PAD4 are also transcriptionally upregulated in a feedback loop that is initiated by accumulating SA (Falk et al., 1999; Feys et al., 2001; Jirage et al., 1999). How this feedback loop works and how it is attenuated after pathogen growth is halted, remains unknown.

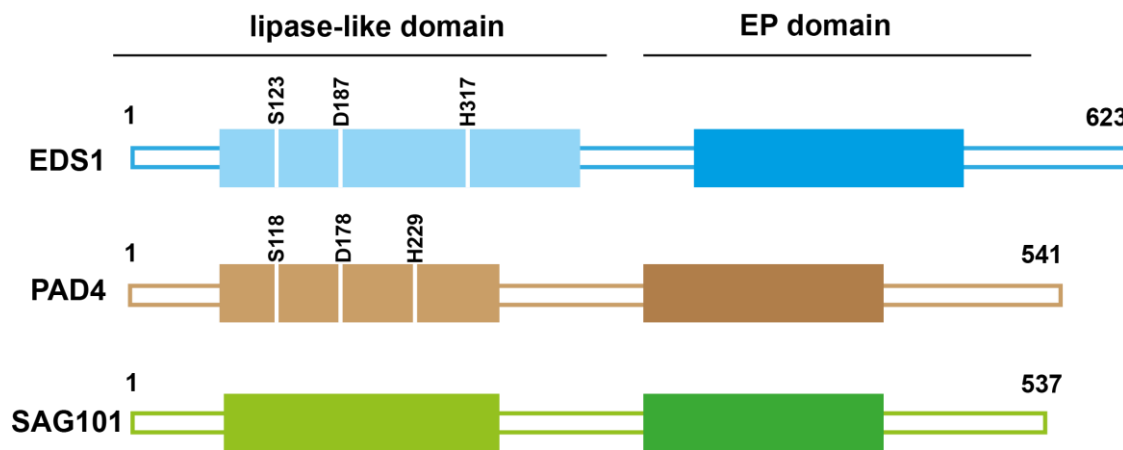


**Figure 1.3: Domain organisation of the EDS1 protein family.** Full-length *Arabidopsis* EDS1, PAD4 and SAG101 proteins are depicted with their lipase-like (light shade) and EP domains (dark shade). The catalytic triad residues serine-aspartic acid-histidine (S-D-H) in the lipase-like domain are highlighted.

A unique role of SAG101 in *Arabidopsis* basal resistance and TNL-triggered immunity is unlikely because its loss in a *sag101* mutant is fully compensated for by PAD4. However, SAG101 contributes to basal and TNL resistance in the absence of PAD4 (Feys et al., 2005; Rietz et al., 2011) and a non-redundant SAG101 activity was observed in CNL-triggered immunity to TCV (Jeong et al., 2012), suggesting a degree of signalling discrimination might occur between EDS1 family proteins. It is hypothesised that EDS1-SAG101 might have diverged from EDS1-PAD4, to modulate and add robustness to TNL-triggered processes. SAG101 and PAD4 also have unique



roles in viral resistance conferred by the *Arabidopsis* CNL receptor, HRT (Zhu et al., 2011) and, strikingly *PAD4* alone is necessary for *Arabidopsis* resistance to green peach aphid feeding in phloem tissues (Pegadaraju et al., 2007). It is possible that SAG101 stabilizes EDS1 inside nuclei, consistent with data of Feys et al. (2005) and Zhu et al. (2011), by acting as a “base station” to provide sufficient nuclear EDS1 for transfer to PAD4 in order to boost transcriptional reprogramming during ETI (García et al., 2009; Heidrich et al., 2011; Rietz et al., 2011). The absence of catalytic residues in SAG101 would fit with it being a less active component of the EDS1 system. Alternatively, separate EDS1 complexes might be recruited by TNLs and CNLs in different ways to regulate distinct ETI outputs (Venugopal et al., 2009; Wagner et al., 2013). Dynamic exchange between EDS1-SAG101 and EDS1-PAD4 heterodimers might provide a mechanism for fine-tuning pcd and defence pathways during ETI.

The EDS1-SAG101 crystal structure and the tested EDS1-PAD4 structural model provide insights to the mode of protein binding between these three proteins (Wagner et al., 2013). Here I summarize knowledge of the EDS1-SAG101 structure at the beginning of my thesis. The EDS1-SAG101 heterodimer (Figure 1.4) is formed via the juxtaposition of the lipase-like domains, bringing the ‘EP’ domains into close proximity and possibly creating new surfaces for further interactions. Binding of these proteins is facilitated through a large interface, which is conserved in EDS1 across different species (Ashkenazy et al., 2010). Two-thirds of the predicted binding strength comes from the N-terminal lipase-like domains which are stabilized by hydrophobic interactions. The lipase-like domain of EDS1 has a hydrophobic helix fitting into the groove of SAG101. The amino acids comprising the helix are necessary for heterodimer formation since simultaneous but not individual mutations in the helix causes a loss of interaction and resistance function (Wagner et al., 2013). This mutated variant of EDS1, EDS1<sup>LLIF</sup> loses its ability to interact with both PAD4 and SAG101 signifying that PAD4 and SAG101 bind to the same interface of EDS1. An EDS1-PAD4-SAG101 ternary complex as proposed by (Zhu et al., 2011) is not supported by the structural evidence from the EDS1-SAG101 crystal. However, EDS1<sup>LLIF</sup> is able to retain binding to EDS1 and forms homodimers in Y2H implying that EDS1 homodimers are structurally distinct from EDS1 heterodimers (Wagner, 2013). It could be possible that due to transient expression in tobacco the heterodimers of EDS1-SAG101 and EDS1-PAD4 could form hetero-complexes utilizing the EDS1 homodimerization interface. Whether this hetero-complex of

EDS1-PAD4-SAG101 has a biological significance or not remains a matter of speculation since PAD4 is able to largely compensate for the loss of SAG101 in basal and TNL-triggered immunity (Feys et al., 2005). However, specific roles of SAG101 in CNL-triggered immunity are emerging (Venugopal et al., 2009).

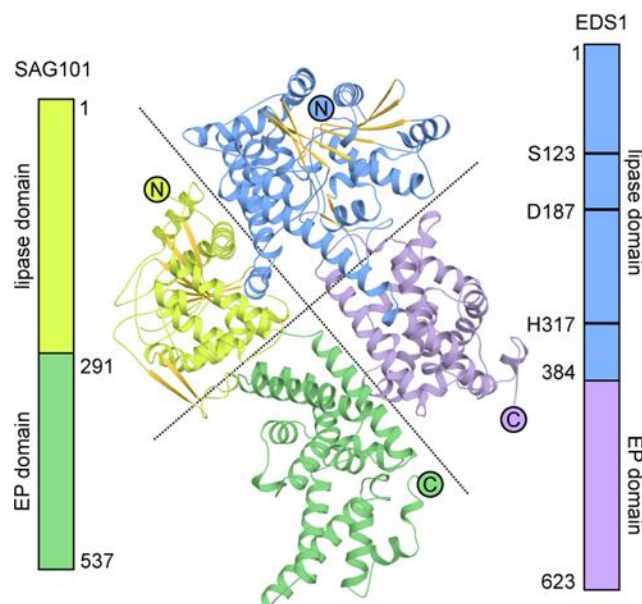


**Figure 1.4: Structural features of EDS1-SAG101.** Crystal structure of EDS1-SAG101 heterodimer, represented in a cartoon form. EDS1 lipase-like domain (light blue) is juxtaposed with the lipase like domain of SAG101 (lime green), while the EP domains of EDS1 (violet) and SAG101 (green) interact with each other. The molecular arrangement of the heterodimer is represented in vertical bars. (Adapted from Wagner et al., 2013).

Although the N-terminus of the EDS1 family proteins is comprised of a lipase-like domain, no lipase/hydrolase activity was detected. The lipase-like domain although stable and maintaining interaction with PAD4 and SAG101, is not sufficient for EDS1 immune functions, suggesting that the EP domain is essential for EDS1 mediated immunity (Wagner, 2013). The EP domain in the absence of the lipase-like domain was unstable in yeast and in transgenic *Arabidopsis* plants (Wagner et al., 2013). Interestingly, in an earlier study (Feys et al., 2001) the lipase-like domain failed to interact with EDS1 or PAD4 in Y2H whereas the EP domain maintained interaction with EDS1 but not PAD4. It is worth noting that the lipase-like domain studied by Wagner et al. is 34 amino acids longer than the lipase-like domain studied by Feys et al. Since, the study by Wagner

et al. is supported by multiple evidences (structural, transgenic, transient and *in-vitro* studies), I use their definition of lipase-like (1-384 aa) and EP (385-623 aa) – domains in this study. The instability of the essential EP domain without its lipase-like domain, suggests that the N-terminal interface acts as a scaffold to facilitate interaction between the EP domains in the heterodimers rather than functioning as a lipase (Wagner et al., 2013).

EDS1, PAD4 and SAG101 exist in diverse flowering plants, underpinning their functional relevance as an immune signalling family (Wagner et al., 2013). Though functional research on EDS1 immune functions has largely been limited to the model plant *Arabidopsis thaliana*, the assimilated knowledge from the model plant is being transferred to crop plants. *In-silico* studies suggest that EDS1 and PAD4 exist as dimers in rice (Singh & Shah, 2012). In soybean, EDS1 (*Gm* EDS1) and PAD4 (*Gm* PAD4) recognize the effector AvrA1 and are required for Rpg2-mediated resistance (Wang et al., 2014). Intriguingly, while *Gm* EDS1 and *Gm* PAD4 complemented the pathogen resistance phenotypes of *eds1* and *pad4* they did not upregulate SA upon pathogen infection (Wang et al., 2014). Similarly, EDS1 from grapevine *Vitis vinifera* (*Vv* EDS1) was able to complement the pathogen resistance phenotypes of *At* EDS1 in *eds1-1* against *Pst*/AvrRps4 (F. Gao et al., 2010a). In contrast to the above studies, Ke et al., (2014) observed that rice PAD4 (*Os* PAD4) functions differently compared to *At* PAD4. Unlike the nucleo-cytoplasmic *At* PAD4, *Os* PAD4 is plasma membrane bound but required for resistance against the biotrophic pathogen *Xanthomonas oryzae* pv. *oryzae*. *Os* PAD4 appear to be required for JA-induced resistance of rice to the *Xanthomonas* pathogen (Ke et al., 2014), while *At*PAD4 activity in the regulation of the JA-pathway is not known. These studies suggest that EDS1-PAD4 might have evolved variable functions in different plant lineages to defend against specific pathogens. The importance of EDS1 in immune signalling across diverse seed plants and the manifold pathways it operates in reinforces the significance of studying this defence hub of plant innate immunity.

## 1.7 Thesis aims

Pathogens have evolved mechanisms to overcome plant basal innate immunity or to disable ETI. In turn, plants have evolved pathways to ensure robustness of ETI against pathogen attack. Recognitionally diverse NLRs converge on conserved immune signalling hubs such as EDS1.

However, molecular mechanisms of signal transduction from the activated NLR immune receptors to transcriptional regulation are not clear. Extensive studies in *Arabidopsis* place both genetically and physically the conserved EDS1-protein family downstream the TIR subclass of NLRs and upstream transcription regulation (Bhattacharjee et al., 2011; Heidrich et al., 2011). The EDS1 protein family mediates basal resistance, ETI and hormonal crosstalk in resistance against different pathogens (Feys et al., 2001; Wagner et al., 2013). EDS1 and PAD4 contribute to SA-dependent and –independent immune signalling pathways (Bartsch et al., 2006; Tsuda et al., 2009; Zhou et al., 1998).

Structure-guided analysis of the *Arabidopsis* EDS1-PAD4 and EDS1-SAG101 revealed that the EDS1 lipase-like domain is stable but insufficient for EDS1 immune functions suggesting that the plant specific C-terminal EP domain of the EDS1 protein is critical for the TNL-signalling (Wagner et al., 2013). However, due to the instability of EP domain it was unclear which molecular surfaces of the EP domain/s are responsible for this function, and their mechanism of immune signalling. Thus, the central aim of my thesis was the identification and functional characterization of the EDS1 EP domain in immune signalling. An extension of this question is whether the EP domains of either PAD4 or SAG101 play an active role in EDS1-dependent signalling or if they act as scaffold proteins to create novel interfaces.

The EP domains of EDS1 family proteins do not have significant sequence similarity to other proteins (Feys et al., 2005). Necessity of the EDS1 heterodimer formation signifies that amino acids mediating EDS1 immune signalling would potentially be situated at the interface between the proteins. This makes them ideal candidates for structure-guided mutagenesis to analyse the immune signalling mechanism of EDS1. My ultimate aim therefore is to identify and functionally characterize specific amino acid residues in the EDS1 EP domain, this would form a basis for (1) establishing the role of EDS1 EP domain, (2) predicting the role of EP domains in PAD4 and SAG101, (3) attempting to dissect EDS1 molecular functions in response to different pathogens, (4) uncoupling of EDS1 controlled SA-dependent and SA-independent pathways.

## 2. Results

### 2.1 Architecture of the EP domain

The EDS1 protein is organized into two domains, an N-terminal lipase-like domain and a unique C-terminal EP domain. EDS1-PAD4 and EDS1-SAG101 heterodimer formations are necessary for a complete immune response against effectors recognized by TNLs (Rietz et al., 2011; Wagner et al., 2013). Though EDS1 heterodimer formation is driven chiefly by the lipase-like domains of EDS1 and its partners PAD4 or SAG101, the EP domain also contributes to heterodimer formation (Wagner et al., 2013). Sequence analysis shows that the EP domain is unique to the EDS1 family and has no homologues on sequence level. For this study, a C-terminal region between 385-623 amino acids of EDS1 was examined in accordance with (Wagner et al., 2013), although a patch of residues comprising the originally defined EDS1 EP domain is smaller (405-554 amino acids) (Feys et al., 2001). The EP domain consists mainly of  $\alpha$ -helical bundles which often support protein-protein interactions and was therefore hypothesised to be a protein interaction surface and/or act as a platform for larger complex formation (Wagner et al., 2013). To search for structural homologues of the EDS1, EP domain (385-623 amino acids) was compared to known protein structures in the PDB using the Dali algorithm (Holm & Rosenstrom, 2010). A similar analysis was reported by (Wagner et al., 2013), Table 2.1 lists the updated structural homologues of the EDS1 EP domain since then.

SAG101 EP domain showed closest homology to EDS1 with a Z-score of 17.5, re-iterating the unique motif in the EP domain shared by proteins of the EDS1 family. Other similar structures were less related (Z-score lower than 10) and could be attributed to small patches of similar protein folds. Structurally homologous proteins to the EP domain, grouped mainly into proteins involved in multi-protein complexes (TPR-like proteins, Nro1), components of the proteasome complex (PRE3, COP9, Rpn6) and proteins involved in nuclear transport (NRO1, TREX-2) (Lingaraju et al., 2014; Pathare et al., 2012; Rispal et al., 2011; Schneider et al., 2015; Wu et al., 2006). Interestingly, Rpn6, a regulatory subunit of 26S proteasome has high similarity to the EDS1 EP domain (Wagner et al., 2013), and EDS1 was found to interact with Rpt2a in Y2H assays (H. cui, personal communication). Another protein with high similarity to EDS1 EP domain is Rcd-1 from humans. Rcd-1 has armadillo-like-repeat proteins and exhibits nucleic acid binding properties

(Garces & Gillon, 2007), pointing towards possible roles of the EP domain in DNA binding. These varied functional/interactional possibilities of EDS1, reinforces the notion that heterodimer formation could introduce novel interfaces of the EP domain which transduce downstream signalling.

EDS1 <sup>385-623</sup>	PDB	Z	rmsd	id%
SAG101	4nfu-B	17.5	2.7	30
PROTEASOME COMPONENT PRE3	4cr2-Q	5.4	3.5	8
Nro1/Ett1	3qtm-A	4.8	4.3	10
COP9 SIGNALOSOME COMPLEX SUBUNIT 1	4d10-J	4.8	3.5	8
TPR REPEAT-CONTAINING PROTEIN YHR117W	3fp3-A	4.7	3.4	7
EUKARYOTIC TRANSLATION INITIATION FACTOR 3	4k51-B	4.7	4	6
MITOCHONDRIAL PRECURSOR PROTEINS IMPORT RECEPTOR	2gw1-B	4.7	3.5	11
BRO1 DOMAIN-CONTAINING PROTEIN BROX	3um2-D	4.5	4.6	8
AH RECEPTOR-INTERACTING PROTEIN	4aif-B	4.5	4.8	7
26S PROTEASOME REGULATORY COMPLEX SUBUNIT P42B	3txm-A	4.5	3.4	11
NUCLEAR IMPORT ADAPTOR, NRO1	3msv-B	4.5	4.2	10

**Table 2.1: The ten closest structural homologues of the EDS1 EP domain as identified by the DALI-server.** For each entry, the PDB entry code (PDB), the DALI Z-score (Z), the average distance between aligned atoms (rmsd) and percentage of sequence identity (id%). Homologues repeated due to occurrence of multiple side chain PDB entries were ignored.

$\alpha$ -helical bundles have modular structural properties and can form novel interfaces with different interacting partners, thus potentially functioning in multiple ways (Groves & Barford, 1999). The crystal structure of EDS1-SAG101 heterodimer (Figure 2.1) reveals a cavity (coloured mesh) formed by conserved residues within the EDS1-SAG101 EP domains which could act as a potential docking platform for such interacting proteins or nucleic acids.

## 2.2 Selection of EDS1 residues for targeted mutagenesis

I focussed on functional analysis of EDS1 EP domain based on structural information from the EDS1-SAG101 heterodimer (Wagner et al., 2013). EDS1 EP domain residues that are conserved between orthologues across seed plant lineages and line the cavity formed by the heterodimer were selected (Figure 2.2). Mutations in these residues were further sorted based on (1) residue accessibility to the surface, (2) prediction that they will not abolish heterodimer associations and

(3) that they will not disturb overall structural integrity. In addition, amino acid residues (366 and 440) in the predicted NLS (nuclear localisation signal) region of EDS1 were not selected for mutational analysis (García et al., 2010). Because the EP domains of the EDS1 protein family likely facilitate protein-protein or protein-nucleic acid interactions upon heterodimer formation (Wagner et al., 2013), the ability of EDS1-SAG101 to be in proximity or association with DNA was probed using the DISPLAR programme (Tjong & Zhou, 2007).

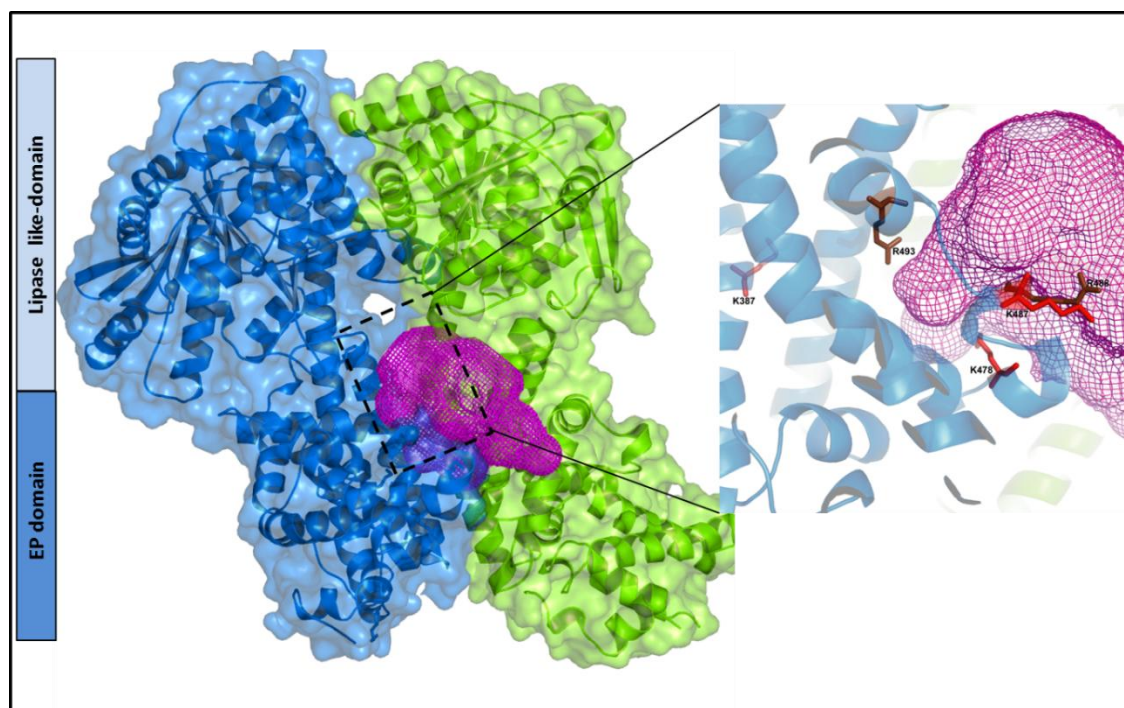


**Figure 2.1: Selection of targets for site-directed mutagenesis of the *Arabidopsis* EDS1 EP domain.** EDS1 (blue) - SAG101 (green) heterodimer is organised into two distinct domains, an N-terminal lipase-like domain and a C-terminal EP domain. Formation of EDS1-SAG101 heterodimer creates a cavity (magenta mesh) involving conserved residues within the EDS1 and SAG101 EP domains. Zoom out: Five EDS1 residues from this cavity (represented as sticks) were selected as targets for mutational analysis; R488, R493 (brown) and K387, K478, K487 (red).

DISPLAR uses a neural network utilizing structural information on sequence-specific position and solvent accessibility of amino acids from crystal structures to predict protein-DNA binding (Tjong & Zhou, 2007). DISPLAR predicted two clusters - one in the EDS1 lipase-like and one in the EP

domain that have potential DNA binding capability (Table S1). Two arginine residues R488 and R493 were selected from the DISPLAR analysis for mutation. In a parallel set of experiments, Laurent Deslandes and colleagues (LIPM, Toulouse) tested the ability of PopP2 to acetylate wild-type *Arabidopsis* EDS1 in tobacco transient co-expression assays. PopP2 is a YopJ family bacterial effector from *Ralstonia solanacearum* with transacetylation activity (Meinzer et al., 2012; Tasset et al., 2010). In these assays, three lysine residues (K387, K478 and K487) in the EDS1 EP domain were found to be acetylated by PopP2 in multiple experiments (L. Deslandes, personal communication).

	K478	K487 R488	R493
<i>A. thaliana</i>	LKNE	KRGRPTRY	
<i>A. lyrata</i>	LKNE	RRGRPNRY	
<i>C. rubella</i>	LKNE	LRGRPNRY	
<i>A. alpina</i>	LKNE	VKGRPNRY	
<i>G. max</i>	LKNE	IRARPKRY	
<i>P. trichocarpa</i>	LKNE	GKGRPRRY	
<i>C. sativus</i>	SKND	IKGRPKRY	
<i>S. tuberosum</i>	LKNE	IRGRPKRY	
<i>A. coerulea</i>	SKND	IKGRPRRY	
<i>M. truncatula</i>	GGKD	TTERSSHRY	
<i>N. benthamiana</i>	LKNE	IRARPKRY	
<i>N. tabacum</i>	SKNE	IRARPKRY	
<i>B. distachyon</i>	SKNE	SKGRPRRY	
<i>O. sativa</i>	SKNE	SKGRPRRY	
<i>Z. mays</i>	SKNE	SKGRPRRY	
<i>S. italica</i>	SKNE	SKGRPRRY	

**Figure 2.2: Conservation of EDS1 EP domain residues across seed plant EDS1 orthologues.** Conservation of EDS1 EP domain residues lining the cavity formed by the EDS1-SAG101 heterodimer. Sequences were aligned using MUSCLE multiple sequence alignment tool (Edgar, 2004). Residues selected for mutational analysis are highlighted. K387 is not conserved and is not depicted here.



Five EDS1 EP domain residues K387, K478, K487, R488 and R493 were selected for mutation to neutral alanine (A) (Figure 2.1). Since PopP2 acetylation activity is necessary for pathogen virulence (Le Roux et al., 2015) and might also target EDS1 to alter its function, lysine residues K387, K478, K487 were mutated to arginine (R) to mimic the positive charge of non-acetylated lysine. K478 was also mutated to glutamine (Q) which mimics acetylated lysine. In addition, double (K478/K487) and triple mutants (K387/K478/K487) were generated for these lysine residues, which are hereafter referred to as 2K\_A or 3K\_A and 2K\_R or 3K\_R, respectively, to denote alanine or arginine substitutions.

### 2.3 Disease resistance phenotypes of T<sub>1</sub> transgenic mutant plants

The EDS1 EP domain mutant variants were expressed under control of the EDS1 native promoter and fused to YFP at the N-terminus (Figure 2.3). A cDNA construct of wild-type (WT) EDS1 from accession Landsberg-*erecta* (*Ler*) (cEDS1) was used for mutagenesis because this was previously shown to complement EDS1 immune functions in a Col *eds1-2* null mutant (Wagner et al., 2013).

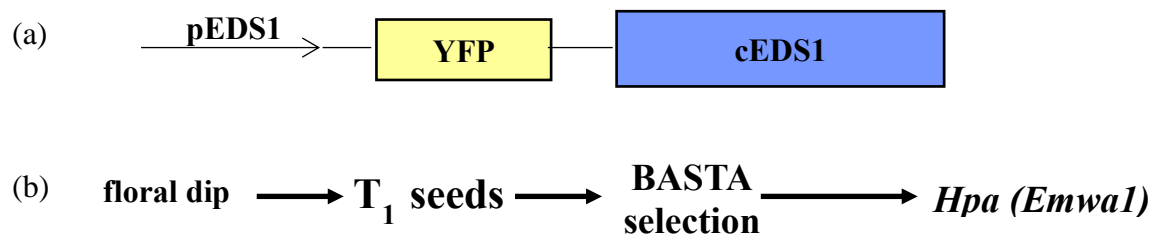


**Figure 2.3: EDS1 T<sub>1</sub> generation transgenic line complementation analysis.** (a) Schematic of EDS1 construct design. Full length cDNA of wild-type EDS1 and mutant variants were expressed under the EDS1 native promoter and with an N-terminal yellow fluorescent protein (YFP) tag. (b) T<sub>1</sub> complementation workflow. EDS1 mutant variants were transformed by a floral dip method (see M&M) into Col *eds1-2* and transgenic plants were selected for resistance to BASTA. T<sub>1</sub> (primary transformant) generation seedlings were tested for EDS1 functional complementation in a TNL disease resistance assay with the oomycete pathogen *Hyaloperonospora arabidopsidis* isolate EMWA1 (*Hpa* EMWA1).

BASTA-resistant primary transformant (T<sub>1</sub> generation) *eds1-2* mutant plants were selected. The transgenic seedlings were then tested for their ability to complement EDS1-dependent TNL

resistance against the obligate biotrophic oomycete *Hyaloperonospora arabidopsidis* isolate EMWA1 (*Hpa* EMWA1), which is recognized by the TNL *RPP4* (Biezen et al., 2002). Plants were semi-quantitatively scored based on macroscopic spores/sporangia formed (Table 2.2). Col-0, Wild-type EDS1 (YFP-cEDS1), K387A/R, K487A/R and R488A mutants complemented *RPP4* resistance to *Hpa* EMWA1, while K478A/R, 2K\_A/R, 3K\_A/R showed partial resistance and R493A exhibited *eds1-2* like hypersusceptibility to *Hpa* EMWA1. EDS1 resistance complementation analysis was done only once on independent T<sub>1</sub> lines and the plants were rescued post *Hpa* infection with a fungicide (Ridomil Gold). I concluded from these results that mutating K478 and R493 result in partial and full loss of EDS1 immune functions, respectively. I also inferred from the complementation test that the 2K\_A/R and 3K\_A/R variants do not additively increase the susceptibility of K478A/R variant. Thus, the partial loss of TNL resistance in the double and triple mutant is likely due to mutation of K478. For further analysis, the susceptibility-inducing EDS1 EP domain residues K478, R493 and 3K were studied.

## 2.4 The EP domain of EDS1 is critical for immune functions

The lipase-like domain of EDS1 is unable to complement an *eds1-2* mutant, although it is stable and interacts with PAD4 and SAG101 (Wagner et al., 2013). Therefore, the EDS1 EP domain is critical for immune signalling after heterodimer formation. The EP domain alone is unstable in transgenic plants (Wagner et al., 2013). Given the resistance complementation data in T<sub>1</sub> generation, I selected stable homozygous transgenic lines in *Arabidopsis* from independent T<sub>1</sub> transformants in Table 2.2 (details of selection in materials and methods). In this section I will present results that point to the functional importance of residues K478 and R493 in the EP domain using stable transgenic lines. These residues form the periphery of the EP domain cavity described in Figure 2.2 and contribute to EDS1 protein function or stability.

### 2.4.1 EDS1 EP domain variants disrupt TNL mediated-ETI

TNL triggered immunity operates entirely via the EDS1 resistance signalling node (comprising EDS1 with PAD4 or SAG101) (Aarts et al., 1998; Wiermer et al., 2005). EDS1 was shown to interact with the TNL RPS4 inside nuclei (Heidrich et al., 2011). Also, EDS1 interacted with

bacterial effectors AvrRps4 and HopA1 and was therefore proposed to be a potential virulence target of these bacterial effectors in modulating plant basal defences (Bhattacharjee et al., 2011).

Mutation	T <sub>1</sub> disease resistance
Col-0	16/16
<i>eds1-2</i>	0/24
cEDS1 (w.t)	16/16
K387A	22/22
K387R	20/20
K478A	3/22
K478R	4/20
K487A	20/21
K487R	21/21
K478A/K487A	3/21
K478R/K487R	1/17
3A (K387/K478/K487)	5/21
3R (K387/K478/K487)	4/17
R488A	24/24
R493A	0/23

**Table 2.2: Summary of TNL (*RPP4*) complementation assay in T<sub>1</sub> plants expressing EDS1 EP domain variants.** For each EDS-YFP transgene, 24 individual BASTA-resistant T<sub>1</sub> seedlings were monitored for TNL-triggered resistance to *Hpa* EMWA1 (at 5 dpi). Seedlings showing conidiospores on leaves were scored as disease susceptible. Shown is the ratio of resistant / total number of plants.

To study the effect of the selected EDS1 EP domain variants K478R, 3K\_R and R493A on TNL-triggered immunity, pathogens recognized by different TNLs in *Arabidopsis thaliana* (*A. th*) were tested in stable *Arabidopsis* transgenics. As mentioned in infection assays of T<sub>1</sub> generation, transgenic lines with *Hpa* EMWA1 (Table 2.2) recognized by the TNL RPP4 was used (van der Biezen et al., 2002). Resistance against *Hpa* CALA2 recognized by RPP2 and *Pst*/DC3000 expressing *AvrRps4* (*Pst*/*AvrRps4*) recognized by the TNL pair of RPS4-RRS1 were studied in stable (T<sub>3</sub>) transgenic lines.

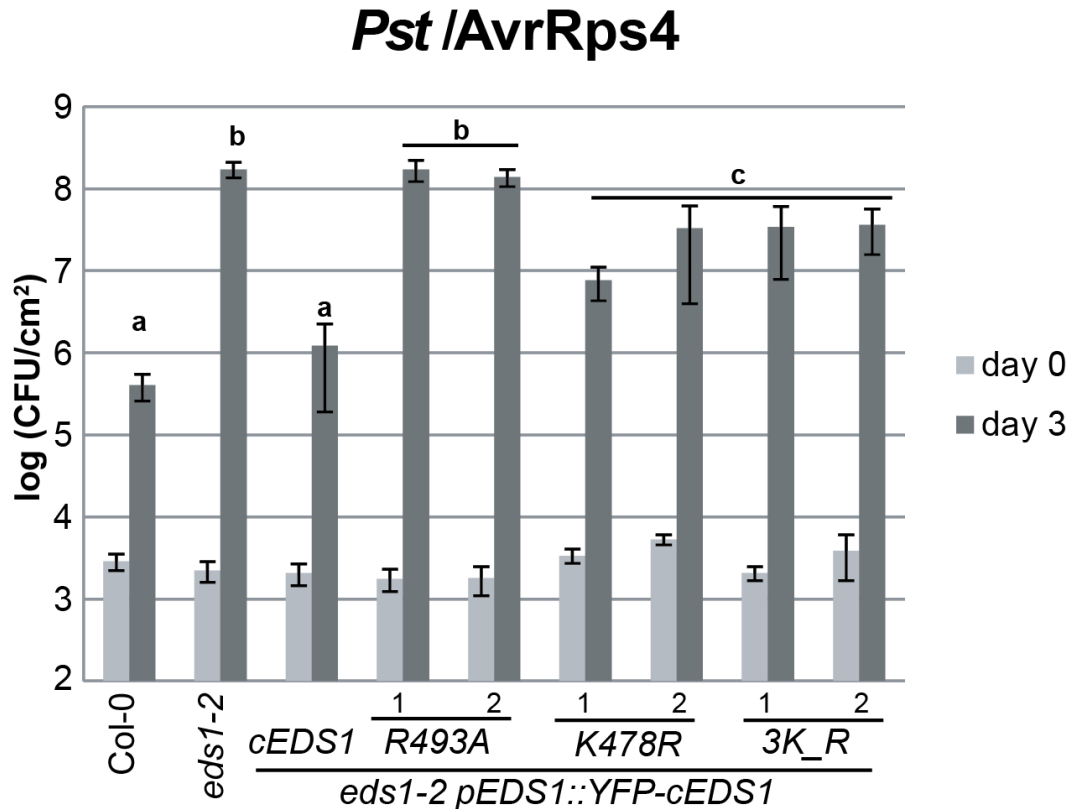


**Figure 2.4: Susceptible phenotypes of EDS1 transgenic lines expressing EP variants in *Pst*/AvrRps4-triggered TNL resistance.** Four-week old plants of the indicated genotypes were spray-inoculated ( $OD_{600}$  - 0.2) with avirulent *Pst*/AvrRps4 and bacterial titers determined at 0 and 3 days post inoculation (dpi). Bars represent means of 4 replicates  $\pm$  standard error. Differences between genotypes were analysed using TukeyHSD ( $p$ -value  $< 0.005$ ). Similar results were obtained in three independent experiments. Independent transgenic lines of each mutant are indicated with numbers (1 and 2).

Spray infection with the avirulent strain *Pst*/AvrRps4 on leaves of 4-week old plants led to different resistance phenotypes (Figure 2.4). In accordance with the macroscopic phenotypes observed in analysis of  $T_1$  transformants infected with *Hpa* EMWA1; R493A lines exhibited a susceptible phenotype that was as extreme as *eds1-2*. By contrast, plants expressing the lysine variants K478R and 3K\_R displayed partial resistance to *Pst*/AvrRps4 with intermediate bacterial titers that were higher than wild-type Col-0 but lower than *eds1-2* or R493A lines (Figure 2.4). Higher susceptibility was not observed in the triple Lysine mutant (3K\_R) compared to the Lysine variant K478R. Two independent transgenic lines for each mutant were tested and no significant difference in disease resistance was observed within the same mutant.

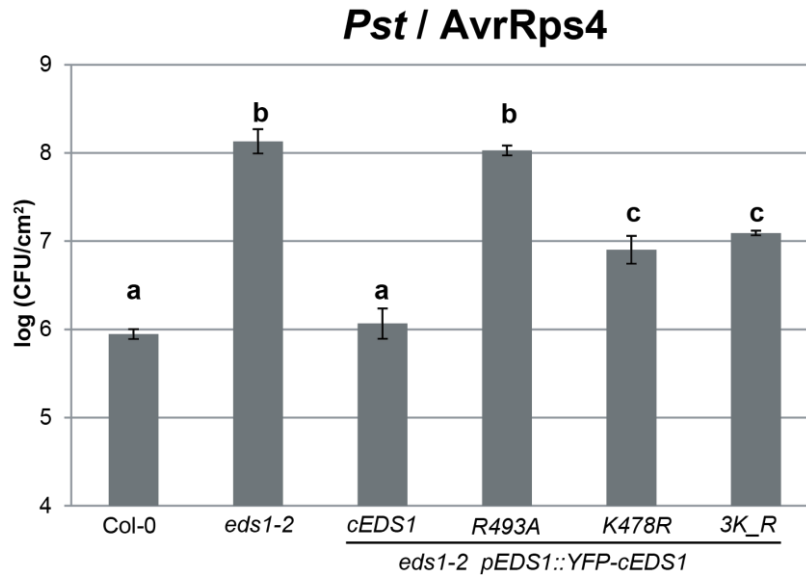


**Figure 2.5: Bacterial growth titers in plants expressing EDS1 EP variants upon infiltration of *Pst/AvrRps4*.** Four-week old plants were hand-infiltrated ( $OD_{600}$  - 0.0002) with avirulent *Pst/AvrRps4* and bacterial titers determined 3 days post infiltration. Bars represent means of 4 replicates  $\pm$  standard error. Differences between genotypes were analysed using TukeyHSD. Significant differences were not observed between different lines at day 0. Similar results were obtained in two independent experiments.

Similar pathogen phenotypes were observed when *Pst/AvrRps4* was hand-infiltrated onto leaves with a 1000-fold diluted bacterial suspension (Figure 2.5). Direct infiltration of bacteria into the leaf apoplast using a syringe by-passes a stomatal resistance layer that contributes to resistance against bacteria sprayed onto the leaf surface (Melotto et al., 2006). These results established that the disease phenotypes of the EDS1-YFP EP mutant lines are consistent using the two modes of inoculation. They also show that loss of TNL resistance in these lines is likely to be post-stomatal. Hereafter, infiltration assays were used for all *P.syringae* infection experiments.

I then tested whether plants expressing the EDS1 EP domain variants were compromised in resistance conferred by other TNL receptors by spraying with *Hpa* CALA2 which is recognized by TNLs *RPP2a* and *RPP2b* (Sinapidou et al., 2004). In line with the T<sub>1</sub> analysis (*Hpa* EMWA1) and bacterial (*Pst/AvrRps4*) resistance phenotypes, Col-0 and cEDS1 were resistant to *Hpa* CALA2. In these infection assays, I stained infected *Arabidopsis* leaves with Trypan Blue (TB) to visualize pathogen growth in plant tissues or hypersensitive response (HR) which is a classical symptom of pathogen recognition and effective ETI which halts pathogen proliferation (Figure

2.6). The *eds1-2* null mutant is susceptible to *Hpa* CALA2 as seen by extensive pathogen growth in leaves (Figure 2.6).

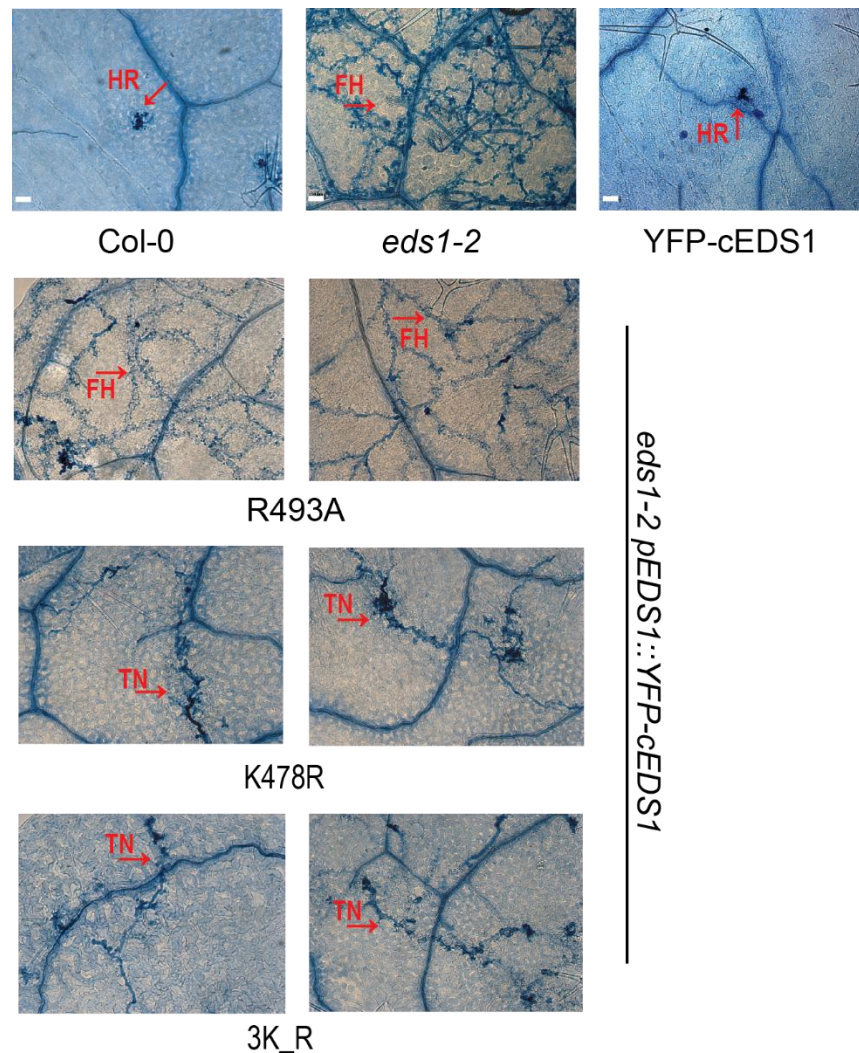


**Figure 2.6: Plants expressing EDS1 EP variants fail to trigger TNL (*RPP2*) resistance to *Hpa* CALA2.** *RPP2* resistance phenotypes of 3-week-old control and homozygous ( $T_3$  generation) transgenic lines expressing YFP-cEDS1 or EP domain mutated variants, as indicated. *Hpa* CALA2 infected leaves were stained with Trypan Blue at 5 dpi. The scale bar represents 50 μm. Images are representative of 24 leaves from two different experiments on the same independent plant lines as used in Figure 2.4. HR-hypersensitive response; FH-pathogen free hyphae; TN-trailing host cell necrosis.

I found R493A plants to be as susceptible as *eds1-2* with free hyphal growth without obvious host resistance (Figure 2.6). By contrast, plants expressing the K478R and 3K\_R variants produced trailing necrosis in response to growing *Hpa* hyphae. Trailing necrosis is considered an indication of a weak or late defence response. Therefore, these mutants have a TNL resistance phenotype that is intermediate between Col-0 (fully resistant) and *eds1-2* (hypersusceptible). I concluded that in resistance conferred by different TNLs against two different pathogens (*Hpa* and DC3000), the EDS1 EP domain variants exhibit partial (in case of K478R) or complete loss (R493A) of resistance (table 2.2, Figure 2.4 & 2.6). These data reinforce the importance of EDS1 as a signalling hub acting as a bridge between upstream TNL activation and orchestrating downstream immune signalling (Heidrich et al., 2011; Wagner et al., 2013; Wiermer et al., 2005). These data also clearly point to the requirement of critical residues in the EDS1 EP domain for TNL resistance against different pathogens.

#### **2.4.2 EDS1 EP domain variants cause a complete loss of basal resistance to virulent pathogens**

*Arabidopsis eds1* null mutant plants are hypersusceptible to virulent strains of *P.syringae* or *Hpa* (Parker et al., 1996), as measured by increased pathogen growth compared to that on wild-type genetically susceptible *Arabidopsis* parental genotypes. EDS1 with PAD4 forms an indispensable component in basal resistance against virulent pathogens (B J Feys et al., 2001; Jirage et al., 1999; Wagner et al., 2013).

Whether basal resistance functions of EDS1 are affected by mutations in the EDS1 EP domain that compromise EDS1 immune functions in TNL resistance, EDS1 EP domain mutants were infected with the virulent strain *P. syringae* pv *tomato* DC3000 (*Pst*/DC3000). Upon infection with *Pst*/DC3000 both wild-type Col-0 and YFP-cEDS1 were resistant to bacteria (Figure 2.7). However, I consistently observed marginally higher (but statistically insignificant) *Pst*/DC3000 titers in YFP-cEDS1 in independent experiments (Figure 2.7). Surprisingly, the EP domain variants (K478R, 3K\_R and R493A) did not complement EDS1 and showed bacterial titers similar to *eds1-2*. Two independent transgenic lines for each mutant were tested as in 2.4.1. Thus, single

amino acid mutations in the EP domain completely compromise EDS1 functions in basal immunity against virulent pathogens but show variable resistance in TNL-triggered immunity.

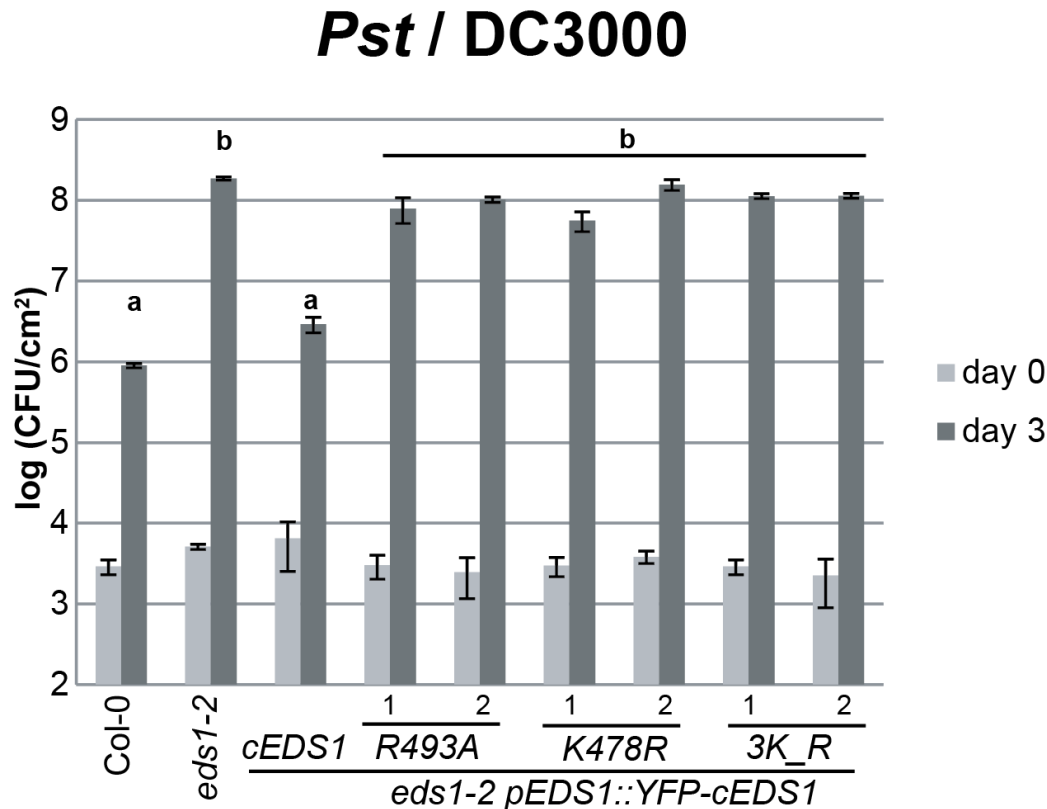


**Figure 2.7: EDS1 EP variants cause complete loss of basal resistance to *Pst*/DC3000.** Four-week old *Arabidopsis* plants of the indicated genotypes were spray-inoculated (OD<sub>600</sub> - 0.2) with a virulent *Pst*/DC3000 and bacterial titers determined at 0 and 3 days post inoculation (dpi). Bars represent means of 4 replicates  $\pm$  standard error. Differences between genotypes were analysed using TukeyHSD ( $p$ -value  $< 0.005$ ). Similar results were obtained in three independent experiments. Two independent transgenic lines for each mutant were tested, numbering of lines similar to that in Figure 2.4.

## 2.5 EP domain mutations do not alter EDS1 nucleocytoplasmic localization

EDS1 is a nucleocytoplasmic protein and proper spatio-temporal regulation of EDS1 accumulation in the nucleus, is essential for a robust immune response (García et al., 2010; Rietz et al., 2011; Wiermer et al., 2005). I first tested whether intracellular localization of the selected EDS1 variants was altered in transient expression assays in *Nicotiana benthamiana* (Figure 2.8).



Functional (K387R, K487R, R488A) and non-functional (K478R, R493A) variants of EDS1 displayed a nucleo-cytoplasmic localization in *N. benthamiana* (Figure 2.8). As controls, YFP-cEDS1 and EDS1-NLS-YFP (localizing only to the nucleus), respectively, accumulated expectedly as nucleocytoplasmic and nuclear proteins in *N.benthamiana* (Figure2.8).

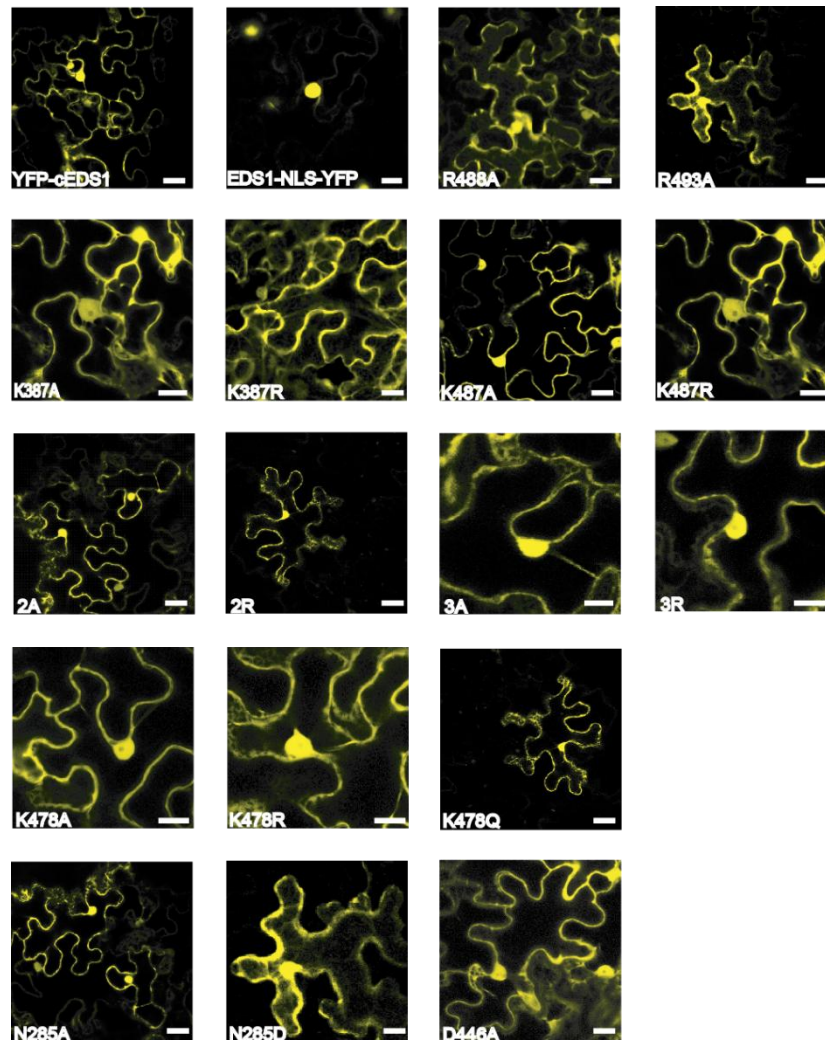


**Figure 2.8: Localization of EDS1 EP domain variants in *N.benthamiana* transient expression assays.** Confocal images of YFP-tagged EDS1 variants transiently expressed in *N.benthamiana* leaf epidermal cells taken at 3 days. Wild-type (YFP-cEDS1) and nuclear-localized (EDS1<sup>NLS</sup>-YFP; N. Peine et al., unpublished) variants are shown as controls for nucleo-cytoplasmic and nuclear localization, respectively. 2K\_A, 2K\_R represent K478/K487 to alanine and arginine variants, respectively. 3K\_A and 3K\_R represent K387/K478/K487 triple mutations to Alanine or Arginine. Images are representative of six different leaves from two independent biological experiments. Images were taken at identical light settings. Scale bar of 20µm.

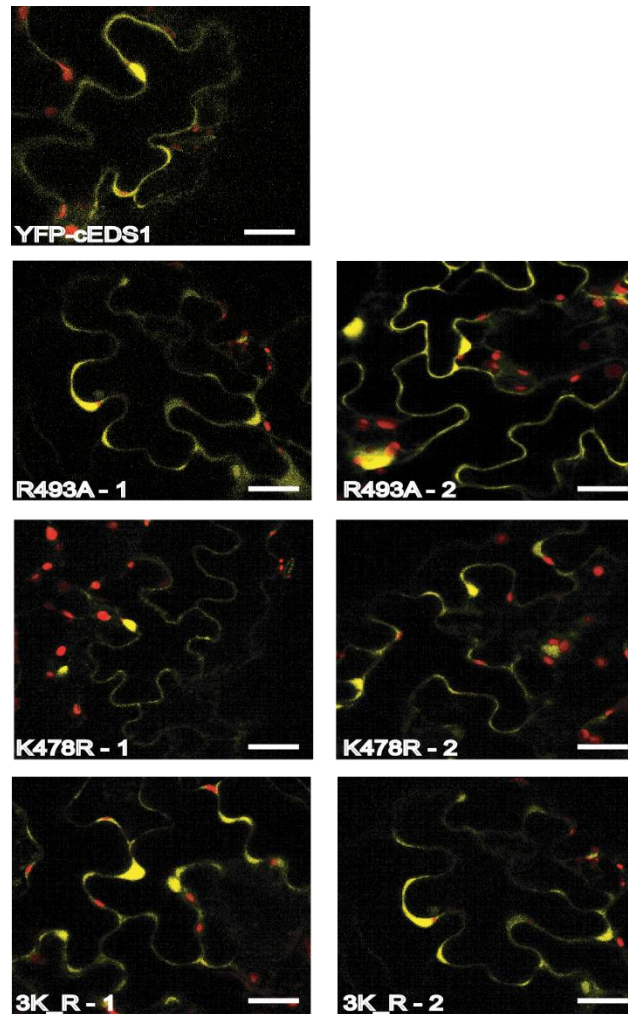


**Figure 2.9: Nucleo-cytoplasmic localization of EDS1 variants in *Arabidopsis eds1-2* homozygous transgenic lines.** Confocal images of leaves expressing YFP-tagged wild-type and mutant EDS1 forms displayed nucleo-cytoplasmic localization at 24 hpi with *Pst/AvrRps4*. Chloroplasts in mesophyll cells produce red fluorescence. Images are representative of three independent treatments, at identical settings. Scale bar of 20µm.

I then monitored intracellular localization of the EDS1-YFP K478R, 3K\_R and R493A variants compared to wild-type YFP-cEDS1 in the selected *Arabidopsis* transgenic lines after infiltration of leaf tissues with *Pst/AvrRps4*. As expected, YFP-cEDS1 showed a nucleo-cytoplasmic localization, as monitored under confocal microscope. Independent homozygous T<sub>3</sub> transgenic lines of the disease susceptible EDS1 EP domain K478R, 3K\_R and R493A mutants also showed

nucleo-cytoplasmic localization after infection with *Pst*/AvrRps4 (Figure 2.9), suggesting that the disease susceptibility of the mutants is not due to their failure to accumulate inside nuclei. Wild-type like localization of mutant EDS1 transgenic lines also underpins that protein stability is not completely lost in these mutants.

## 2.6 Interaction with PAD4 and SAG101 is maintained in EDS1 EP domain variants

After establishing the localization of the YFP-EDS1 K478R, 3K\_R and R493A variants, I tested their ability to homo-dimerize and interact with PAD4 and SAG101 in a yeast-two hybrid (Y2H) assay. Here, the EDS1 variants were fused to the GAL4 activation domain (prey) and WT EDS1, PAD4 or SAG101 were used as baits fused to the GAL4 DNA binding domain (BD). I found that the EDS1 EP domain variants maintained homo- and hetero-interactions with itself and its interaction partners (Figure 2.10A). BD-p53 and AD-T7 constructs were tested alongside as negative controls for bait and prey, respectively (for a full list of interactions, see Table S2).

In an independent manner, I tested the ability of transiently expressed EDS1 variants to immunoprecipitate (IP) PAD4 or SAG101 in *N.benthamiana*. R493A, K478R, 3K\_R variants of YFP-EDS1 were co-infiltrated with StrepII-3xHA-tagged PAD4 or SAG101 into young *N.benthamiana* leaves. Infiltrated leaves expressing the proteins were harvested 3 days later. Leaf tissue extracts were incubated with GFP-trap beads to facilitate binding and purification of YFP-tagged WT EDS1 and mutant variants. Co-purification of strep-HA-tagged PAD4 or SAG101 with YFP-tagged EDS1 mutants was tested on Western blots (materials and methods). The EDS1 EP domain mutants (R493A, K478R, 3K\_R,) interacted with PAD4 and SAG101. A variant of EDS1 (EDS1<sup>LLIF</sup>) which fails to interact with PAD4 and SAG101 (Wagner et al., 2013) was used as a negative control and WT cEDS1 as a positive control for EDS1 interaction with PAD4 and SAG101. The ability of EP domain variants to form EDS1 hetero- and homo-dimers suggests that the pathogen susceptibility of these variants cannot be attributed to loss of EDS1 binding to either PAD4 or SAG101.

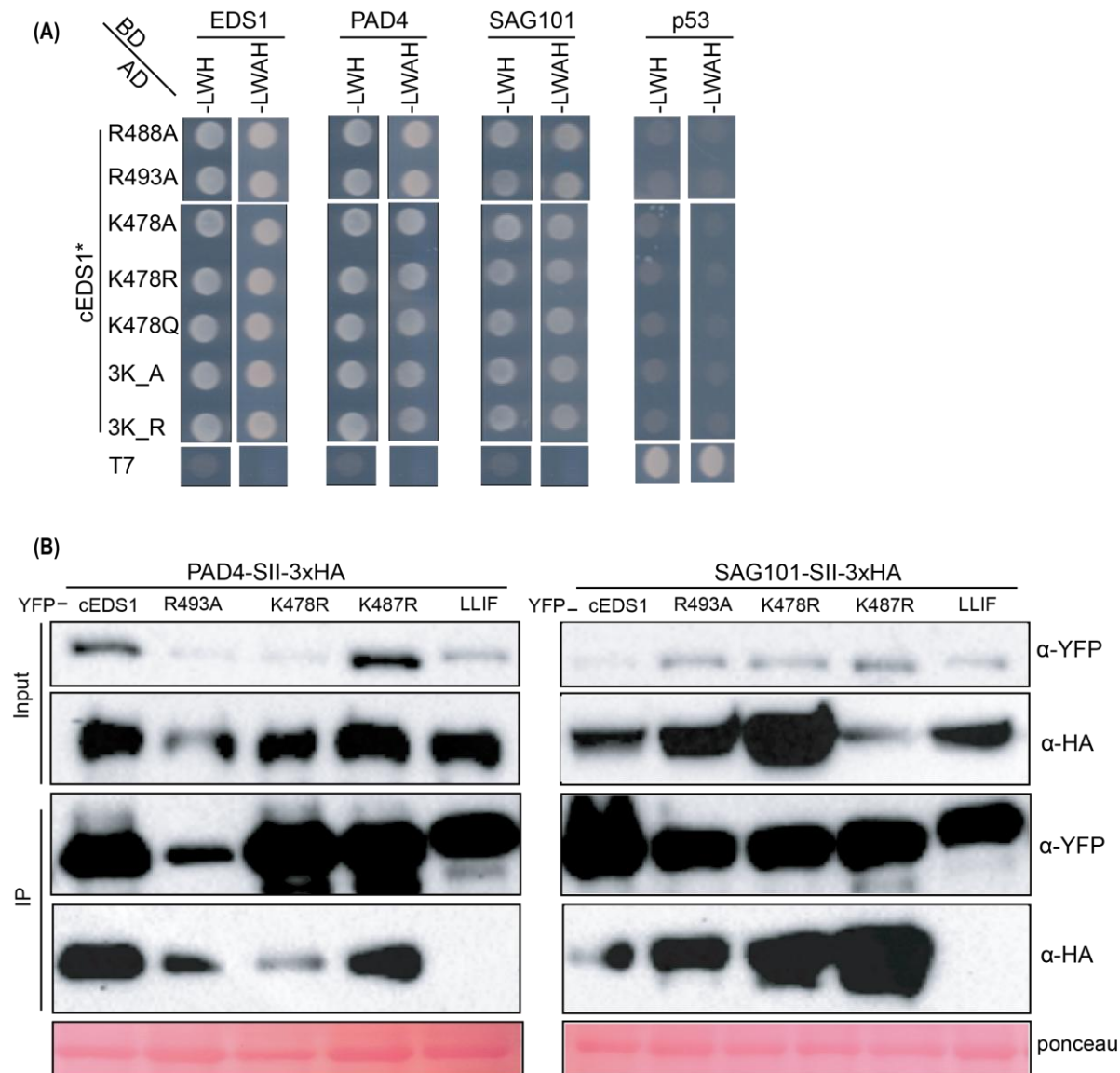


**Figure 2.10: EDS1 variants can form homo-dimers and maintain interaction with partners PAD4 and SAG101.** (A) Y2H interactions between activation domain (AD) fusions of EDS1 variants and full-length EDS1, PAD4 or SAG101 binding domain (BD) fusions. Yeast viability, weak (-LWH) or strong (-LWAH) protein interactions are shown. BD-p53 and AD-T7 were used as negative controls in the GAL4 matchmaker Y2H system. (B) EDS1 variants expressed transiently in *N.benthamiana* were co-immunoprecipitated with transiently co-expressed PAD4 or SAG101. Inputs of different YFP-cEDS1 variants under the native EDS1 promoter and PAD4-SII-3xHA or SAG101-SII-3xHA protein under a constitutive CaMV 35S promoter are shown in top panels. Note the different levels of protein expression. Proteins were immunoprecipitated with  $\alpha$ -GFP beads and co-immunoprecipitated SII-3xHA proteins were detected with anti-HA (IP). Image is representative of four independent experiments. Disease susceptible EDS1 variants (R493A, K478R) are able to IP PAD4 and SAG101. The LLIF variant of EDS1 was used as a control for loss of binding to PAD4 or SAG101.

## 2.7 Disease susceptibility of EDS1 EP domain mutants cannot be explained by low protein accumulation

### 2.7.1 EDS1 variant proteins accumulate upon pathogen infection

In western blot analysis of the YFP-cEDS1 EP variant transgenic lines probed with anti-EDS1 antibodies I found that steady state protein accumulation in mutated variants was overall lower than the transgenic WT YFP-cEDS1 line or endogenous native EDS1 in Col-0 uninfected leaf extracts (Figure 2.11). Because all known TNLs signal *via* the EDS1 regulatory node, I tested YFP-cEDS1 protein accumulation at 24 hpi with *Pst*/AvrRps4. In two independent transgenic lines for each EP domain variant, EDS1 protein accumulation was observed post infection with *Pst*/AvrRps4 (Figure 2.11 B). Notably, all the EP variants accumulated higher steady state protein at 24 h post *Pst*/AvrRps4 infection (Figure 2.11). The fully susceptible mutant R493A accumulated protein in comparable amounts to WT YFP-cEDS1 (Figure 2.11). I concluded that the EDS1 EP domain variants detected AvrRps4 and likely initiated immune signalling leading to protein upregulation and accumulation.

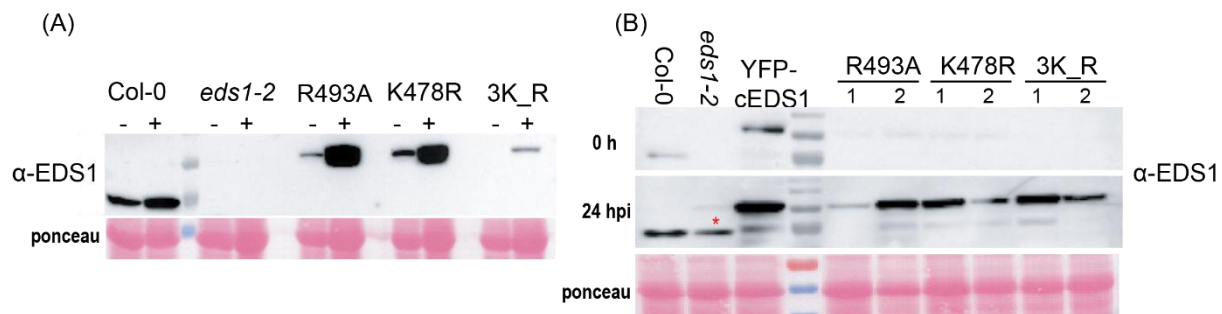


**Figure 2.11: EDS1 variant proteins accumulate in ETI response to *Pst*/AvrRps4.** (A) EDS1 protein accumulation in Col-0 and mutant EDS1 transgenics in uninfected (-) and 24 hpi (+) with *Pst*/AvrRps4. Ponceau staining shows protein loading. (B) Two independent transgenic lines of EDS1 variants shows variable levels of protein accumulation at 24 hpi with *Pst*/AvrRps4. Ponceau staining shows protein loading. YFP-tagged EDS1 lines run at higher molecular mass of 100 kDa compared to native EDS1 protein (72 kDa). \*- a contaminating band likely due to spill over from adjoining lanes.



### 2.7.2 Disease susceptibility does not correlate with low initial EDS1 protein levels

Low steady state protein accumulation in susceptible R493A variant compared to YFP-cEDS1 (Figure 2.11) and their disease susceptible phenotypes (Figure 2.4, 2.6, 2.7) suggested that the disease susceptibility might be due to low initial EDS1 protein amounts in cells. As shown above (Figure 2.11), the EP domain variants accumulated protein 24 hpi with *Pst*/AvrRps4. EDS1 EP domain variants with single mutations in lysine residues K387R and K487R did not have compromised pathogen resistance (Table 2.2, Figure 2.12) but accumulated similar pre-infection proteins levels as the loss-of-resistance R493A variant (Figure 2.12).

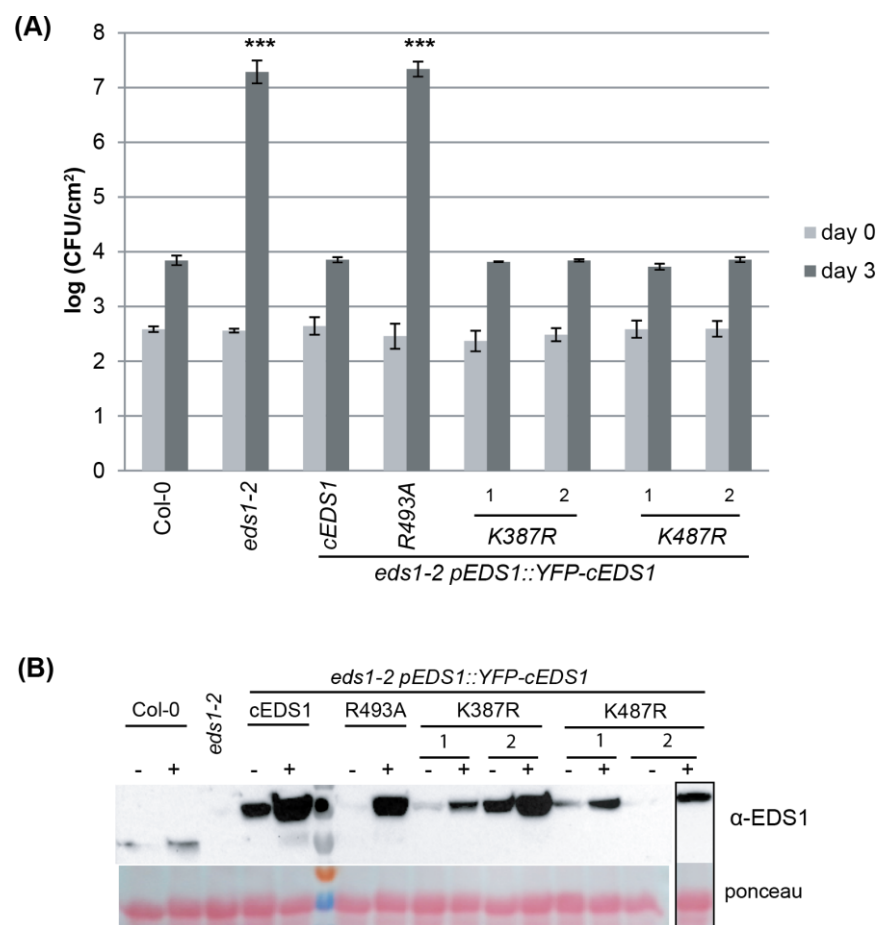


**Figure 2.12: Low starting levels of EDS1 protein are sufficient to generate a robust TNL immune response.** (A) The indicated genotypes (susceptible- R493A and resistant- K387R, K487R) were infiltrated with avirulent *Pst*/AvrRps4 and bacterial titers measured at 3 dpi. Bars represent means of 3 replicates  $\pm$  standard error. Similar trends were observed in two independent experiments. *t*-test (p-value \*\*\* <0.005). (B) Protein accumulation pre (-) and post infection (+) at 24 hpi was measured in leaves from the same experiment as shown in (A).

Interestingly, R493A lines accumulated more protein post infection with *Pst*/AvrRps4 than the K387R and K487R mutants which are resistant to *Pst*/AvrRps4 (Figure 2.12). The different starting protein levels in independent transgenic lines #1 and #2 of K387R and K487R did not confer enhanced resistance to *Pst*/AvrRps4. This is consistent with the observation that overexpression of EDS1 does not enhance resistance (Wagner et al., 2013).

In summary, the EP-domain variants have variable pre-infection steady state protein levels but accumulate to wild-type like levels post infection with *Pst*/AvrRps4 whether they confer resistance (K387R, K487R) or not (R493A) (Figure 2.12). Also notable is that, though low protein levels of R493A, K387R #1 and K487R #2 are comparable, their resistance phenotypes are different, R493A is susceptible while K387R and K487R are resistant. This lack of correlation between protein levels and resistance phenotypes highlights the requirement of very low levels of basal EDS1 protein to carry out its immune functions. I concluded that basal EDS1 protein and accumulation post-infection with *Pst*/AvrRps4 do not correlate with EDS1 immune signalling competence.

## 2.8 EDS1 EP domain mutants accumulate salicylic acid after TNL activation

As described in the Introduction, the stress hormone salicylic acid (SA) plays a major role in plant defence against biotrophic pathogens. EDS1 and PAD4 are necessary for pathogen mediated SA accumulation in TNL and basal immunity (B J Feys et al., 2001; Jirage et al., 1999). In ETI mediated by several CNL receptors, EDS1 and SA signalling were shown to act redundantly (Aarts et al., 1998; Venugopal et al., 2009). I therefore measured the effect of mutations in EP domain on EDS1-mediated SA accumulation in response to pathogen infection.

Four-week old plants were infiltrated with *Pst*/AvrRps4 and SA was measured 24 hpi. Col-0 and the YFP-cEDS1 control transgenic line accumulated SA but the Col *eds1-2* null mutant did not, in line with previous reports (B J Feys et al., 2001) and the model of EDS1-dependent SA accumulation in TNL triggered immunity (Figure 2.13). Surprisingly, independent lines of the EDS1 EP domain variants K478R and 3K\_R that were (partially) disabled in defence against *Pst*/AvrRps4 (Figure 2.4) accumulated SA to YFP-cEDS1-like levels at 24 hpi with *Pst*/AvrRps4 (Figure 2.13).

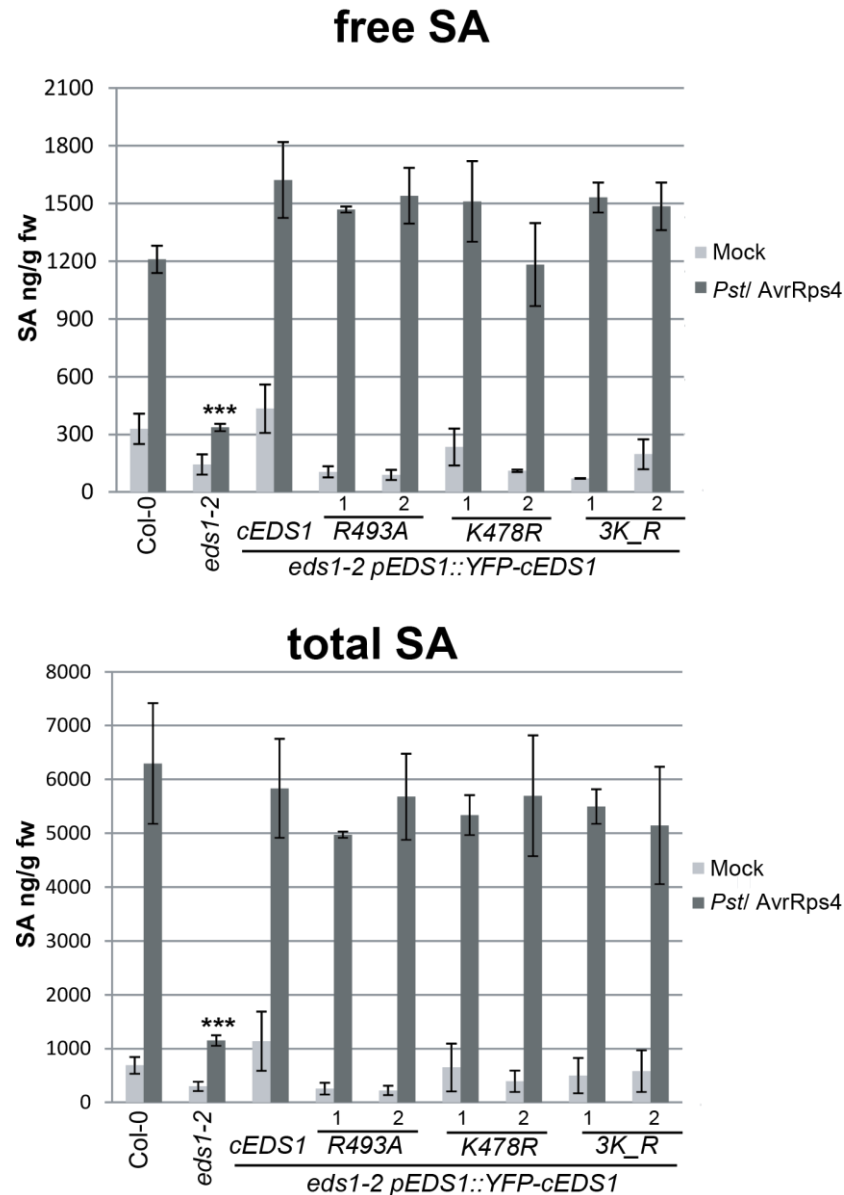


**Figure 2.13: EDS1 EP-domain disease susceptible variants trigger SA accumulation in response to *Pst/AvrRps4* infiltration.** Free SA and total SA (SA + SA-glucose conjugate) were quantified at 24 hpi with mock (10mM MgCl<sub>2</sub>) or *Pst/AvrRps4* (O.D<sub>600</sub>- 0.005). Two independent transgenic lines per variant were tested. Bars represent means of 4 replicates pooled from different biological experiments  $\pm$  standard error. Differences between genotypes were analysed using TukeyHSD ( $p$ -value : \*\*\*< 0.001). fw, fresh weight.

Remarkably, independent transgenic lines #1 and #2 of R493A which displayed a complete *eds1-2* like disease susceptibility phenotype (Figure 2.4, 2.6) also accumulated SA to similar levels as



Col-0 or YFP-cEDS1, suggesting that the R493A mutation does not get perturbed by the SA-dependent defence pathway, at least as measured at 24 hpi. I concluded that the resistance defect in EDS1 EP variant R493A is likely to be in an EDS1 SA-independent signalling function.

SA accumulation is antagonized by the JA pathway which reduces SA by converting active free SA to an inactive glucosylated SA form (SAG) via BSMT1 (SABATH methyl transferase 1) (F. Chen et al., 2003; Thaler, Humphrey, & Whiteman, 2012). I found no significant difference between cEDS1 and EDS1 mutant variants in absolute amounts of SAG at 24 hpi with *Pst*/AvrRps4 (Figure 2.13), suggesting that altered conversion of free SA to SAG does not explain disconnect between SA accumulation and disease susceptibility in variant R493A. However, while R493A accumulated SA at 24 hpi with *Pst*/AvrRps4, it did not upregulate the SA-response marker *PR1* (pathogenesis related 1) (Nawrath, 1999; Yalpani et al., 1991) (Figure2.14).

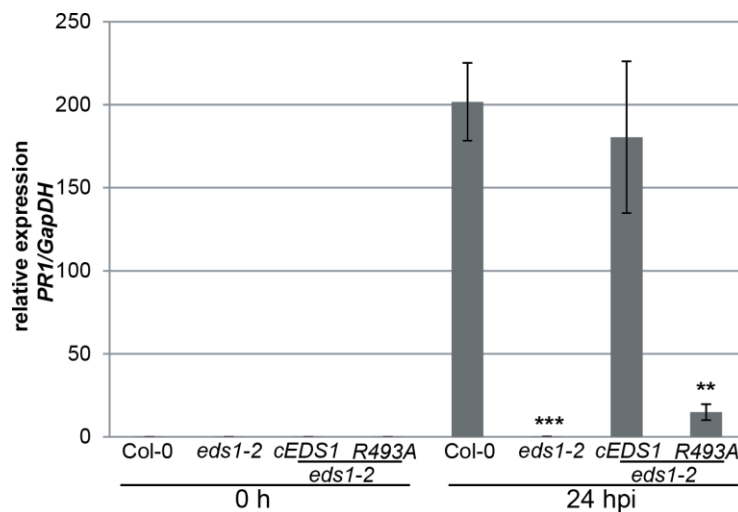


**Figure 2.14: The SA marker gene *PR1* is not induced in R493A despite SA accumulation.** Leaves of 4-week-old plants were infiltrated with *Pst*/AvrRps4 (O.D<sub>600</sub> = 0.005) and *PR1* and *EDS1* transcript levels were measured at 0 h (untreated) and 24 hpi. Transcripts were determined by qRT-PCR and normalized using the internal control *GapDH*. Bars represent means of 3 replicates  $\pm$  standard error. Similar trends were observed in three independent experiments. *t*-test (p-values \*\*\*<0.001, \*\* <0.005).

The YFP-cEDS1 line showed similar induced *PR1* expression, measured by qRT-PCR as in Col-0 at 24 hpi with *Pst*/AvrRps4 (Figure2.14). By contrast, YFP-cEDS1 R493A variant lines produced 10-fold lower *PR1* expression than YFP-cEDS1 (Figure2.14), despite high SA

accumulation (Figure 2.13). The observed low *PR1* upregulation indicated that R493A does not behave as a complete *eds1* loss-of-function mutant (*eds1-2*) in which *PR1* was not induced (figure 2.14).

### 2.8.1 Exogenous SA induces *PR1* in EDS1 R493A EP variant

To ascertain whether the uncoupling of SA accumulation and *PR1* upregulation in YFP-cEDS1 variant R493A is due to the repression or failure of signalling pathways downstream of SA, I measured *PR1* transcript levels in R493A plants after application of exogenous SA.

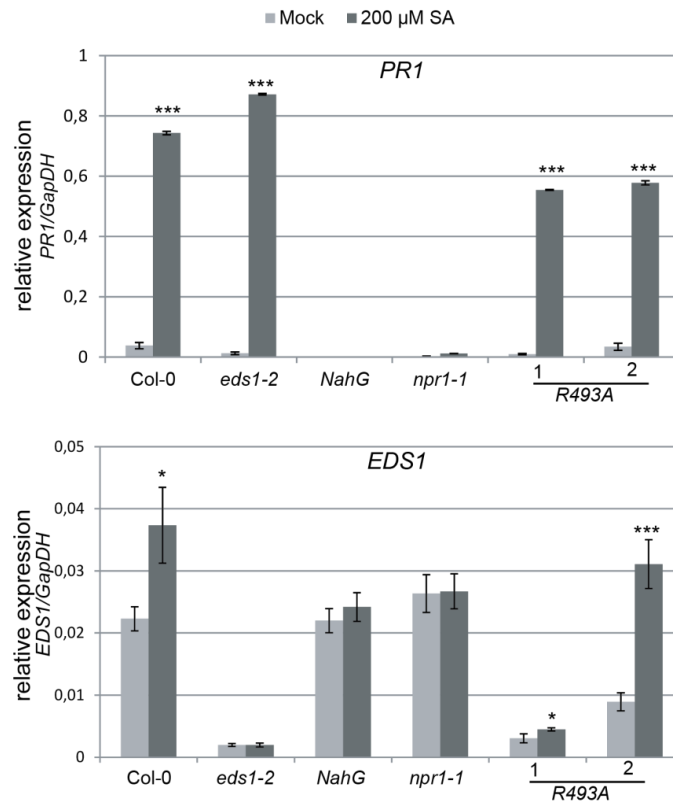


**Figure 2.15: EDS1 R493A is competent in SA-mediated *PR1* up-regulation.** Mock (10mM  $\text{MgCl}_2$ ) or 200 $\mu$ M SA were added to 2-week old seedlings of the indicated genotypes grown in liquid MS medium, *PR1* and *EDS1* transcripts were measured 24 h post treatment with SA. Independent transgenic lines #1 and #2 were tested for the YFP-cEDS1 R493A variant. Bars represent means of 3 replicates  $\pm$  standard error. A similar trend was observed in two independent experiments *t*-test (*p*-values \*\*\* $<0.001$ , \* $<0.01$ ).

Upon exogenous application of SA, *PR1* was found to be upregulated in Col-0, *eds1-2* and R493A but not in a *NahG* expressing line (encoding SA hydroxylase that converts SA to catechol) or in the SA response regulator NPR1 (non-expressor of PR1) knock out *npr1-1* (Yue Wu et al., 2012), which do not relay signals from SA to *PR1* (Cao et al., 1994; Yue Wu et al., 2012). Independent transgenic lines #1 and #2 of R493A were tested. No significant difference was observed in SA-induced *PR1* expression between Col-0 and R493A (Figure 2.15). The upregulation of *PR1* in R493A in response to SA suggests that defects in R493A resistance signalling are not downstream of SA. This is in line with positioning EDS1 upstream of SA in TNL and basal immunity pathways (B J Feys et al., 2001). Notably, expression of the R493A transgene also responded positively to exogenous SA (Figure 2.15), consistent with operation of an intact SA feed-forward loop promoting *EDS1* (B J Feys et al., 2001). By contrast, *EDS1* was not up regulated in response to SA in the *NahG* line (Figure 2.15). Thus, R493A does not interfere with signalling downstream of SA and feed forward action of SA on *EDS1* expression.

### 2.8.2 Plants expressing EDS1 EP variant R493A display full CNL (RPS2) immunity

Genetic evidence suggests that EDS1 and SA operate redundantly in CNL-triggered immunity (Aarts et al., 1998; Venugopal et al., 2009). To assess whether the R493A mutation compromises redundancy between SA and EDS1, R493A transgenic lines #1 and #2 were infiltrated with *Pst/AvrRpt2*. AvrRpt2 is recognized by the CNL receptor RPS2 (Kunkel et al., 1993). Four-week old plants were infiltrated with *Pst/AvrRpt2* and bacterial growth was measured 3 dpi. As expected, Col-0 and cEDS1 were resistant to *Pst/AvrRpt2* (Figure 2.16).

An *rpm1/rps2* double mutant which does not recognize the AvrRpt2 (Belkhadir et al., 2004) was susceptible to *Pst/AvrRpt2* (Figure 2.16). The *eds1-2* mutant was resistant consistent with (Pieterse et al., 2009) compensation by SA (Figure 2.16). Although *eds1-2* and R493A lines had slightly higher bacterial growth compared to Col-0 and YFP-cEDS1, the difference in growth was not significant (Figure 2.16). These data show that the EDS1 R493A mutation does not disrupt RPS2 resistance and are consistent with RPS2 signalling downstream of SA being intact and able to compensate for defective EDS1 in the R493A mutant lines.

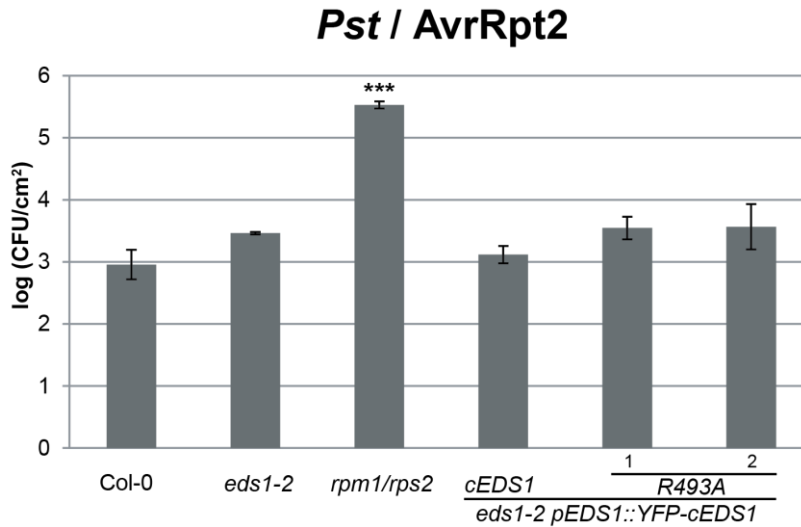


**Figure 2.16: EDS1 R493A does not affect CNL triggered resistance.** The indicated genotypes were infiltrated with avirulent *Pst*/*AvrRpt2* suspension (O.D<sub>600</sub> 0.0002) and bacterial titers were determined 3 dpi. Bars represent means of 3 replicates  $\pm$  standard error. Similar trend was observed in two independent experiments. *t*-test (p-values \*\*\*<0.005).

## 2.9 Effect of R493A variant on EDS1-mediated SA-JA pathway crosstalk

In plants, the activation of immune responses involves synergistic and antagonistic interactions between hormone pathways (Pieterse et al., 2009). Crosstalk between plant hormones is essential to maintain the balance between defence and growth (Barbara N. Kunkel & Brooks, 2002; Pieterse et al., 2009). It is well established that SA and its derivatives play an important role in defence against bio- and hemi-biotrophic pathogens, whereas JA (Jasmonic acid) derivatives are active against herbivores and necrotrophic pathogens (Caarls et al., 2015). Crosstalk between SA and JA signalling is mediated at transcriptional and post-transcriptional levels and is mainly antagonistic (Caarls et al., 2015; Y. Kim et al., 2014; Pré et al., 2008). Pathogens such as *P. syringae* (Mittal & Davis, 1995) and *Hpa* (Caillaud et al., 2013) use SA-JA antagonism to their advantage by eliciting molecules such as coronatine (COR) which mimics biologically active jasmonic acid-Isoleucine (JA-Ile) to upregulate the JA pathway and suppress SA signalling (X.-Y. Zheng et al., 2012).

Because the disease resistance defect in R493A lines was not at the level of intrinsic SA signalling (Figure 2.4, 2.13), I tested whether the R493A variant was altered in EDS1-mediated SA-JA pathway antagonism. For this, I infiltrated leaves of 4-week-old plants with *Pst* DC3000 strain

expressing AvrRps4 but lacking COR (*Pst*/AvrRps4<sup>COR-</sup>). Strikingly, EDS1 variants R493A, K478R and 3K\_R which showed various levels of susceptibility against *Pst*/AvrRps4 (Figure 2.4) were fully resistant to *Pst*/AvrRps4<sup>COR-</sup> at 3 dpi (Figure 2.17). While *eds1-2* was susceptible to both the bacterial strains, it displayed 1.5 log lower bacterial growth when infiltrated with *Pst*/AvrRps4<sup>COR-</sup> compared to *Pst*/AvrRps4. There was no significant difference in bacterial titers between Col-0 or cEDS1 plants treated with *Pst*/AvrRps4 and *Pst*/AvrRps4<sup>COR-</sup> (Figure 2.17). These data suggest that wild-type (functional) EDS1 counteracts the negative effect of COR produced by the pathogen on resistance (Figure 2.17). Thus, increased susceptibility to *Pst*/AvrRps4 in the EDS1 EP-domain mutants appears to be chiefly due to reinstated negative regulation by the toxin, COR, which is normally suppressed by EDS1.

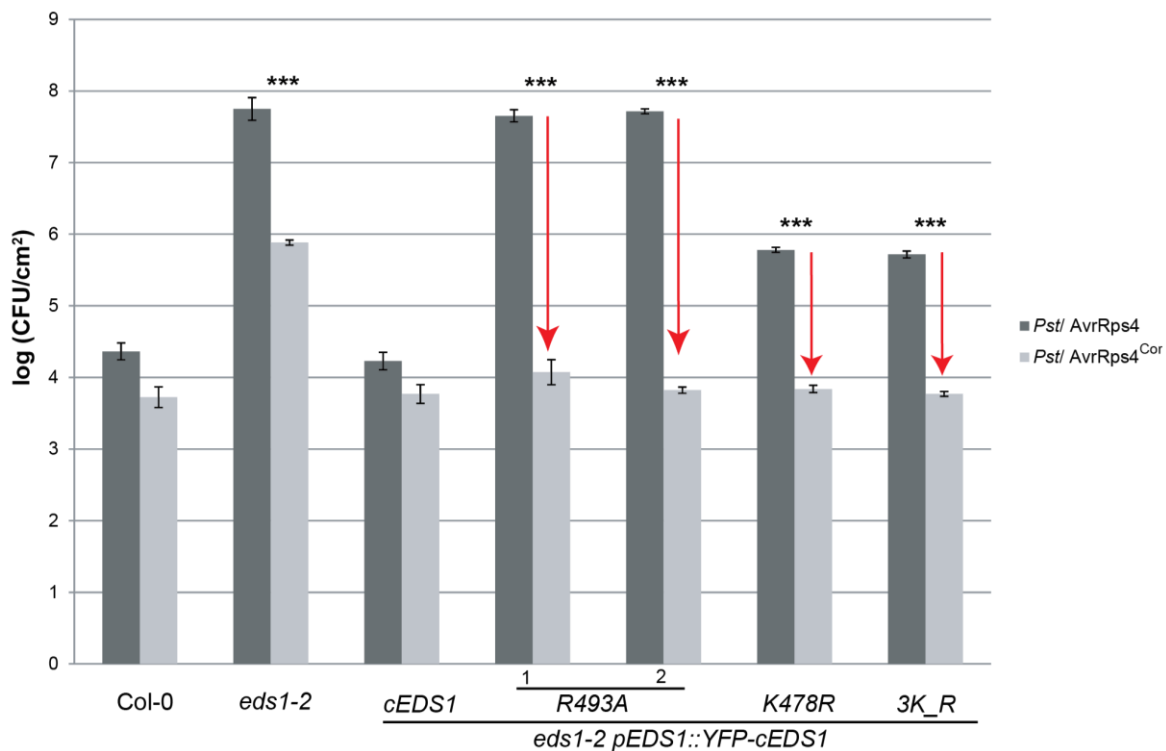


**Figure 2.17: Bacterial coronatine promotes virulence of *Pst*/AvrRps4 in EDS1 EP variants.** The indicated genotypes were infiltrated (OD<sub>600</sub> - 0.0002) with *Pst*/AvrRps4 or coronatine lacking *Pst*/AvrRps4 (*Pst*/AvrRps4<sup>COR-</sup>). Bacterial titers were determined at 3 dpi. Bars represent means of 3 replicates ± standard error. Differences between genotypes (emphasised with red arrows) were analysed using *t*-test (Bonferroni corrected, *p*-value - \*\*\*<0.001). Similar results were obtained in three independent experiments.

*P. syringae* uses COR to suppress SA upregulation in plants (Mittal & Davis, 1995; Uppalapati et al., 2007). I observed that coronatine can suppress EDS1 upregulation (Figure 2.19) during the early phase of infection (4 hpi). At 4 hpi, *EDS1* transcripts were 1.4-fold higher (*t*-test,  $p < 0.005$ ) when infected with *Pst*/AvrRps4<sup>cor-</sup> compared to *Pst*/AvrRps4. This difference also manifested into differences in EDS1 protein accumulation evident at 8 hpi when there is higher EDS1 accumulation in response to *Pst*/AvrRps4<sup>cor-</sup> as compared to *Pst*/AvrRps4 (Figure 2.18 B).

Consistently, higher EDS1 protein accumulation was observed in *Arabidopsis* plants infected with *Pst*/AvrRps4<sup>cor-</sup> across different EDS1 variant transgenic lines, suggesting that EDS1 might be a target of coronatine mediated SA-defence suppression (Figure 2.18 A). At the level of gene expression, R493A was induced to low levels at 4 hpi with both *Pst*/AvrRps4<sup>cor-</sup> and *Pst*/AvrRps4 (Figure 2.19). Significantly, at 8 hpi R493A showed similar levels of *EDS1* upregulation against *Pst*/AvrRps4<sup>cor-</sup> but significantly lower transcripts when infected with *Pst*/AvrRps4 (Figure 2.19). This indicates that suppression of EDS1 in R493A occurs between 4-8 hpi with *Pst*/AvrRps4. This suppression is due to the secretion of coronatine by *P. syringae*, since *Pst*/AvrRps4<sup>cor-</sup> lacking coronatine does not affect *EDS1* expression in R493A (Figure 2.19). This difference in *EDS1* mRNA levels manifested as lower protein in R493A compared to YFP-cEDS1 at 8hpi. However, at 24 hpi, R493A and cEDS1 protein accumulation were similar (Figure 2.18 B). In summary, the gene expression and protein accumulation data of YFP-cEDS1 and R493A prove conclusively that the difference in resistance of R493A mutant to *Pst*/AvrRps4<sup>cor-</sup> (resistant) and *Pst*/AvrRps4 (susceptible) is due to delay in EDS1 signalling which is dampened by bacterial coronatine.

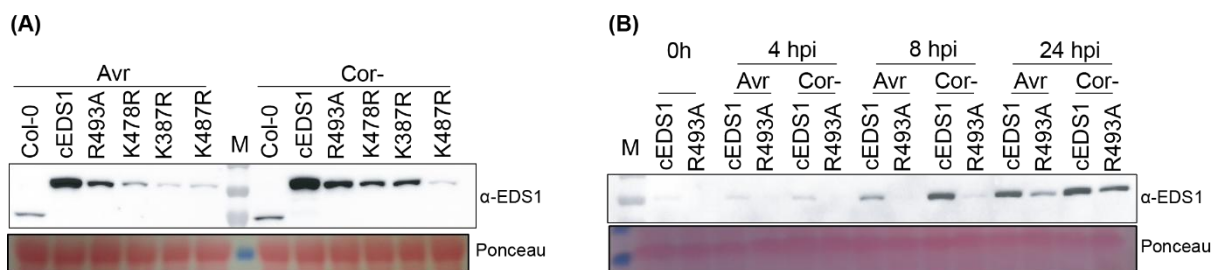


**Figure 2.18: Coronatine has negative effect on EDS1 protein accumulation upon bacterial infection.** (A) Protein accumulation at 8 hpi with *Pst*/AvrRps4 (Avr) or coronatine lacking *Pst*/AvrRps4 (Cor-) in wild-type and mutant EDS1 transgenics in *eds1-2*. (B) Time course of protein accumulation in wild-type (cEDS1) and R493A EDS1 transgenics showing EDS1 protein accumulation in uninfected (0 h) and pathogen-infected samples.

At 8 hpi, significant differences were not observed in *PAD4* transcripts of cEDS1 between *Pst/AvrRps4* and *Pst/AvrRps4<sup>cor-</sup>* (Figure 2.19). *PAD4* was not expressed in *eds1-2*, while consistently lower expression levels were observed in R493A. At 8 hpi with *Pst/AvrRps4<sup>cor-</sup>* *PAD4* transcripts were 2.5-fold higher (*t*-test,  $p < 0.05$ ) compared to *Pst/AvrRps4* infection. *PAD4* transcripts were upregulated in both cEDS1 and R493A at 24 hpi (Figure 2.19), suggesting that R493A eventually reaches levels of cEDS1 expression at later time points after infection (Figure 2.19). *PAD4* was not upregulated upon infection with *Pst/AvrRps4<sup>cor-</sup>* suggesting that resistance to *P. syringae* lacking coronatine does not require *PAD4*.

Although the effect of coronatine on JA-mediated suppression of SA signalling is well studied (X.-Y. Zheng et al., 2012), little is known about the impact of coronatine on EDS1/*PAD4* immune signalling. My results show that EDS1 EP domain variants are able to mediate full TNL resistance to *Pst/AvrRps4* in the absence of bacterial coronatine. *ICS1* and *PR1* expression patterns in cEDS1 and R493A transgenic lines were similar at 8 hpi between *Pst/AvrRps4* and *Pst/AvrRps4<sup>cor-</sup>* (Figure 2.19). In plants infected with *Pst/AvrRps4<sup>cor-</sup>*, *ICS1* transcripts were higher at 8 hpi in cEDS1 but were reduced at 24 hpi. R493A did not show any significant difference in *ICS1* expression between 8 and 24 hpi, when infected with *Pst/AvrRps4<sup>cor-</sup>*. *ICS1* transcripts in both cEDS1 and R493A at 24 hpi were higher in plants infected with *Pst/AvrRps4* (Figure 2.19). At 24 hpi infiltration with *Pst/AvrRps4* resulted in a 6-fold lower expression of *PR1* in R493A compared to cEDS1 (*t*-test,  $p < 0.005$ ) when infected with (Figure 2.19). At 24 hpi, no significant difference was observed in *PR1* levels between cEDS1 and R493A when infected with *Pst/AvrRps4<sup>cor-</sup>*. The expression of *ICS1* and *PR1* in cEDS1 was attenuated at 24 hpi in plants infected with *Pst/AvrRps4<sup>cor-</sup>*. R493A expressed *ICS1* to cEDS1 like levels, which would explain the high levels of accumulated SA at 24 hpi (Figure 2.13). It is thus likely that *Pst/AvrRps4<sup>cor-</sup>* and *Pst/AvrRps4* encounter different modes/pathways of host resistance. Intriguingly, the lack of upregulation in R493A at mRNA and protein level at early time points post infection with *Pst/AvrRps4* suggested a delay in EDS1 signalling which might explain the R493A susceptibility to *Pst/AvrRps4*.

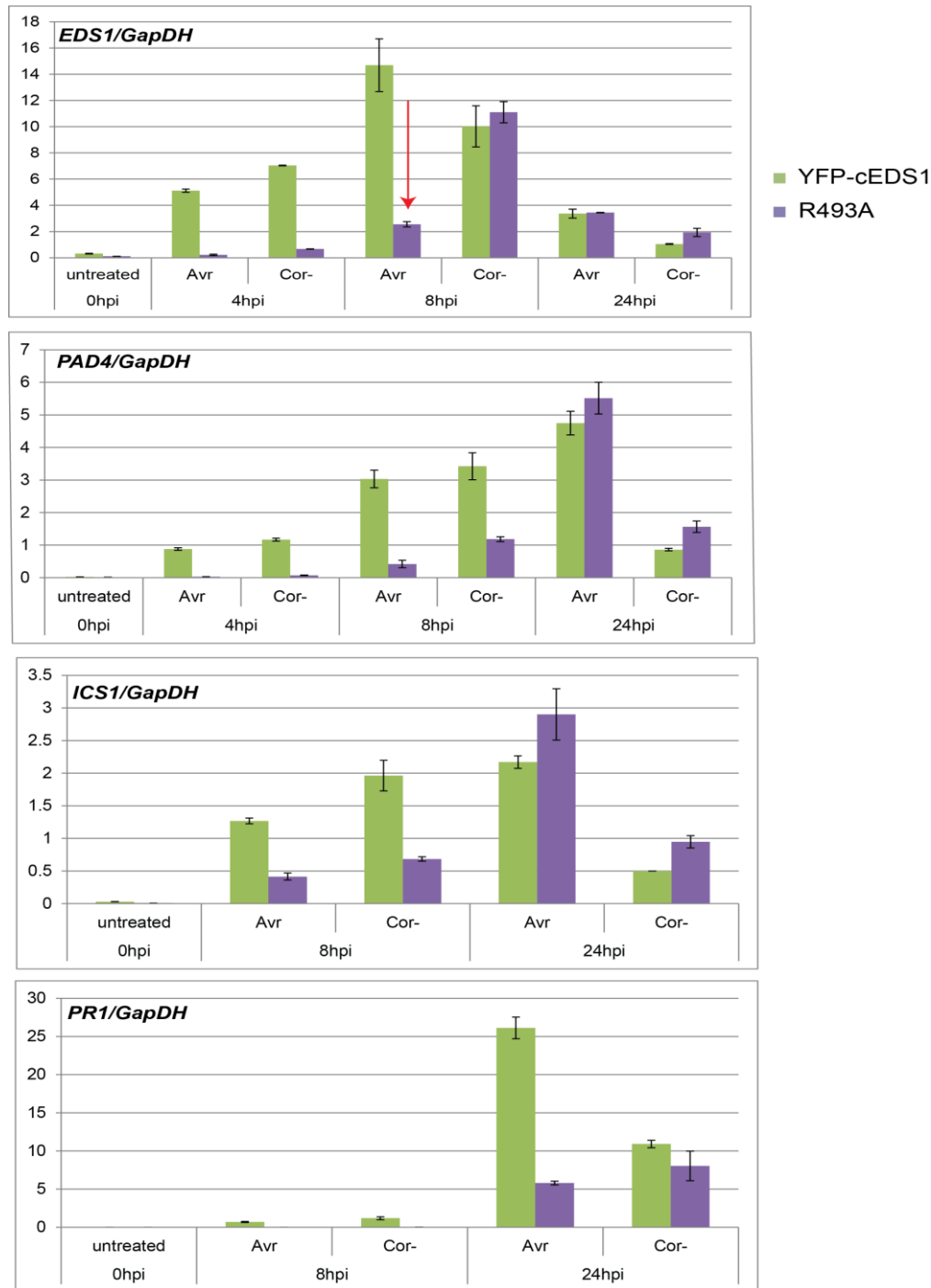


**Figure 2.19: Bacterial coronatine has a negative effect on *EDS1* transcript accumulation.** Transcript levels of *EDS1*-dependant genes in TNL-triggered resistance were measured over a 24 h time course and normalized to *GapDH*. Four-week-old leaves of wild-type (cEDS1) and R493A *EDS1* variant line (#1) were infiltrated with *Pst*/AvrRps4 (Avr) or coronatine lacking *Pst*/AvrRps4 (Cor-). Samples were collected at the indicated time points, total mRNA was extracted and quantified with qRT-PCR ( $n = 2$  biological replicates). Bars represent expression of transcripts relative to *GapDH*  $\pm$  standard error. Similar expression trends observed in 2 independent experiments.



## 2.10 R493A delays SA accumulation upon infection with *Pst*/AvrRps4

At 8 hpi with *Pst*/AvrRps4, *EDS1* transcripts were lower in R493A compared to cEDS1 (Figure 2.19). EDS1 protein levels were also reduced in R493A compared to cEDS1 (Figure 2.18). To check if this was also true for R493A-mediated SA accumulation, 4-week old plants were infiltrated with *Pst*/AvrRps4 and samples were harvested at 0, 8 and 24 hpi. In this experiment, the two independent transgenic lines of R493A (#1 and #2) were assayed alongside one line each of the partially resistant K478R and 3K\_R transgenics and resistant mutants K387R and K487R, and controls Col-0, *eds1-2* and YFP-cEDS1. As observed earlier (Figure 2.13) in response to *Pst*/AvrRps4, free SA levels in all EP domain mutants were similar to those of Col-0 and cEDS1 at 24 hpi (Figure 2.20). SA was not induced in *eds1-2* at 8 and 24 hpi (Figure 2.20). At 8 hpi, R493A SA levels were similar to *eds1-2*. However, by 24 hpi, SA levels in R493A were comparable to the YFP-cEDS1 line (Figure 2.20). These data suggest that free SA accumulation is delayed in R493A in TNL mediated ETI against *Pst*/AvrRps4.

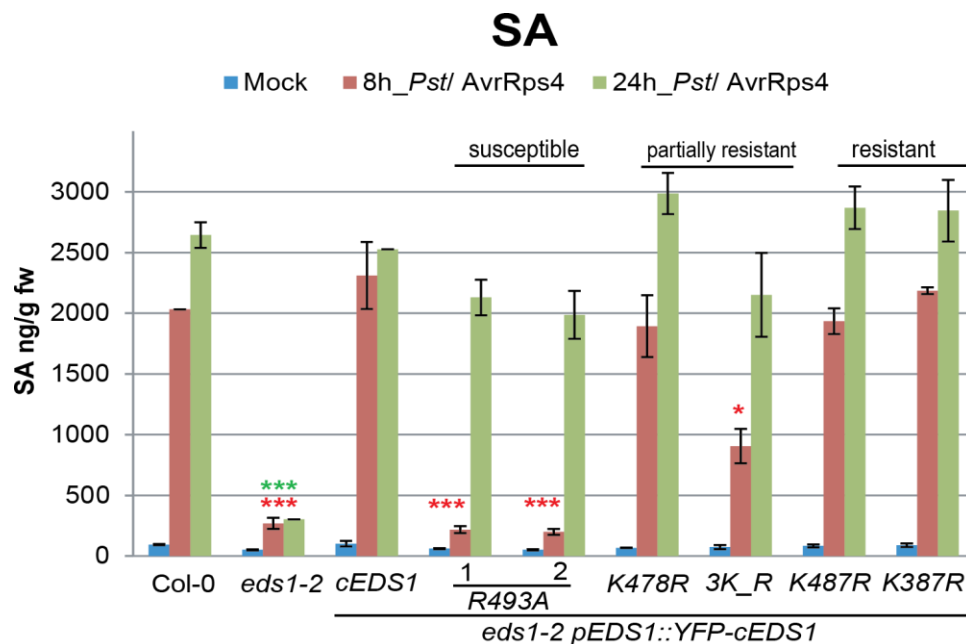


**Figure 2.20: R493A delays free SA accumulation upon *Pst*/AvrRps4 infection.** The indicated genotypes were infiltrated with mock (10mM MgCl<sub>2</sub>, blue bars) or *Pst*/AvrRps4 (O.D<sub>600</sub> 0.005) and free SA was measured at 8 (Red bars) and 24 (green bars) hpi. Bars represent means of 3 biological replicates  $\pm$  standard error. Differences between genotypes were analysed using *t*-test (Bonferroni corrected, *p*-value -\*\*\*< 0.001, \*<0.05). Green and red asterisks denote comparison between genotypes at 8 and 24 hpi, respectively. TNL (*RRS1/RPS4*) resistance phenotypes are indicated for each mutant variant.

Intriguingly, the EDS1 K478R partially susceptible variant accumulated similar SA levels as the YFP-cEDS1 control line at both 8 and 24 hpi, suggesting that K478R partial susceptibility is not due to a delay in SA induction, in contrast to R493A (Figure 2.20). Other fully resistant EDS1 EP domain lysine variants (K387R, K487R) accumulated SA to wild-type levels (Figure 2.20). Unexpectedly, the 3K\_R (lysine triple mutant) variant which shows a partially resistant phenotype similar to K478R, accumulated less free SA compared to the K478R single mutant at 8 hpi but again caught up at 24 hpi (Figure 2.20). The delay in free SA accumulation in R493A at 8 hpi with *Pst*/AvrRps4 (Figure 2.20) underpins that the disease susceptibility of R493A (Figure 2.4) is due to delay in signalling at this critical time point.

### 2.10.1 EDS1 R493A but not other EP domain mutations cause delayed SA accumulation

To assess the influence of bacterial coronatine on the ability of the EDS1 R493A EP domain variant to mobilize the SA pathway, free SA was measured in leaves after infection with *Pst*/AvrRps4<sup>cor-</sup> or *Pst*/AvrRps4 at the critical time point of 8 hpi. R493A had lower SA accumulation at 8 hpi with both *Pst*/AvrRps4<sup>cor-</sup> and *Pst*/AvrRps4 (Figure 2.21). Curiously, although SA levels were similar between *eds1-2* and R493A in response to *Pst*/AvrRps4, *eds1-2* produced lower SA when infected with *Pst*/AvrRps4<sup>cor-</sup>. All other EDS1 variants tested had higher SA accumulation upon infection with either *Pst*/AvrRps4<sup>cor-</sup> or *Pst*/AvrRps4. These data emphasize that a delay in SA accumulation is a characteristic phenotype of the EDS1 R493A mutation (Figure 2.21).

SA levels were uniformly lower in all the plant lines infected with *Pst*/AvrRps4 compared to *Pst*/AvrRps4<sup>cor-</sup>, except in *eds1-2* which showed the opposite trend (Figure 2.21). The triple Lysine mutant (3K\_R) also had low SA accumulation with both infecting strains, hinting towards an additive effect of the individual mutations on SA accumulation even though the individual mutations (except K478R) are resistant to *P. syringae*. Surprisingly, the disease resistant mutant K387R also shows lower SA accumulation upon infection with *Pst*/AvrRps4<sup>cor-</sup> (Figure 2.21), although analysis of further independent transgenic lines for these mutants is necessary to establish whether this is a robust trend.

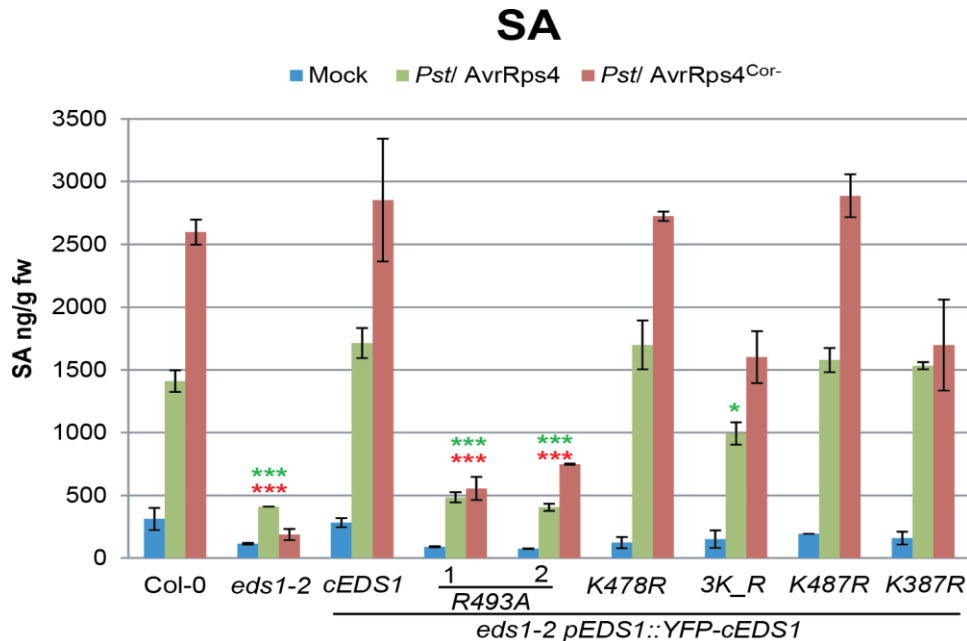


**Figure 2.21: Delay in SA accumulation is an inherent property of R493A and not affected by coronatine in TNL resistance.** Four-week old plants of the indicated genotypes were infiltrated with mock (10mM MgCl<sub>2</sub>) (blue bars), *Pst/AvrRps4*<sup>Cor-</sup> (red bars) or *Pst/AvrRps4* (green bars) (O.D<sub>600</sub> 0.005). Free SA was measured at 8 hpi. Bars represent means of 3 biological replicates  $\pm$  standard error. Differences between genotypes were analysed using *t*-test (Bonferroni corrected *p*-value -\*\*\*< 0.001, \*<0.05). Green and red asterisks denote comparison between genotypes treated with *Pst/AvrRps4* and *Pst/AvrRps4*<sup>Cor-</sup>, respectively.

### 2.11 A positive charge at R493 is essential for EDS1-mediated TNL resistance

The failure of R493A to accumulate SA in a timely manner in a TNL immune response (Figure 2.20), and the position of R493 in the putative DNA-binding region of the EP domain (Figure 2.1, Table S1), hinted that DNA or chromatin binding properties of EDS1 might be important for function. To test if R493A is compromised in immunity because it has lost the Arginine or more generally its positive charge, I mutated Arginine 493 to positively charged Lysine (R493K). In addition, an Arginine to Glutamic acid (R493E) mutant presenting a negatively charged side chain was created as a control. To test for the role of the Arginine side chain, R493 was mutated to Glutamic acid (R493E).

The ability of these mutants (R493K and R493E) to complement EDS1 resistance functions in TNL (*RPP4*) resistance to *Hpa* EMWA1 was tested in T<sub>1</sub> plants. In 10 independent T<sub>1</sub> plants tested,

R493K was able to fully complement the loss of EDS1 in *eds1-2* in TNL resistance (Figure 2.22). The R493K variant produced an HR like wild-type Col-0, while R493E was as susceptible as *eds1-2*, seen by free growing *Hpa* hyphae (Figure 2.22). I concluded that a positively charged amino acid at position 493 rather than specifically an arginine residue is essential for EDS1-mediated immune signalling.

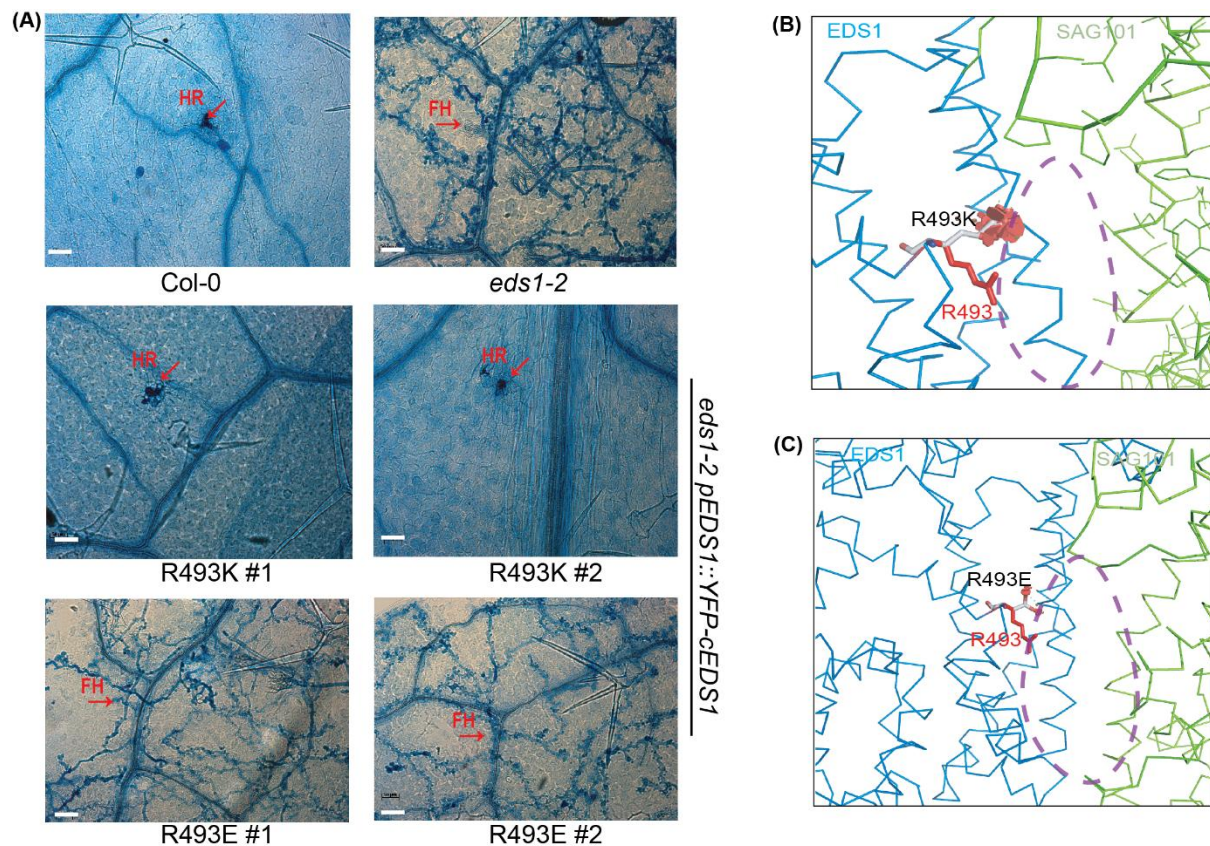


**Figure 2.22: A positive charge at aa 493 is essential for EDS1 mediated TNL-resistance.** (A) *RPP4*-mediated TNL resistance phenotypes of 3-week-old control and  $T_1$  transgenic lines (*eds1-2*) expressing R493K and R493E variants of EDS1. *Hpa* EMWA1-infected leaves were stained with trypan blue at 5 dpi. The scale bar represents 50 μm. HR, hypersensitive response; FH, free hyphae; TN, trailing necrosis. Images are representative of 10 independent transgenic lines from a single experiment in  $T_1$ . (B) Mutation of R493 (red stick) to lysine (K) or (C) glutamic acid (E), is modelled onto the EDS1-SAG101 structure (blue-green). The cavity formed by the heterodimer is depicted as a purple circle (dashed).

## 2.12 Transcriptome analysis of the R493A defence response

The EDS1 EP domain mutant R493A delays SA upregulation and shows different resistance phenotypes in the presence or absence of coronatine. To study when and how the R493A variant disturbs EDS1 mediated immunity, a transcriptome analysis by RNA-sequencing (RNA-seq) was performed. Four-week old Col-0, *eds1-2*, cEDS1 and R493A (line #1) plants were infiltrated with *Pst/AvrRps4* and samples collected at 0 (uninfiltrated), 4, 8 and 24 hpi. 21-32 million reads per sample were generated in three independent biological repeats with 83-98% of the sequences aligning to the *A. thaliana* genome (Table S3). The questions that this study aimed to answer are:

1. Is there a global defect in EDS1 transcriptional reprogramming caused by the R493A mutation?
2. R493A accumulates SA and is upregulated post infection with *Pst/AvrRps4* but is as pathogen susceptible as *eds1-2*. How similar then is the transcriptional profile of R493A to an *eds1-2* null mutant?
3. Which EDS1 reprogrammed pathways or genes are affected by the R493A mutant?

RNA-seq data were initially compared to study general patterns of differentially expressed genes (DEGs) across genotypes (Table S5) and time points (Table S4). Transcriptome profiles across the lines tested (Col-0, *eds1-2*, cEDS1, R493A) at the time points mentioned showed 20573 differentially expressed genes (log 2 FC (fold change),  $p$ -value<0.05). 13667, 12389 and 15968 genes were differentially expressed at 4, 8 and 24 hpi with *Pst/AvrRps4*, respectively when compared to the untreated samples across all the lines. As expected, broad patterns suggested that apart from (60 DEGs) the transgenic line cEDS1 behaved like Col-0 (Figure 2.23). Major differences in transcriptome were observed between *eds1-2* and cEDS1 (5499 DEGs, Table S5). R493A showed expression patterns closer to *eds1-2* at early time points and behaved weakly like cEDS1 at 24h (Figure 2.23). DEGs clustered into 18 groups based on the expression patterns at different time points (Figure 2.23). Though differentially expressed genes were seen at all time points (Table S4), major transcriptional differences were seen at 8 and 24hpi across all genotypes (Figure 2.23).

---

The four samples tested were grouped in six combinations (cEDS1/Col-0, cEDS1/*eds1-2*, cEDS1/R493A, *eds1-2*/Col-0, *eds1-2*/R493A and Col-0/R493A). Analysis of the six combinations across four time points tested, revealed that genes expressed at 0 h and 4 h did not differ in any of the six combinations. 44 DEGs were observed at 0h, since these were differentially expressed in all the four genotypes and were either uncharacterized genes or map back to TE, these were ignored (Figure 2.23). At 4 h, 53 DEGs were observed across genotypes suggesting that major transcriptional reprogramming had not happened at this early time point (Figure 2.23).



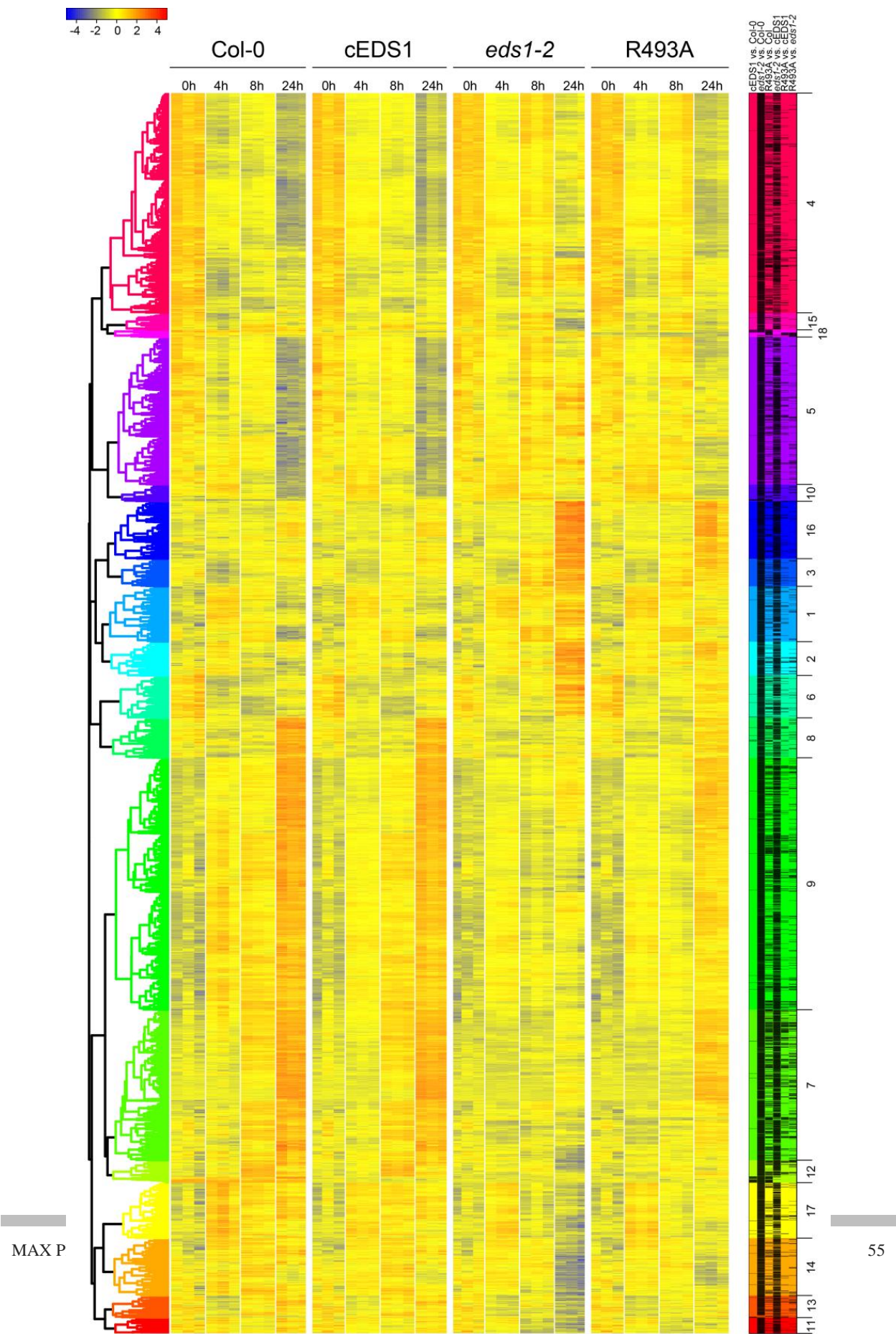


**Figure 2.23: Global expression profile of EDS1 wild-type (cEDS1) and R493A transgenic lines compared to Col-0 and the *eds1-2* null mutant.** A heat map shows genes expressed in the indicated genotypes post infection with *Pst*/AvrRps4 at 0, 4, 8 and 24 hpi. ( $p$ -value < 0.05, > 2-fold change). Right panel shows individual comparison between genotypes and individual DEGs (differentially expressed genes) are marked in black. Genes were separated into 18 clusters based on similarities in expression profiles across time points among the genotypes analysed. The left panel depicts a dendrogram highlighting the similarity between genes expressed within a cluster and distances between closely related clusters.

The few genes that were differentially expressed at 4 h between R493A/cEDS1 or between R493A/*eds1-2* were weakly differentially expressed with a low  $p$ -value and less than 2-fold change. Genes that were differentially expressed at 4 h show a pattern similar to expression in Col-0, thus are most likely genes that are affected by the mutant background of *eds1-2* (Figure 2.23). Because the cEDS1 and R493A transgenes were expressed in an *eds1-2* background, these genes show up as differentially expressed but are lost in the comparison between R493A/*eds1-2* (5 DEGs) or R493A/cEDS1 (7 DEGs).

Transcriptional differences between genotypes manifested most clearly at 8 h and were further reinforced at 24 h (Figure 2.23). At 8 h and 24 h there were no major DEGs between Col-0 and cEDS1 (Figure 2.23), corroborating with their complete disease resistance phenotypes (Figure 2.4). By contrast, R493A showed an expression pattern that was most similar to *eds1-2* at 8h with only 14 DEGs (Figure 2.23). This indicates that at the critical point of 8 hpi with *Pst*/AvrRps4, R493A behaves like an *eds1* null mutant. Strikingly, at 24 h R493A had an expression pattern that was markedly different from *eds1-2* and cEDS1. This suggests that R493A expresses defence genes later than the cEDS1 line and at 24 h has not caught up. This might explain why R493A displays wild-type SA accumulation at 24 hpi but not at 8 hpi with *Pst*/AvrRps4 (Figure 2.20).

In a complimentary analysis of the Col-0, *eds1-2*, cEDS1 and R493A transcriptomes, I plotted all DEGs on a multidimensional scatter plot (MDS). The MDS plot revealed that the pathogen unchallenged samples (0 h) are scattered across different replicates, likely due to environmental and between-experiment variations (Figure 2.24). At 4 hpi all the samples clustered into one group, although Col-0 and cEDS1 showed a minor tendency to cluster away from *eds1-2* and R493A, suggesting that although no major difference in expression is manifested, early transcriptional changes were being mobilized in the wild-type lines (Figure 2.24). Major grouping differences



were evident at 8 h, at which point replicates of Col-0 and cEDS1 clustered together and away from R493A and *eds1-2*. While R493A clustered with *eds1-2* at 8 h, by 24 h it clustered separately and had moved away from *eds1-2* towards cEDS1 but did not fit with cEDS1 and Col-0 cluster (Figure 2.24). These results point to a general delay in transcriptional reprogramming in R493A compared to the wild-type immune response. The delay rather than the inability to respond might be the reason for the susceptibility of R493A against *Pst*/AvrRps4. The clustering analysis thus assisted in identifying a critical time frame for EDS1 immune functions to be transduced to effective resistance.

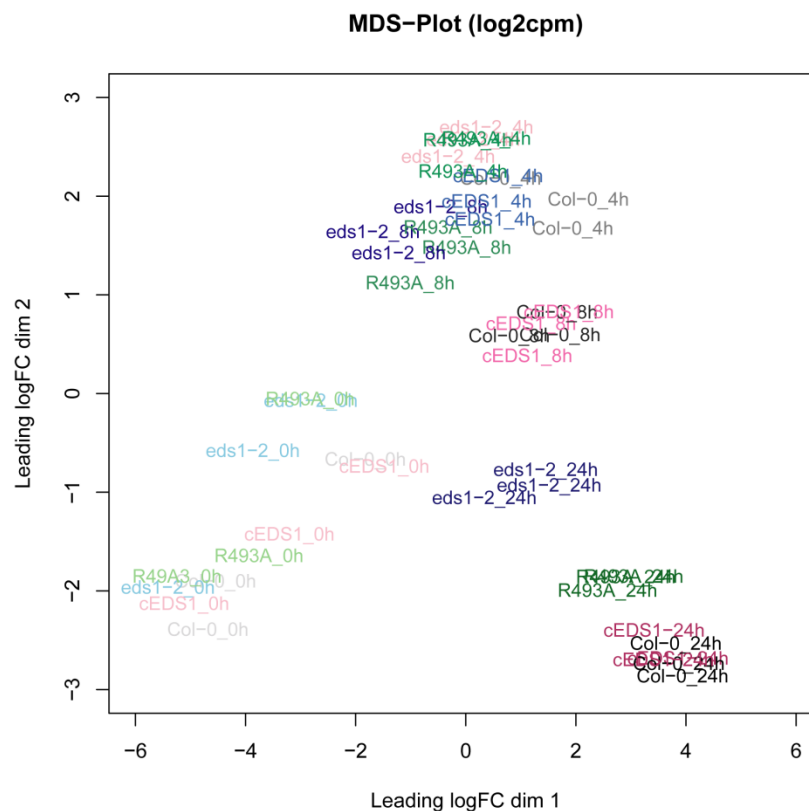


**Figure 2.24: Mutation of R493A delays EDS1 dependent transcriptional reprogramming in ETI.** A multidimension scatter plot of differentially expressed genes in the indicated genotypes across tested time points. Clustering of biological replicates and the differences between treated samples at different time points is shown based on genotype. Major transcriptional differences start appearing at 8 hpi in the form of two clusters 1) cEDS1 & Col-0 and 2) R493A & *eds1-2*. By contrast, at 24 hpi R493A separates from *eds1-2*.

The aim of this analysis was to study differences caused by the EDS1 R493A variant in defence transcriptional reprogramming. Because cEDS1 largely phenocopied Col-0 (Figure 2.4, 2.6), the absolute expression changes in the other three genotypes (cEDS1, R493A, *eds1-2*) were normalized to the changes in Col-0 across all time points and fitted to a single scale. Genewise normalization of all lines with Col-0 provided crucial insights on the expression profile of R493A in comparison with either cEDS1 or *eds1-2* (Figure 2.26).

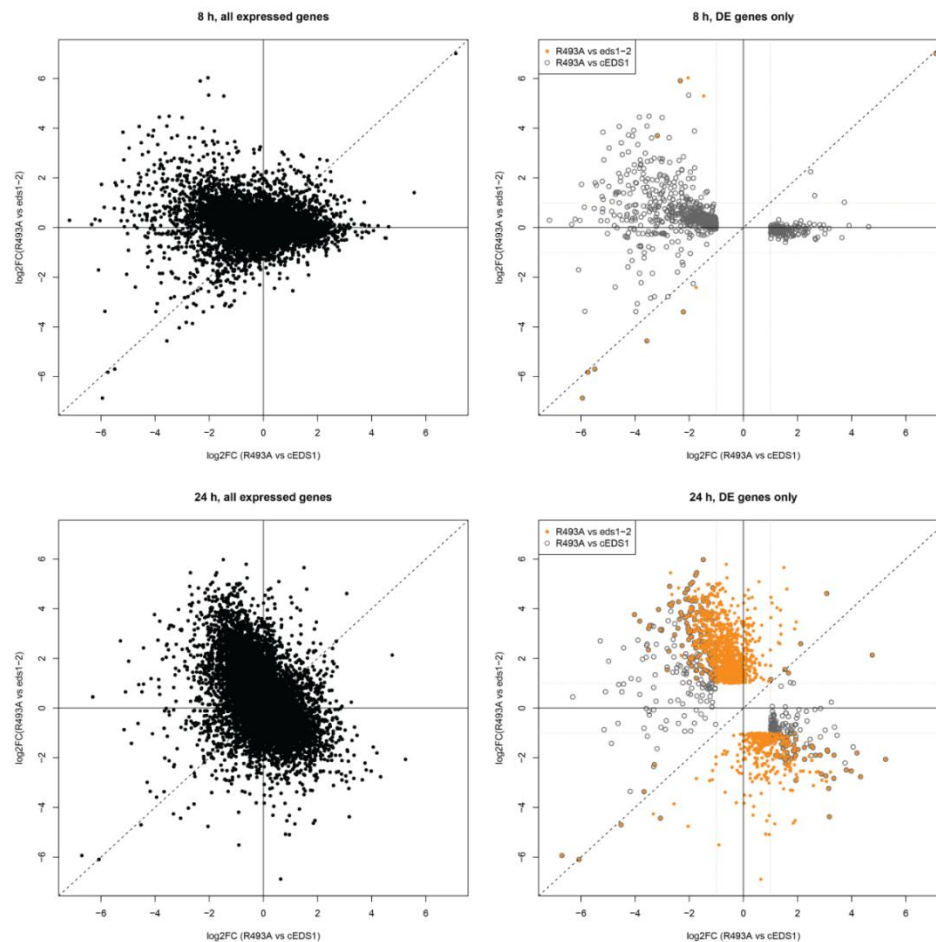


**Figure 2.25: Comparison of differential gene expression between R493A, cEDS1 and *eds1-2* at 8 h and 24 hpi.** A 2-dimensional scatter plot compares R493A vs *eds1-2* against R493A vs cEDS1 at 8h and 24 hpi with *Pst*/AvrRps4. Plots on the left (solid black dots) represent all expressed genes and show that at 8h genes cluster around the *x*-axis of *eds1-2* whereas at 24h the expressed genes cluster towards *y*-axis. Plots on the right (coloured) show DEGs between R493A vs *eds1-2* (solid orange) and R493A vs cEDS1 (open gray dots) at 8h and 24h. Differentially expressed genes represented have been filtered with a log two-fold change cut-off. Note the marked difference between DEGs at 8h and 24h.

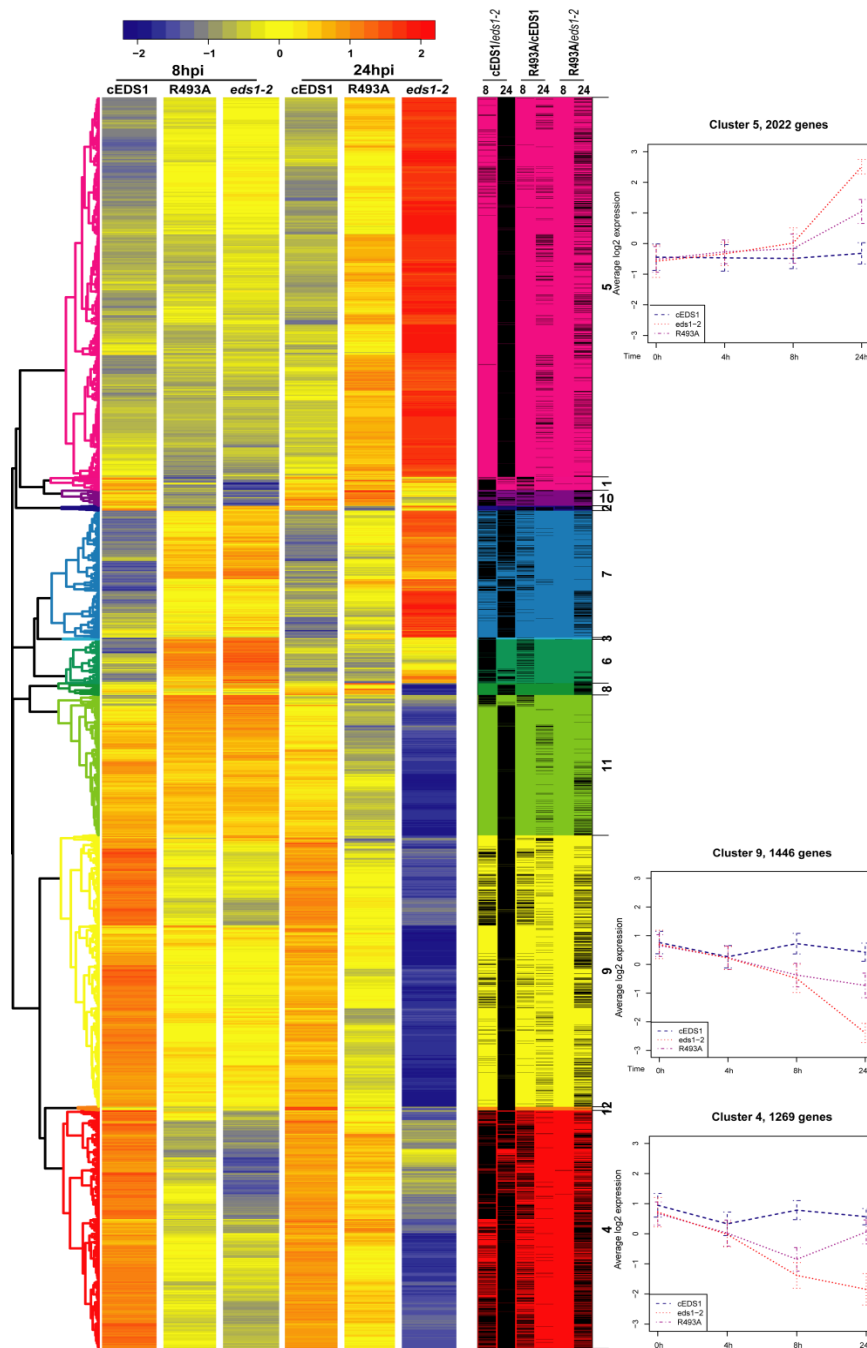


**Figure 2.26: Gene expression profiles of cEDS1, R493A and *eds1-2* normalized to Col-0 at 8 and 24 hpi with *Pst/AvrRps4*.** The heatmap shows genes expressed in the indicated genotypes normalized to Col-0 post infection with *Pst/AvrRps4* at 8 and 24 hpi. ( $p$ -value < 0.05, > 2-fold change). The right panel shows individual comparisons between genotypes and individual DEGs are marked in black. Genes separate into 12 clusters based on the similarities in expression profiles. Boxes on the far right depict clusters 5, 9 and 4 and their general expression patterns. The left panel depicts a dendrogram highlighting similarities between genes expressed within a cluster and distances between clusters.

Genewise normalization was done across three biological replicates and normalized to expression of each gene in Col-0 and a heatmap was created based on relative expression values. The heatmap (Figure 2.26) is colour-coded based on the average differential expression between cEDS1, R493A and *eds1-2*, and does not provide a comparison between these genotypes and Col-0. Thus, upon averaging differential expression of up-/down- regulated genes is enhanced and cEDS1 would show differential expression compared to Col-0 instead of the expected non-differential expression (0-fold change). This is evident in the normalized heat map with cEDS1 showing differential expression and a very small number of genes are not differentially expressed (yellow) as the comparison is now essentially between cEDS1 (resistant), *eds1-2* (susceptible) and R493A (susceptible but partially signalling competent) (Figure 2.26). This approach emphasizes differences between R493A/*eds1-2* and R493A/cEDS1. In addition to highlighting the critical time point at which the R493A immune response shifts from *eds1-2*-like to cEDS1-like, this approach should help to identify particular genes or pathways that determine a robust EDS1-mediated immune response.

Post-normalization to Col-0, all genes expressed in the R493A variant tended to cluster with *eds1-2* (Figure 2.25, top left) at 8 hpi. Only 12 DEGs (Figure 2.25, top right panel- orange dots) were found between R493A and *eds1-2* at 8 hpi. These included *EDS1* and *PBS3* (AvrPphB susceptible 3; early marker for EDS1 dependent immune resistance). By contrast, 1021 genes (open grey dots) were differentially expressed between R493A and cEDS1. GO (gene ontology) enrichment analysis (agriGO, <http://bioinfo.cau.edu.cn/agriGO/analysis.php>) clustered these genes into two major groups of defence processes and chloroplast organization. The trend was reversed at 24 h with 153 DEGs between R493A and cEDS1 and 2053 genes differentially expressed between R493A and *eds1-2*, which is evident by the increase in orange dots at 24 h (Figure 2.25, bottom right). The same trend was seen in all the genes expressed at 24 h, with a marked shift from the *x*-axis (R493A vs *eds1-2*) to *y*-axis (R493A vs cEDS1). Interestingly, not all the expressed genes aligned perfectly with the *y*-axis, reinforcing the notion that at 24 h R493A does not behave like cEDS1.

DEGs between R493A and cEDS1 belong mainly to the category of transcriptional regulation enriched with transcription factors such as bHLH (basic helix-loop-helix), TCPs etc. The DEGs between R493A and *eds1-2* belong to defence responses, apoptosis and innate immunity. Overall

differences in DEGs between cEDS1 and *eds1-2* was pronounced at both 8 h (1880 DEGs) and 24 h (5993 DEGs).

6667 genes were significantly differentially expressed between the three genotypes (cEDS1, *eds1-2* and R493A) post normalization to Col-0, compared to the 20573 DEGs before normalization. Normalized gene expression data while reinforcing the trends observed in previous analysis (R493A is delayed at 8 h and shows intermediate expression at 24 h) provided deeper insights into the expression patterns of R493A (Figure 2.26). This also shows that normalization with Col-0 does not affect the expression patterns observed prior to normalization. The 6667 DEGs grouped into 12 clusters based on the expression pattern at each time point (Figure 2.27). At 8 h, though R493A clustered with *eds1-2* (Figure 2.26), it shows weaker expression across 6641 genes expressed. It is also very clear that at 8 h, R493A and *eds1-2* have similar expression patterns with just 2 genes differentially expressed (*EDS1* and *PBS3*), whereas cEDS1 and R493A have a large number of genes differentially expressed (Figure 2.25, right panel).

At 24 h, the expression pattern of R493A shifts and it shows intermediate expression compared to either cEDS1 or *eds1-2*. Due to normalization with Col-0 and averaging of relative expression, the up-/down- regulated genes in *eds1-2* are enhanced as observed by the extreme expression levels in the heatmap (Figure 2.26). While the number of DEGs between cEDS1 vs *eds1-2* and R493A vs *eds1-2* increased at 24 h (Figure 2.25, right panel), the number of DEGs between cEDS1 and R493A decreased reinforcing the ability of R493A to function weakly like cEDS1.

The differences in expression patterns which grouped into 12 clusters are represented in Figure 2.27. Clusters 1, 2, 3, 10 and 12 were removed from further analysis as they did not have any significant GO enrichment. Moreover, these 5 clusters combined together represented only 210 out of 6667 DEGs.

In cluster 8, R493A shows similar expression pattern as cEDS1, suggesting that genes making up this cluster are not responsible for the susceptible phenotype of R493A against *Pst*/AvrRps4 (Figure 2.27). Clusters 6, 7 and 11 consist of genes involved in developmental or metabolic processes, which though interesting in itself is not the focus of my study (agriGO). Thus, these clusters were not analysed further for R493A-dependent immune functions but might provide a

good basis for studying the processes affected by the mutation. A major chunk of (4737/6667) DEGs are grouped into three clusters 4, 5 and 9 (Figure 2.26 & 2.27).

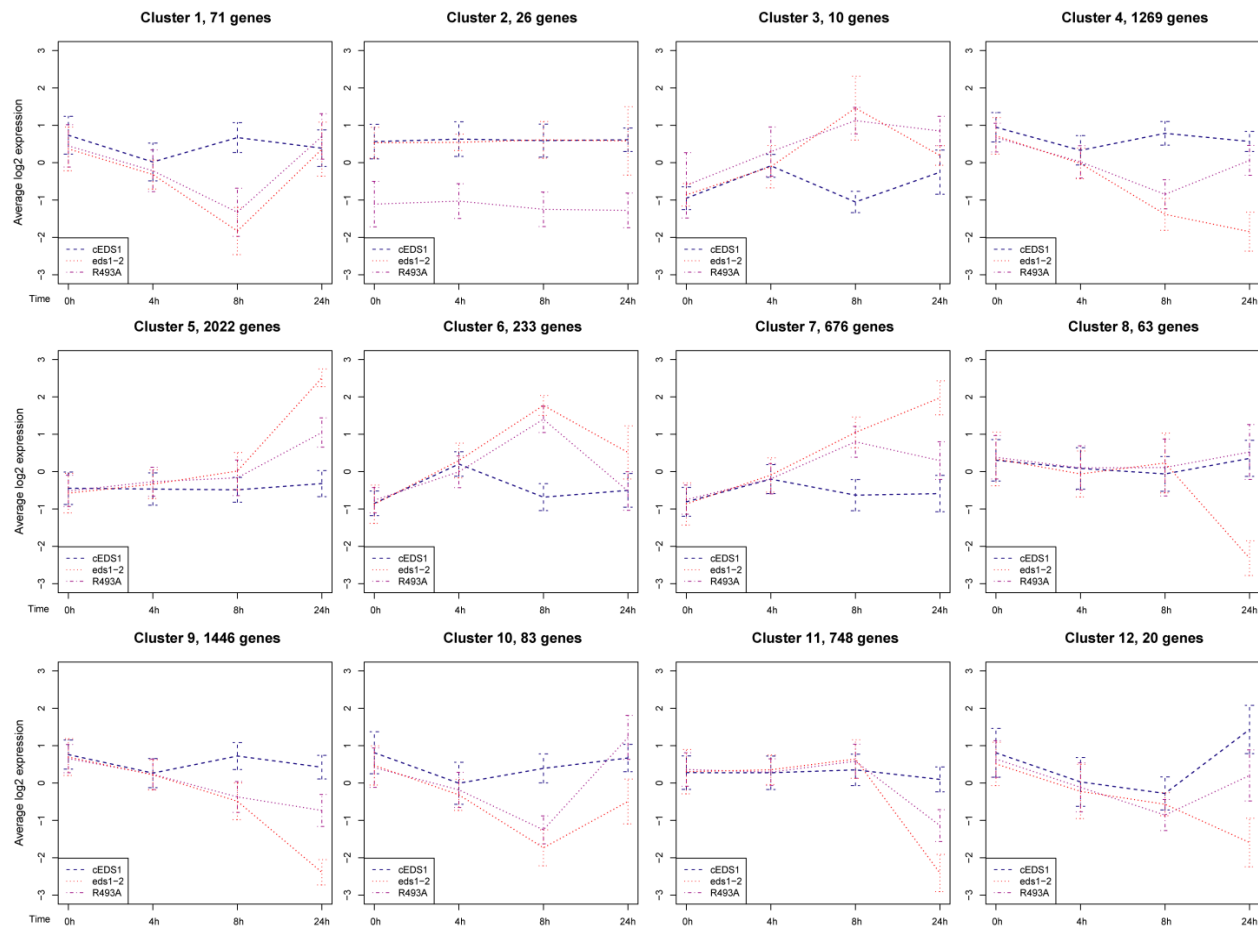


**Figure 2.27: Clustering of DEGs at 8 and 24 hpi with *Pst*/AvrRps4.** Differentially expressed genes grouped into 12 clusters after normalizing the expression of each genotype to the expression of Col-0 at the tested time points.

Cluster 5 comprises of genes that show similar expression pattern at 8 h between cEDS1, R493A and *eds1-2* but at 24 hpi both R493A and *eds1-2* move away from cEDS1. In cluster 5 *eds1-2* shows extreme variation with almost 3 log<sub>2</sub>FC from cEDS1 (Figure 2.27). Cluster 5 consists of genes chiefly involved in metabolic and biosynthetic processes for eg., *components of the 40s and 60s ribosomal unit*. Clusters 4 and 9 are comprised of genes that are similarly regulated at 8 h between R493A and *eds1-2* but markedly different from cEDS1 At 24 hpi genes in R493A express

similar/intermediate to cEDS1 but clearly different from *eds1-2*. This pattern of gene expression would fit the pathogen phenotypes observed earlier where R493A behaves like a *compromised* form of cEDS1 at late time points (Figure 2.20) and like *eds1-2* at early time points (Figure 2.24).

Cluster 4 is comprised of 1269 DEGs with significant enrichment of genes involved in immune responses, apoptosis and protein modification (Table S6). This cluster is thus most interesting in terms of EDS1 dependent immune functions that might have been compromised by the mutant R493A. Upon deeper analysis it was found that only 3 genes were differentially expressed between R493A and *eds1-2* at 8 h which including *EDS1*; this number increased to 705 DEGs at 24 h underpinning the ability of R493A to respond to biotic stimuli albeit belatedly (Figure 2.28). This cluster represents genes associated with EDS1-dependent immune signalling such as *PAD4*, *FMO1*, *ICS1*, *PR1*, *RPS4* etc.

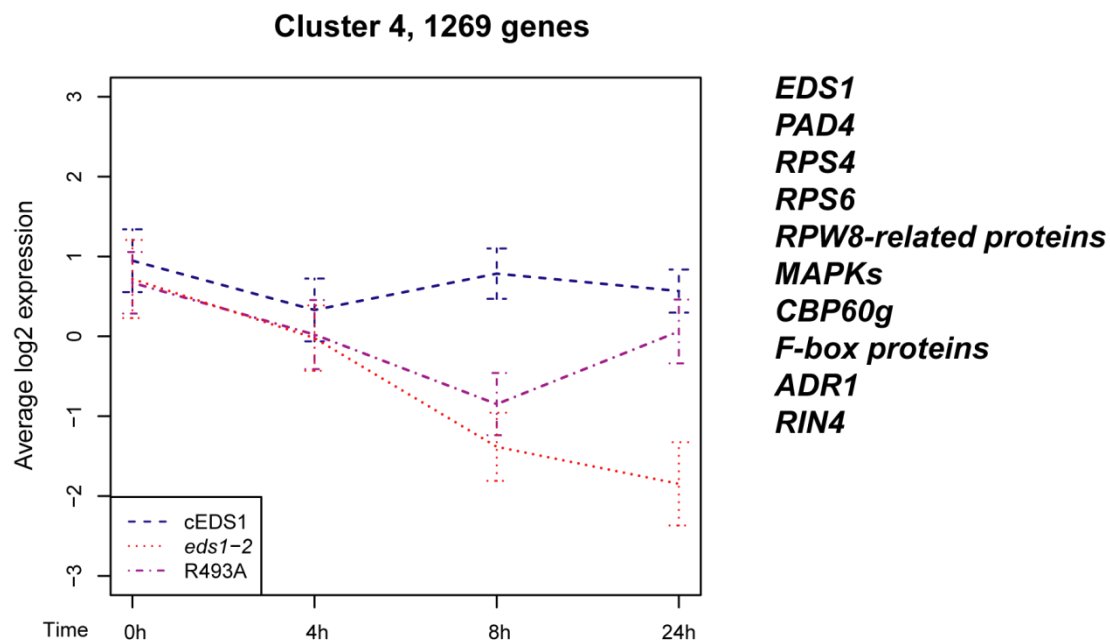


**Figure 2.28: Cluster 4- R493A dependent delayed genes that catch up with cEDS1.** 1269 DEGs in cluster 4. Cluster 4 comprises of R493A dependent genes that are differentially expressed weakly from *eds1-2* at 8 hpi and segregate from *eds1-2* at 24 hpi to catch up with cEDS1. Representative genes are listed on the right panel.

Cluster 9 comprising of 1446 DEGs is chiefly enriched with genes involved in signalling transduction and ubiquitin dependent processes (Figure 2.29). This cluster provides an interesting facet of R493A dependent immune functioning upon infection with *Pst*/AvrRps4. It is similar to cluster 4 in its tendency to be similar to *eds1-2* at 8 h (0 DEGs) (Table S6) but unlike cluster 4, cluster 9 genes (of R493A) do not catch up with cEDS1 but maintain a steady level of expression at 24 h whereas genes in *eds1-2* are significantly downregulated (3 log<sub>2</sub>FC). This cluster might thus represent genes that are critical in determining the influence of EDS1 dependent immune reprogramming, since cEDS1 also does not show major transcriptional differences between 8 and 24 hpi (Figure 2.29). This cluster is comprised of genes that form part of major proteasomal degradation pathways such as components of 26s proteasome, SUMO conjugating enzymes, E2 Ub-conjugating enzymes, E3 ligases etc. This cluster might help in understanding how EDS1 affects hormonal cross talk by modulating protein turnover and de-repression of immune suppressors.

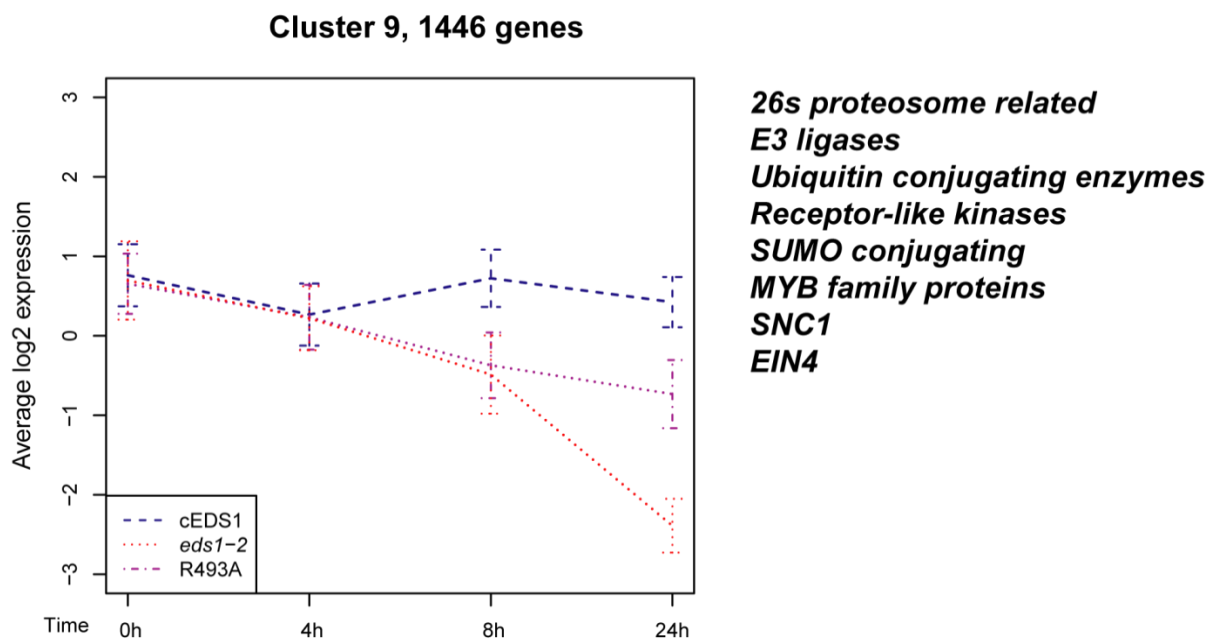


**Figure 2.29: Cluster 9- R493A dependent delayed genes that do not catch up with cEDS1.** 1446 DEGs in cluster 9 represent R493A dependent genes that show *eds1-2* like expression pattern at 8 hpi but unlike *eds1-2* are not downregulated at 24 hpi. Representative genes are listed on the right panel.



### 3. Structure-guided analysis of EDS1 self-association

#### 3.1 Introduction

EDS1 homodimers have been reported in Y2H (Feys et al., 2001; Wagner et al., 2013) and in FRET assays (Feys et al., 2005) but direct interaction by protein pulldowns has not been reported. PAD4 and SAG101 homodimers have not been observed in-planta or in transient assays, suggesting that EDS1 homo-dimerization in transient assays might not be an artefact. Recombinant EDS1 was consistently eluted at a higher molecular weight of 142 kDa (as compared to 72 kDa for a monomer) hinting towards EDS1 homodimers (Rietz et al., 2011). The biological significance of EDS1 homodimers in plant innate immunity and their existence in physiological conditions is unknown. Overexpression of nucleo-cytoplasmic EDS1 does not lead to autoimmunity (N. Peine-MPIPZ, unpublished) and plants overexpressing EDS1 are susceptible to *Hpa* CALA2 (*RPP2*) in the absence of PAD4 and SAG101 (Wagner et al., 2013).

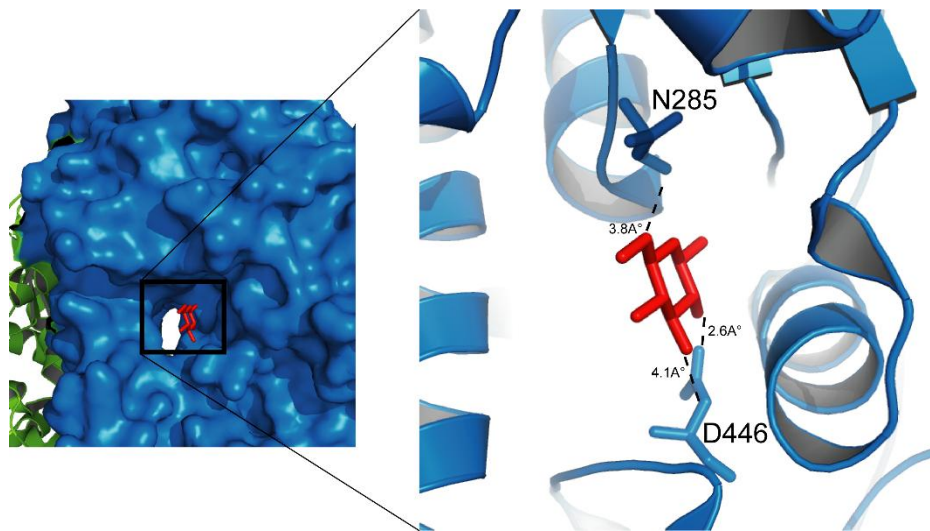


**Figure 3.1: EDS1 glucose binding pocket.** A Glucose molecule (red stick) sitting in the pocket of EDS1-SAG101 (blue-green) is highlighted. **Zoom in.** H-bond formation between glucose, aspartic acid (D446) and asparagine (N285) residues are shown.

I tested the hypothesis that EDS1 homomers exist in immune unchallenged conditions and upon pathogen challenge leading to upregulation of PAD4 and SAG101, the balance is shifted from

EDS1-EDS1 homodimers to EDS1-PAD4 or EDS1-SAG101 heterodimers which are essential for transcription reprogramming leading to immune signalling (Wagner et al., 2013).

*Arabidopsis* PAD4 and SAG101 compete for the same surface of EDS1 (Wagner et al., 2013), while a ternary complex of EDS1-PAD4-SAG101 has been observed (Zhu et al., 2011) by transient expression in *N. benthamiana*. This led to the search for an alternative site for EDS1-EDS1 dimerization.

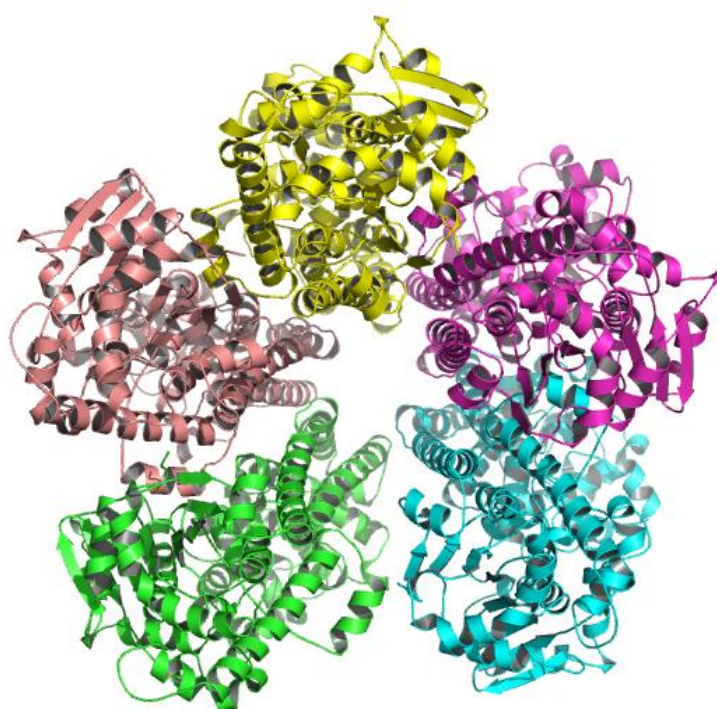


**Figure 3.2: EDS1 pentamer model.** A putative model of EDS1 self-association based on EDS1-SAG101 crystal structure. EDS1 chain from the crystal structure was fitted onto the SAG101 chain, followed by deletion of the SAG101 chain in the crystal structure. This process was repeated thrice to obtain a pentamer model of EDS1 without any obvious steric hindrance (modified from K. Niefind, University of Köln).

Analysis of *Arabidopsis* EDS1-SAG101 crystal structure revealed a small pocket, on the opposite side of EDS1-SAG101 interface, which could accommodate a glucose molecule (Figure 3.1). This glucose molecule was in close proximity to two residues, aspartic acid - D446 (2.6Å) and asparagine - N285 (3.8Å) (Figure 3.1). The  $\alpha$ -helix H of EDS1 (Wagner et al., 2013) would fit perfectly in this pocket (Figure 3.2). Based on EDS1-SAG101 crystal structure a simplistic model was generated by superimposing EDS1-SAG101 heterodimer structure multiple times on itself.

The formation of a pentamer could be a way of stabilizing EDS1 self-associations. Thus, it could also be conceived that a glucose-like small molecule could play an important role in shifting the balance from EDS1 homomers to EDS1-PAD4 or EDS1-SAG101 heterodimers. To test this hypothesis, I mutated N285 and D446 to disturb the interaction between these residues and the glucose molecule. The working hypothesis was that abolition of the interaction would either lead to loss of EDS1-EDS1 interaction and/or affect the dynamics of EDS1-PAD4 or EDS1-SAG101 thereby leading to compromised immune functions.

### 3.2 Results and discussion

In Y2H assays, EDS1 mutants N285A, N285D and D446A maintained interaction with EDS1 (Figure 3.3) suggesting that this pocket was not responsible for EDS1 self-associations. This observation would fit with the observation of (Feys et al., 2001) that C-terminal (351-623) of EDS1 was sufficient for homo-dimerization. Conversely, a 35-amino acid shorter C-terminal EP domain (385-623) was found to be unstable in Y2H and in *Arabidopsis* (Wagner et al., 2013).

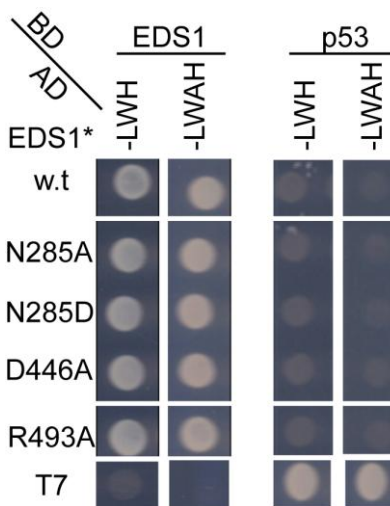


**Figure 3.3: N285 and D446 variants maintain interaction with EDS1.** Y2H interactions between activation domain (AD) fusions of EDS1 variants and full-length EDS1 binding domain (BD) fusion. The susceptible mutant R493A from EDS1 EP domain is shown as an additional control. Yeast viability, weak (-LWH) or strong (-LWAH) protein interactions are shown. BD-p53 and AD-T7 were used as negative controls in the GAL4 matchmaker Y2H system.

To assess the effect of these mutations on the immune functions of EDS1, their ability to resist the oomycete *Hpa* CALA2 recognized by the TNL *RPP2* was tested. Expectedly, *eds1-2* null mutant was susceptible as seen by extensive free hyphal growth, while Col-0 was resistant showing HR (Figure 3.4). Mutations in N285 and D446 did not affect EDS1 TNL-resistance functions against *Hpa* CALA2 as seen by HR (Figure 3.4).

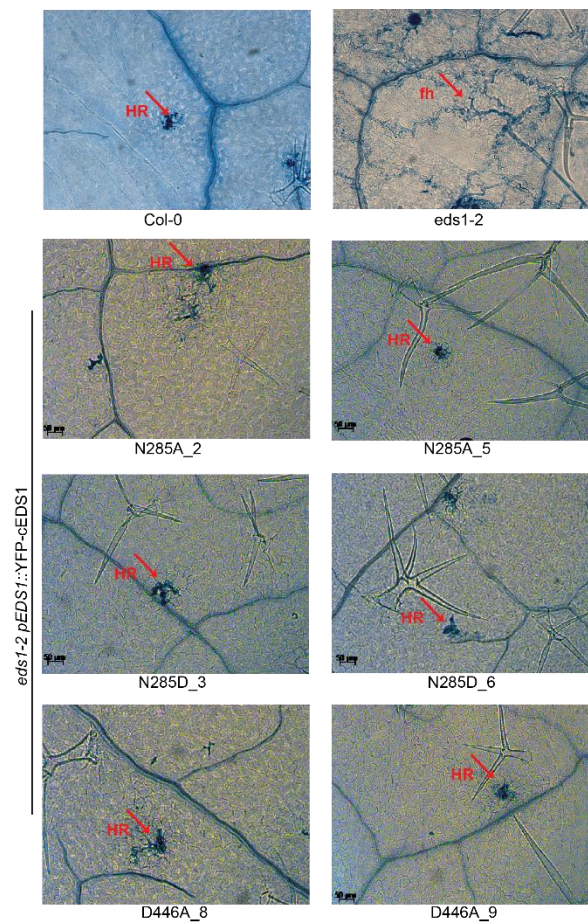


**Figure 3.4: Plants expressing N285 and D446 variants are competent in triggering TNL (*RPP2*) resistance to *Hpa* CALA2.** *RPP2* resistance phenotypes of 3-week-old control and homozygous ( $T_3$  generation) independent transgenic lines expressing N285A, N285D and D446A variants of EDS1. *Hpa* CALA2 infected leaves were stained with Trypan Blue at 4 dpi. The scale bar represents 50  $\mu$ m. Images are representative of 12 leaves from two different experiments on two independent transgenic lines. HR-hypersensitive response; fh-pathogen free hyphae.

Putative dimerization of EDS1 might have some immune functions like maintaining a basal inactive state or guarding against ectopic activation of competent immune signalling complexes. By contrast, overexpression of EDS1 does not activate immunity negating a role of EDS1 homomers in plant immune signalling (Wagner et al., 2013). The inability of EDS1 to interact with and pull down itself from plant extracts (AG-Parker, MPIPZ) also points to the possibility that EDS1 interaction with itself in Y2H might be an artefact. Interestingly, overexpression of exclusively nuclear localized EDS1 shows symptoms of TNL-triggered autoimmunity (Stuttman et al., unpublished) hinting towards possible roles of EDS1 homomers in nucleo-cytoplasmic trafficking.

The idea of plant metabolites affecting EDS1 immune signalling although valid, can be excluded due to the resistance shown by N285A and D446A mutants. It is possible that a double mutant of N285 and D446 is required for the complete abolition of glucose binding, which was not tested in this study, but is unlikely given the close interaction of D446 with the glucose molecule. A crystal structure of these mutants will confirm if these individual mutants retain binding with a glucose molecule. Another residue that is in the vicinity of the glucose molecule is serine 176. Mutational analysis of S176, which lies parallel to the glucose molecule at a distance of 3Å° could contribute to the binding and stability of the glucose molecule and might affect EDS1 immune signalling.

Accumulating evidences point towards the EDS1-PAD4 and EDS1-SAG101 complexes being stable rather than transient (Wagner et al., 2013). Thus, shuttling of proteins from EDS1 homomers to EDS1-PAD4 or EDS1-SAG101 heterodimers is less likely.



## 4. Discussion

EDS1 is an essential component of plant immunity, signalling in basal and NLR-triggered immunity (Aarts et al., 1998; Parker et al., 1996; Rietz et al., 2011). While EDS1 is genetically indispensable for TNL resistance, it acts redundantly with SA, and is able to compensate for SA signalling defects in certain CNL resistance responses (Venugopal et al., 2009). Evidence for *Arabidopsis* EDS1 association with the TNLs such as RPS4, RPS6, SNC1, VICTR in the nucleus and the *P. syringae* effector AvrRps4 point to EDS1 serving not only as a convergence point for different activated TNLs, but also as a target for pathogen effectors in their quest to dampen the immune system (Bhattacharjee et al., 2011; Heidrich et al., 2011; Kim et al., 2012; Le Roux et al., 2015; Li et al., 2001; Sarris et al., 2015).

Molecular and genetic analyses of *Arabidopsis* EDS1 have identified its functional interaction partners, PAD4 and SAG101 (Feys et al., 2001; Feys et al., 2005; Jirage et al., 1999), their spatial organization (Feys et al., 2005; Rietz et al., 2011). Also, nuclear accumulation of EDS1 upon TNL activation is essential for its immune signalling (García et al., 2010). EDS1-PAD4 regulate the accumulation of SA during pathogen challenge (Zhou et al., 1998). Genome wide microarray analysis revealed EDS1-dependent SA-independent immune signalling components (Bartsch et al., 2006), making EDS1 a bifurcating node signalling in both SA-dependent and SA-independent pathways. Although genetic analyses of EDS1, has revealed many facets of this central immune protein, the precise EDS1 molecular function has been elusive.

Fresh insights to how EDS1 might operate have been provided by an initial functional characterization of the *Arabidopsis* EDS1-SAG101 heterodimer crystal structure (Wagner et al., 2013). In the crystal structure, EDS1-SAG101 interact via a large conserved interface dominated by the juxtaposed N-terminal lipase-like domains. Formation of either EDS1-PAD4 or EDS1-SAG101 heterodimers is essential for immune signalling and mutation of *PAD4* or *SAG101* were not at all circumvented by overexpressing EDS1 alone (Wagner et al., 2013). Structure-guided functional analysis also showed that PAD4 and SAG101 compete for the same conserved surface of EDS1 to form stable heterodimers (Wagner et al., 2013), which argues against formation of an EDS1-PAD4-SAG101 ternary complex as suggested by Zhu et al. (2009). However, higher order complexes of EDS1 with PAD4 and/or SAG101 utilizing other surfaces of EDS1 cannot be



excluded (Wagner et al., 2013). The individual (stable) lipase-like or (unstable) EP domains of *Arabidopsis* EDS1 did not have disease resistance signalling activity, emphasizing the importance of the full length protein (Wagner et al., 2013). By contrast, and surprisingly, highly conserved  $\alpha/\beta$ -hydrolase catalytic residues in the lipase-like domain were dispensable for EDS1 immune signalling (Wagner et al., 2013). Strong interactions between the EDS1 and SAG101 lipase-like domains, combined with instability of the essential EP domain, suggested that the lipase-like domains act as scaffold for the functional EP domains to interact (Wagner et al., 2013).

At the beginning of my thesis work little was known about the EDS1 EP domain, although there were indications that the EP domain is a signalling module of EDS1 family proteins because (1) it is structurally unique, (2) the EDS1 lipase-like domain is stable but does not have signalling activity, and (3) there is a propensity of  $\alpha$ -helical bundles to mediate protein-protein interactions (Ghoorah et al., 2015; Guharoy & Chakrabarti, 2007). The aim of my work was to perform a targeted structure-function dissection of the EDS1 EP domain from the information provided by the EDS1-SAG101 heterodimer structure.

In this thesis, I used structure-guided mutations in the *Arabidopsis* EDS1 EP domain to elucidate its function. My body of work shows that the EDS1 EP domain is the functional module of the heterodimer, although complementary studies on PAD4 and SAG101 EP domains need to be done to assess their role/s in the heterodimer. A patch of conserved residues on the EDS1 EP domain that includes R493 and K478 is important for EDS1 immune signalling. Independent transgenic plants carrying mutations in these key residues compromise EDS1 immunity (Figures 2.4, 2.6, 2.7) without obviously affecting EDS1 nucleo-cytoplasmic localization or interactions with its partners (Figures 2.9, 2.10). R493A delays EDS1 signalling and renders the plants susceptible to bacterial (*Pst*) and oomycete (*Hpa*) biotrophic pathogen strains (Figures 2.4, 2.7). The delay in R493A defence signalling cannot be explained simply by reduced R493A protein steady state accumulation because low protein levels of other EDS1 variants (eg. K387R#1, K487R#2) are sufficient for EDS1 signalling (Figure 2.12). The difference in resistance of EP domain mutants against *Pst*/AvrRps4 and *Pst*/AvrRps4<sup>COR-</sup> (Figure 2.17) suggests that the EDS1 EP domain is a target of the bacterial virulence factor, coronatine (COR), in dampening the plant immune system, whereas wild-type EDS1 (cEDS1) suppresses COR mediated virulence. Functional analysis of R493A also revealed that this mutant is hampered in timely immune signalling (Figures 2.20, 2.24,



2.26). SA accumulation in R493A, but not K478 and cEDS1, is delayed irrespective of the presence or absence of COR (Figure 2.21). I also show indirect but compelling evidence that EDS1 is associated with DNA/chromatin, and that this association is due to a positive charge at R493 in the EP domain (Figure 2.22). I shall discuss these results, their implications within the current knowledge of EDS1 functioning, their shortfalls and further experiments required in detail below.

Although the structural homology search was done using EDS1 from the EDS1-SAG101 heterodimer, the lack of immune signalling in plants overexpressing EDS1 (Wagner et al., 2013) point towards novel interfaces formed by EDS1 heterodimers that likely interact with other proteins.

#### **4.1 The EDS1 EP domain represents a key immunity signalling module**

The  $\alpha$ -helical bundles of the EDS1 C-terminal EP domain, owing to their modular nature (Groves & Barford, 1999), have low structural similarity to other proteins compared to homologues of the EDS1 N-terminal lipase-like domain. The lack of sequence homology of the EDS1 family EP domains to other proteins and its instability without the lipase-like domain led to the hypothesis that the EP domain provides a key signalling function in EDS1 heterodimer complexes (Wagner et al., 2013). Some structural similarities between the EDS1 EP domain (385-623 aa) and other  $\alpha$ -helical proteins that are chiefly involved in multi-protein complexes (Table 2.1) strengthens the notion that the EDS1 EP domain facilitates protein-protein binding within multi-protein complexes to confer immune signalling.

The EP domain of EDS1 has some structural similarity to the human COP9 signalosome subunit 1 (Table 2.1, PDB id: 4d10-J). COP9 signalosome is involved in the regulation of Ubiquitin-proteasome system (Schwechheimer et al., 2002). Although COP9 subunits are generally conserved across *A. thaliana*, *D. melanogaster* and human COP9 (Lingaraju et al., 2014), the EDS1 EP domain has higher structural similarity to human COP9 signalosome than to *Arabidopsis* COP9 (Lingaraju et al., 2014; Serino et al., 2003), which would be inconsistent with a close functional relationship between EDS1 family proteins and COP9. *Arabidopsis* COP9 interacts with RAR1 (required for *Mla* 12 conditioned resistance) and SGT1 (suppressor of G2 allele of *skp1*)

which are HSP90 (heat shock protein 90) co-chaperone proteins required for resistance triggered by NLRs of both the CNL and TNL types by assisting receptor accumulation (Austin et al., 2002; Azevedo et al., 2002, 2006; Bieri et al., 2004). It is notable that the EP domain has significant similarity to components of the 26S proteasome such as Rpn6 (PDB id: 3txm-A) and PRE3 (PDB id: 4cr2-Q). Thus, it is possible that EDS1 EP domain regulates TNL turnover by degradation via the 26S proteasome in concert with co-chaperones such as SGT1 (Azevedo et al., 2002; Schulze-Lefert, 2004). A possible link has also been proposed for the EP domain to interact with the TNL repressor, SRFR1 (Wagner, 2013). SRFR1 contains  $\alpha$ -helical tetratricopeptide repeats and is a negative regulator of immunity (Kwon et al., 2009). SRFR1 was found in a complex with EDS1 and TNLs RPS4 and RPS6 (Bhattacharjee et al., 2011). Reduced interaction between SRFR1 and EDS1 upon effector recognition suggested that their interaction might set a threshold for TNL activation (Bhattacharjee et al., 2011). These various functional interaction possibilities of EDS1 reinforce the notion that heterodimer formation could introduce novel interfaces of the EP domain which transduce downstream signalling. Although EDS1 associations with various TNLs has been reported (Bhattacharjee et al., 2011; Kim et al., 2012), the nature of these associations (direct or indirect) and the mechanism or mediators (EP domain or lipase-like domain) is not yet known.

#### 4.1.1 EDS1 EP domain mutants are compromised in TNL resistance

Several EDS1 EP domain mutants I generated exhibited disease susceptibility phenotypes in TNL (*RPP2*, *RPP4* and *RPS4-RRS1*) resistance against different pathogens (Figures 2.4, 2.6, Table 2.2). Stable homozygous ( $T_3$ ) transgenic lines expressing EP domain mutant variants showed the same phenotypes observed in the initial segregating  $T_1$  lines, giving credence to the  $T_1$  analysis as an efficient tool for testing functional complementation. The lysine variants (K478R and 3K\_R) were partially resistant to *Pst*/AvrRps4 and showed trailing necrosis against *Hpa* CALA2, signifying reduced TNL resistance (Figure 2.6). By contrast, R493A was as susceptible as *eds1-2* to both these pathogenic strains, although all EP domain mutants maintained a nucleo-cytoplasmic localization (Figure 2.9) and interaction with PAD4 and SAG101 (Figure 2.10). Not all residues that line the cavity formed by the EDS1-SAG101 heterodimer are essential for EDS1-mediated TNL resistance, as observed by the fully resistant mutants K487R and R488A (Table 2.2, Figure 2.4). Both K487 and R488 are in close proximity to the EP ‘cavity’ (Figure 2.1) and have access

to the solvent, but are clearly not essential for EDS1 function. K487 and R488 are not as highly conserved as the essential K478 and R493 residues and thus might be less constrained. The different degrees of TNL resistance in K478R (partial resistance) and R493A (fully susceptible) suggests that individual amino acids within the EDS1 EP domain are required to different extents or affect different facets of EDS1 heterodimer function, possibly by affecting interactions with other components to different degrees.

Compromised resistance in the EP domain mutants is unlikely to be due simply to low EDS1 protein accumulation in the disease susceptible mutants (K478R, R493A) compared to cEDS1, because although the transgenic mutant proteins are less abundant in healthy tissues, they accumulate comparable protein levels as cEDS1 in response to *Pst*/AvrRps4 inoculation (Figure 2.11). Individual transgenic lines of EP domain mutants with similar resistance phenotypes accumulated different protein amounts pre- and post-infection with *Pst*/AvrRps4 (Figures 2.11, 2.12B). Additionally, both K478R and 3K\_R mutants gave similar partial TNL resistance to *Pst*/AvrRps4, but had different protein levels (Figure 2.11 A). Wagner et al. (2013) demonstrated using EDS1 lipase-like domain mutants (EDS1<sup>LL</sup>, EDS1<sup>LLI</sup>, EDS1<sup>SDFHV</sup>) that low levels of EDS1 protein are sufficient for immune functions if partner interactions are maintained. Resistance of EP domain mutants K387R (line #1) and K487R (line #2) against *Pst*/AvrRps4 also supports this conclusion, because these mutants had lower EDS1 steady state protein levels than R493A, which is susceptible (Figure 2.12). Therefore, I concluded that the resistance defects in R493A and K478R are not due to low protein accumulation but rather a problem in signalling.

In accordance with its disease susceptible phenotypes, R493A failed to upregulate the expression of SA-defence marker gene *PR1* in TNL resistance (Figure 2.14) (Vlot et al., 2009). A 10-fold lower accumulation of *PR1* in R493A line #1 (Figure 2.14) and SA accumulation to levels of cEDS1 at 24 hpi (Figure 2.13) suggests that immune signalling is not completely lost in the R493A variant. Few cases are known in which accumulated SA fails to upregulate *PR1*, one is overexpressing WRKY25 (a negative regulator of SA-mediated defence responses) and the other is in mutants of the SA response regulator NPR1 (Ng et al., 2011; Wu et al., 2012; Zheng et al., 2007). Genetic analyses place EDS1 above SA accumulation in defence pathways and a feedback loop from SA amplifies *EDS1* and *PAD4* expression (Feys et al., 2001). Upregulation of *PR1* and *EDS1* in two independent transgenic lines of R493A upon exogenous SA application (Figure 2.15)

implies that the R493A mutant defect does not lie downstream of SA accumulation or in the SA-feedback loop, in accordance with the positioning of EDS1 upstream of SA signalling in TNL resistance (Bartsch et al., 2006; Feys et al., 2001).

It is worth noting that *EDS1* levels were not upregulated in *npr1-1* (Figure 2.15), suggesting that the feedback loop of SA-EDS1 functions via NPR1 probably through transcription factors like TGAs (Brodersen et al., 2006; Caarls et al., 2015; Seyfferth & Tsuda, 2014) (Caarls et al., 2015; Seyfferth & Tsuda, 2014). A similar lack of *EDS1* upregulation was seen in *NahG* plants in which SA is fully depleted. Comparable levels of total SA (free SA + glycosylated SA) in cEDS1 and the EP domain mutants R493A and K478R excluded the possibility of low *PR1* levels as a result of conversion of active SA to glycosylated SA (Figure 2.13). Thus, the compromised TNL resistance in R493A and K478R mutants is not due to lower protein accumulation or an inability to accumulate SA or impaired signalling downstream of SA.

#### 4.1.2 EDS1 EP domain mutants cause a complete loss of basal resistance

Physical association of EDS1 and PAD4 is essential for basal immunity against virulent biotrophic pathogens (Rietz et al., 2011). EDS1, when mutated at leucine 262 to proline (EDS1<sup>L262P</sup>) in the lipase-like domain, lost detectable interaction with PAD4 but not SAG101 and EDS1<sup>L262P</sup> plants were as susceptible to *Pst* DC3000 as an *eds1* loss of function knockout (Rietz et al., 2011). By contrast, the EP variants (K478R, 3K\_R and R493A) retained interaction with PAD4 and SAG101, as measured by transient plant and Y2H assays, but had lost EDS1 functions in basal immunity against *Pst* DC3000 (Figure 2.7). There is therefore a clear difference between the partial loss of TNL resistance and full loss of basal resistance phenotypes of the K478R and 3K\_R mutant lines (Figures 2.4, 2.7). Thus, mutations in the EDS1 EP domain suggest that physical association of EDS1-PAD4 as reported by Rietz et al. (2011) is required but not sufficient for EDS1 basal immune signalling. These data also reinforce that lipase-like domains act as structural scaffolds facilitating heterodimer formation and presenting novel surfaces in the EP domain to mediate immune signalling.

Evidence from previous studies (Falk et al., 1999; Wagner et al., 2013) and disease susceptible EP domain mutants (Table 2.2, Figures 2.4, 2.7) firmly establish that the EP domain is the functional

module of EDS1. Within the EDS1 EP domain conserved residues lining the cavity formed by EDS1-SAG101 heterodimer mediate EDS1 immune signalling and mutations in these residues lead to compromised EDS1 resistance. The ability of EDS1 EP domain mutants to accumulate SA upon infection with the virulent *Pst* DC3000, similar to their SA accumulation post inoculation with *Pst*/AvrRps4, is yet to be tested. Mutations in the lipase-like domain of EDS1 resulted in loss of resistance due to abolition of partner interactions, whereas EP domain mutants are susceptible although they retain partner interaction indicating that these domains have different attributes and functions. Mutations in the EP domain causing loss of EDS1 functions in basal and TNL-triggered immunity also support the existence of a basal immune network that is utilized by various layers of plant innate immunity (Tsuda et al., 2009).

#### 4.2 EDS1 R493A delays immune signalling and SA accumulation

Transcriptional reprogramming is essential for mounting local and systemic defence responses in pathogen resistance (Buscaill & Rivas, 2014; Tsuda & Somssich, 2015; Vlot et al., 2009). Transcriptional reprogramming is not only critical for stimulating defences but also in downregulating defence pathways after the pathogen growth is halted (Rivas, 2012). The balance between plant biotic stress pathways and growth is managed by a network of transcription factors, protein signal intermediates and hormones (Buscaill & Rivas, 2014; Tsuda et al., 2009). Interactions between SA, JA (jasmonic acid), ET (ethylene), ABA (abscisic acid), IAA (auxin) and GA (gibberellic acid) hormone pathways play critical roles in plant-biotic interactions (Pieterse et al., 2012). The scale and timing of defence reprogramming is critical in limiting pathogen growth and priming uninfected tissue (Navarro et al., 2004; Tao et al., 2003; Tsuda & Katagiri, 2010).

The R493A variant has some activity because R493A protein and SA accumulate in TNL resistance at 24 h (Figure 2.13) but there is very poor upregulation of *PR1* and no disease resistance against *Pst*/AvrRps4 and *Hpa* CALA2 (Figures 2.14, 2.4, 2.6). SA-independent mechanisms that regulate SA-responsive genes in ETI such as prolonged activation of MAPKs (Mitogen-Activated Protein Kinases) have been reported (Tsuda et al., 2013). Sustained activation of MAPKs leads to upregulation of *PR1* independent of SA (Tsuda et al., 2013), lack of *PR1* upregulation in R493A

variant suggested that this mutant might interfere with SA-independent pathways also. I assessed more precisely how R493A mutant affects TNL immune signalling and defence gene expression outputs, the Col-0, *eds1-2*, wild-type EDS1 (cEDS1) and R493A line #2 transcriptomes were examined by RNA-seq at 0, 4, 8 and 24 h after infiltration of leaves with *Pst*/AvrRps4.

Transcriptome analysis showed that the genotypes do not differ from each other at 0 h in line with *eds1-2* null mutant having little effect on growth in uninfected tissues (Falk et al., 1999) (Figure 2.23). At 4 hpi, expression patterns across different samples were similar (Figure 2.23) and the different biological replicates clustered together (Figure 2.24), fitting with the lack of measurable changes in expression of *EDS1*-dependent defence marker genes (*EDS1*, *PAD4*, *PBS3*, *FMO1*) at 3 hpi with *Pst*/AvrRps4 (García et al., 2010).

Differences between R493A and cEDS1 became clear at 8 hpi, at which time the R493A expression profile was similar to *eds1-2* (Figures 2.23, 2.24, 2.25). However, by 24 hpi, the R493A expression profile was intermediate between cEDS1 and *eds1-2* (Figures 2.23, 2.26). Clustering of R493A with *eds1-2* at 8 hpi but closer to cEDS1 at 24 hpi points to a general delay in gene expression changes in the R493A mutant compared to wild-type (Figure 2.24). At 8 hpi, only 12 genes were differentially expressed between R493A and *eds1-2*. These include *EDS1* and *PBS3* suggesting that EDS1 immune signalling was operational at 8 hpi (Figure 2.25, top-right panel orange dots). The differentially expressed genes in cEDS1, *eds1-2* and R493A at 8 and 24 hpi were grouped into 12 clusters based on their expression patterns (Figure 2.27). Among these, three clusters (4, 5 and 9) comprising of 4737 DEGs showed similar expression of R493A and *eds1-2* at 8 hpi but not at 24 hpi (Figure 2.27). Deeper analysis of these clusters showed that cluster 4 was comprised of genes known to be involved in EDS1 signalling or associated with EDS1 (Figure 2.28), while cluster 9 represented genes belonging to TF families, proteasome sub-units, post-translational modifications (Figure 2.29). Cluster 4 genes were not upregulated in R493A compared to cEDS1 at 8 hpi but showed increased expression levels, which were similar to cEDS1 at 24 hpi (Figure 2.28) indicating clearly that in R493A, EDS1 immune signalling genes were delayed which can be linked to disease susceptibility. Genes upregulated at 24 hpi but not at 8 hpi, further reinforces that R493A is not non-functional but a weak version of EDS1 which is delayed in defence signalling. Why and how this mutation of R493A results in delayed signalling needs to be examined further with multiple molecular tools to ascertain its mechanism. A cause for disease

susceptibility in R493A might be the delay in *PAD4* upregulation in this mutant (Figure 2.28) because the need for PAD4 and heterodimer formation in EDS1-dependent TNL resistance is well documented (Feys et al., 2001; Jirage et al., 1999; Wagner et al., 2013). As EDS1 with PAD4 is important for SA accumulation (Feys et al., 2001; Rietz et al., 2011; Wagner et al., 2013) a delay in either one component would weaken the SA response.

The role of genes found in cluster 9 (Figure 2.29) is less clear as they are involved in a variety of critical pathways regulating growth and defence (Eichmann & Schäfer, 2015; Fan et al., 2014; Huot et al., 2014). The Ubiquitin-26S proteasome system plays a major role in protein degradation thereby affecting diverse plant functions such as growth, defence, chromatin structure and transcription (Vierstra, 2009). NLRs are also involved in regulating protein degradation for eg. WRKY45, a TF involved in SA signalling is protected from Ubiquitin proteasome machinery by *Pb1* (*Panicle blast 1*), a rice CNL (Inoue et al., 2013). The EDS1 EP domain has structural similarities to Rpn6 (section 3.1.1) and in Y2H assays EDS1 interacts with Rpt2a which is a component of 19S regulatory particle of the 26S proteasome (H. Cui, unpublished data) (Chung & Tasaka, 2011). *Arabidopsis* Rpt2a interacts with a CNL *uni-1D* to activate defence signals (Chung & Tasaka, 2011). Because EDS1 forms complexes inside nuclei with the TNL receptors RPS4 or RPS6 (Bhattacharjee et al., 2011), it is possible that EDS1 bridges between TNLs and the 26S proteasome machinery to regulate protein turnover. The R493A mutant might disrupt these interactions, resulting in delayed transcriptional defence reprogramming.

It is interesting that known EDS1 interactors were found in cluster 4 (e.g. *PAD4*, *RPS4*, *RPS6*) which is delayed in signalling at 8 hpi but not at 24 hpi compared to cEDS1, while proteins dependent on but not necessarily interacting with EDS1 were represented in cluster 9 (e.g. *SNCI*, components of the 26S proteasome) which is delayed at 8 hpi but does not show a cEDS1-like expression at 24 hpi (Figures 2.28, 2.29). There is a strong correlation between transcriptional reprogramming at early time points (4-6 hpi) and robust immune response (AG Tsuda-MPIPZ, personal communication). Delayed reprogramming as seen in R493A would result in a failure to degrade (possibly by the 26S proteasome) immune suppressors resulting in susceptibility. Although, at 4 hpi transcriptional changes were not observed between R493A, cEDS1 and *eds1-2*, the critical window of 4-6 hpi might be affected in the mutant R493A, which is manifested as delay in upregulation of critical immune regulating genes. Measuring expression patterns in a finer

time frame between 4-8 hpi would assist in identifying genes affected due to the R493A mutant. Gene expression patterns over a period of 24 h indicates that the EDS1 EP domain mutant R493A delays upregulation of immune-related genes showing *eds1-2* like expression at 8 hpi. Although, at 24 hpi, R493A shows cEDS1 like expression for a majority of the delayed genes a cluster of genes (cluster 9) does not recover from the delay and these genes show similar expression at 8 hpi and 24 hpi (Figure 2.29). These data alongwith SA accumulation in R493A, reinforce that R493A is a weak version of EDS1 capable of doing limited functions in TNL resistance.

#### 4.2.1 SA accumulation is delayed only in R493A but not in other EP domain mutants

The delayed transcriptional reprogramming (Figures 2.24, 2.26) upon TNL activation in R493A also resulted in delayed SA accumulation at 8 hpi, which, like the *EDS1*-dependent gene expression changes, caught up with cEDS1 at 24 hpi (Figure 2.20). SA in infected tissue is potentiated by a cell death loop (Vlot et al., 2009). Evidence suggests that an initial increase in H<sub>2</sub>O<sub>2</sub> upon pathogen infection upregulates SA synthesis and SA signals with ROS to generate a sustained phase of the oxidative burst which potentiates cell death and defence gene expression (Overmyer et al., 2003). A delay in SA accumulation is likely to delay this resistance and the cell death reinforcement loop. Thus, slow mobilisation of SA signalling might be a key factor in R493A susceptibility to the tested pathogens.

By contrast, the EDS1 EP domain mutant K478R accumulated wild-type levels of SA at both 8 hpi and 24 hpi (Figure 2.20), but exhibited compromised TNL resistance phenotypes (Figures 2.4, 2.7). Because the 3K\_R (triple lysine) mutant displayed similar partial disease susceptibility as K478R but accumulated lower SA at 8 hpi compared to K478R, the additional lysine residues in the EP domain might further augment SA production but not resistance. EDS1/PAD4 confer pathogen resistance in TNL and basal immunity via both SA-dependent and SA-independent pathways (Bartsch et al., 2006; Brodersen et al., 2006). *Arabidopsis MPK4* (MAP kinase 4) is a negative regulator of SA signalling pathway, *mpk4* mutants display autoimmune phenotype with high SA accumulation and retarded growth (Brodersen et al., 2006). *EDS1* and *PAD4* act downstream of *MPK4* to control SA signalling and related pathways. The *mpk4/eds1* and *mpk4/pad4* mutants showed stronger suppression of the growth phenotype which is not related to



SA, as the suppression of SA accumulation was weaker than the *mpk4/nahG* mutant (Brodersen et al., 2006). Thus, EDS1 and PAD4 can regulate immunity in SA-independent pathways, a similar explanation for the difference between K478R and R493A resistance phenotypes might be that EDS1 R493 is required for both SA-dependent and SA-independent outputs whereas K478 is necessary only for SA-independent immune signalling. These EP domain mutants R493A and K478R provide a tool for uncoupling EDS1 SA-dependent and SA-independent signalling.

In summary, mutating R493 in the EDS1 EP domain causes a critical delay in transcriptional reprogramming and SA accumulation (Figures 2.24, 2.25, 2.20). Although SA accumulation recovers at 24 h (Figure 2.20), my data suggest that a window between ~ 4 and 8 hpi is critical for stopping pathogen growth (Figure 2.24). Phenotypic and SA accumulation differences between R493A and K478R suggest their differential roles in SA signalling. Based on the RNA-seq, targeted gene expression analysis on independent lines of R493A and K478R at 4, 8 and 24 hpi with *pst/AvrRps4* will help in identifying similar/different pathways affected by these mutants. In addition, crosses generated of K478R mutant with the SA-induction deficient mutant *sid2-1* and testing the disease resistance phenotype of the mutants will determine the role of SA-independent EDS1 functions.

### **4.3 The EP domain mutant R493A fails to counteract bacterial coronatine-induced susceptibility**

EDS1 positively regulates SA and dampens JA signalling by antagonizing the function of MYC2 (H. Cui, personal communication). The EP domain of EDS1, specifically K478 and R493 mediate this antagonism, since mutations in these residues (to K478R and R493A) lead to compromised resistance against *Pst/AvrRps4*, while the mutants exhibit resistance against *Pst/AvrRps4*<sup>cor-</sup>.

Pathogens manipulate host defence by interfering with plant hormonal pathways in different ways (Duke & Dayan, 2011; Melotto et al., 2006). A well-studied example of pathogen manipulation of hormonal defence is via the phytotoxin coronatine (COR) produced by *P. syringae* and other bacterial strains (Geng et al., 2014; Mittal & Davis, 1995). COR mimics the bioactive hormone JA-Ile and promotes bacterial growth by re-opening stomata for bacterial entry into the leaf apoplast (Brooks et al., 2005; Melotto et al., 2006). COR also inhibits SA accumulation by

activating NAC TFs and the JA-regulator MYC2 (Zheng et al., 2012). The NAC TFs antagonize SA signalling by repressing *ICS1* (*Isochorismate Synthase 1*) and activating *BSMT1* (*SA Methyl Transferase 1*), catalysing SA biosynthesis and conversion of SA to methyl-SA, respectively (Zheng et al., 2012). Because EDS1 operates upstream of SA upregulation and there is a difference in penetrance between the EDS1 EP domain mutants K478R and R493A at the level of SA accumulation and TNL resistance to *Pst*/AvrRps4 (which produces COR), I tested whether these mutants differ in their responses to COR-antagonism of SA signalling.

#### 4.3.1 EP domain mutants are resistant to *P. syringae* lacking coronatine

Notably, the EDS1 EP domain mutants (K478R, 3K\_R, R493A) that were susceptible to *Pst*/AvrRps4 were fully resistant to *Pst*/AvrRps4<sup>COR-</sup> (Figure 2.17). EP domain mutants R493A (susceptible) and K478R, 3K\_R (partially resistant) to *Pst*/AvrRps4 did not show significant differences in bacterial titers when infiltrated with *Pst*/AvrRps4<sup>COR-</sup>. Therefore, the disease susceptibility of EP domain mutants to *Pst*/AvrRps4 is dependent on COR.

*P. syringae* uses COR to hijack the host defence system by simultaneously activating the JA signalling pathway and repressing SA signalling (Brooks et al., 2005; Katsir et al., 2008; Uppalapati et al., 2007). A major effect of COR on the SA pathway is known to occur at the level of *ICS1* expression, but not on genes upstream of SA signalling (Zheng et al., 2012). To date, no effect of COR on EDS1 has been reported. EDS1 interacts with the bHLH (basic helix-loop-helix) TF MYC2 in Y2H (H. Cui, personal communication). My data suggest that *P. syringae* COR causes a reduction in EDS1 at both mRNA (Figure 2.19) and protein levels (Figure 2.20). Whether EDS1 is directly targeted by COR (*e.g.* via MYC2) or indirectly by repressing *ICS1* expression and affecting the positive SA-EDS1 feedback loop remains unclear. Lower bacterial titers of *Pst*/AvrRps4<sup>COR-</sup> than *Pst*/AvrRps4 in *eds1-2* (Figure 2.17) indicate that COR mediated susceptibility is independent of *EDS1*. Thus, EDS1 resistance is most likely affected indirectly by COR by dampening SA accumulation. In my bacterial infection assays, the inability of *Pst*/AvrRps4<sup>COR-</sup> to re-open stomata is not the cause of lower bacterial titers compared to *Pst*/AvrRps4, because both strains were hand-infiltrated into the leaf apoplast, thus by-passing stomatal entry barriers.

Consistently higher protein accumulation of endogenous EDS1 (Col-0), cEDS1, susceptible mutants (R493A, K478R) and resistant mutants (K387R, K487R) upon infiltration with *Pst*/AvrRps4<sup>cor</sup> re-inforce the notion that EDS1 is also targeted (likely indirectly) by COR to dampen SA immune responses (Figure 2.18). Uncoupling the SA-EDS1 feedback loop in the EDS1 EP domain mutants and cEDS1 control lines by testing crosses with *sid2-1* at pathological and biochemical levels is essential to determine whether the effect of COR on EDS1 accumulation is through SA or not.

*EDS1* levels were not different between cEDS1 and R493A at 8 hpi with *Pst*/AvrRps4<sup>cor</sup>, while R493A transcript levels were 8-fold lower than cEDS1 upon *Pst*/AvrRps4 infiltration (Figure 2.19). Also, consistently higher R493A protein accumulation in plants infected with *Pst*/AvrRps4<sup>cor</sup> when compared to *Pst*/AvrRps4 infection (Figure 2.18) suggests that the EDS1 EP domain has an important role in antagonizing COR-mediated dampening of SA signalling. Major differences were not observed in *PAD4*, *ICS1* and *PR1* transcripts between *Pst*/AvrRps4<sup>cor</sup> and *Pst*/AvrRps4 (Figure 2.19) at 8 hpi, suggesting that early signalling responses affect only *EDS1*. Furthermore, RNA-seq analysis has highlighted the need to examine transcriptional differences between the mutants at key time points, multiple transgenic lines tested in these conditions will provide a clear, robust mechanistic understanding of the mutants. In contrast to COR repressing *ICS1* (Zheng et al., 2012), lower *ICS1* and *PR1* levels were observed at 24 hpi when infected with *Pst*/AvrRps4<sup>cor</sup> compared to *Pst*/AvrRps4. An explanation for this could be that the study by Zheng et al., used *Psm* ES4326 and I used *Pst* DC3000 expressing an effector (AvrRps4). COR might have differential effects in a stronger ETI response against *Pst*/AvrRps4 compared to the basal response against *Psm* ES4326.

I have shown that EDS1 EP domain variants are compromised in resistance to *Pst*/AvrRps4 (Figure 2.17) and *Hpa* (Figure 2.6), while a degree of susceptibility to *Pst*/AvrRps4 can be attributed to COR independently of EDS1 action (Figure 2.17). *Hpa* does not produce COR but might use an effector molecule or protein with similar SA pathway dampening actions by upregulating JA-signalling (Caillaud et al., 2013). *Hpa* delivers effector HaRxL44 that interferes with the degradation of MED19 (mediator subunit 19). MED19 is a positive regulator of immunity and the degradation of MED19 leads to increased JA-signalling and reduced SA-signalling correlated with enhanced susceptibility to pathogens (Caillaud et al., 2013). Other examples of pathogens not

producing COR but modulating host immunity by activating JA-signalling include *P.syringae* pv. *syringae*, which produces an effector that acetylates HopZ1 to degrade JAZ repressor proteins and activate JA-signalling (Jiang et al., 2013) or *P.syringae* pv. *tabaci*, which elicits an effector, HopX1, which interacts with and degrades JAZ proteins to activate JA-signalling (Gimenez-Ibanez et al., 2014). Thus, *Hpa* might use a similar strategy by producing effectors to dampen SA-signalling and the EDS1 EP domain mutants fail to counteract this virulence activity.

#### 4.3.2 Delayed SA accumulation is an inherent feature of R493A

A delay in transcriptional reprogramming and accumulation of SA at 8 hpi with *Pst*/AvrRps4 (3.2.2, Figures 2.19, 2.20) is due to the combined effects of the R493A mutation and bacterial COR. Notably, *Pst*/AvrRps4<sup>cor-</sup> did not elicit higher SA accumulation in independent lines of R493A (Figure 2.21), although the mutant lines were resistant to *Pst*/AvrRps4<sup>cor-</sup> (Figure 2.17). While COR dampening of SA signalling is well established (Brooks et al., 2005), its effect on SA accumulation is not very clear. Studies by (Uppalapati et al., 2007; Zheng et al., 2012) established that COR suppressed SA accumulation, on the contrary, there was no difference in the effect of COR on SA accumulation between *Arabidopsis* plants infected with *Pst* DC3000 and *Pst* DC3000<sup>cor-</sup> (Block et al., 2005). At 8 hpi, I observed consistently lower SA accumulation in cEDS1 and lysine mutants (K478R and 3K\_R) infected with *Pst*/AvrRps4 compared to *Pst*/AvrRps4<sup>cor-</sup> (Figure 2.20). By contrast, R493A and *eds1-2* were not different in SA accumulation when infected with either *Pst*/AvrRps4<sup>cor-</sup> or *Pst*/AvrRps4. I conclude that the delay in immune signalling and SA accumulation is due to the mutation of arginine to alanine in EDS1 EP domain, irrespective of the *Pst* COR status.

How R493A confers resistance to *Pst*/AvrRps4<sup>cor-</sup> is not understood, but the above data support the claim that R493A is a weakly active EDS1 variant. Also, evidence for COR-mediated disease susceptibility in EP domain mutants is compelling (Figure 2.17). Identical levels of SA accumulation in R493A with and without COR (Figure 2.18) suggest that, COR works in other pathways to dampen EDS1 signalling in addition to the JA-mediated suppression of SA signalling pathway.

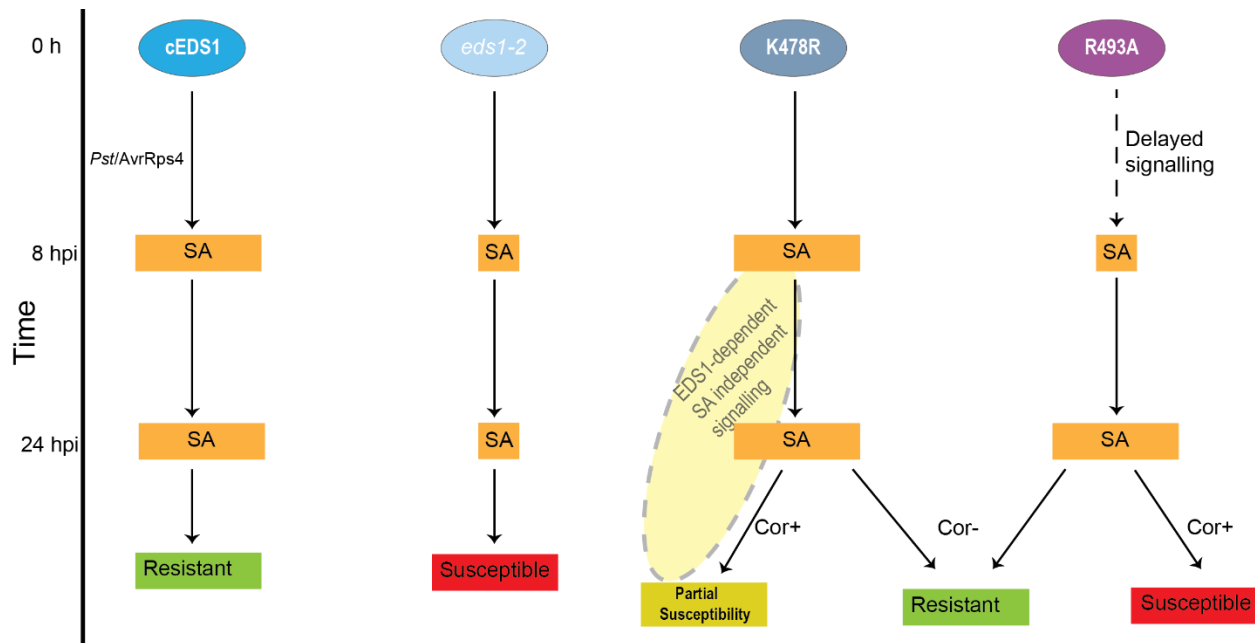


**Figure 4.1: A working model for EDS1 EP domain functions in TNL resistance.** This model is based on a comparison of EP domain mutants R493A and K478R defects in SA signalling and resistance to *Pst/AvrRps4* in the presence or absence of bacterial COR. Set on a time scale of 0-24 hpi with *Pst/AvrRps4*, the model shows actions of wild-type EDS1 (cEDS1), the *eds1-2* null mutant and EP domain mutants K478R and R493A in promoting SA accumulation at 8 and 24 hpi. Delayed signalling in R493A (Figures 2.24, 2.26) is shown as dashed lines. SA accumulation is shown as orange rectangles of different sizes corresponding to a level at the indicated time points. Effect of COR is shown on disease resistance phenotypes only. R493A and *eds1-2* are fully susceptible to *Pst/AvrRps4*, while SA is not upregulated in *eds1-2*, SA accumulation in R493A is similar to cEDS1 at 24 hpi. K478R accumulates cEDS1-like SA levels at 8 and 24 hpi, but is partially resistant suggesting that EDS1-dependent SA-independent signalling is compromised in this mutant. Both K478R and R493A mutants are resistant to *Pst/AvrRps4*<sup>COR-</sup> indicating that disease susceptibility by the phytoxin COR is additive to EDS1 functions. These EP domain mutants provide a tool for uncoupling EDS1 SA-dependent and SA-independent signalling.

In addition, the K478R mutant accumulates SA to cEDS1-like levels but has compromised resistance to *Pst/AvrRps4* (Figures 2.21, 2.17), thus indicating that SA signalling is necessary but not sufficient for a robust EDS1-immune response. Conflicting evidences of EDS1 being either a direct target of COR (via MYC2) or indirectly by the suppression of SA-signalling present a problem, since uncoupling EDS1 signalling from the EDS1-SA feedback loop is difficult. Crosses generated for R493A and K478R in SA induction deficient mutant (*sid2-1*) would assist in determining whether the EDS1 EP domain is targeted by COR directly or not.

EP domain mutants K478R and R493A are resistant to *Pst*/AvrRps4<sup>Cor-</sup>, indicating the effect of COR on their susceptibility against *Pst*/AvrRps4. The difference in SA accumulation at 8 hpi between the mutants suggests that they might regulate immunity via SA-independent pathways. The differential effects exhibited by two closely situated residues provides a valuable tool not only in understanding the role of EDS1 EP domain, but will also serve to uncouple EDS1 SA-dependent and SA-independent pathways (Figure 4.1).

#### 4.4 A positive charge at R493 is essential for EDS1-mediated TNL resistance

Nuclear accumulation of EDS1 after *Pst*/AvrRps4 infiltration (García et al., 2010), combined with the chromatin-association of the TNL receptor pair RPS4-RRS1 (Le Roux et al., 2015; Sarris et al., 2015) and *in-silico* prediction of DNA binding capability of the EDS1-SAG101 crystal structure (Table S1) are suggestive of direct or indirect association of EDS1 with the chromatin. FRET-FLIM (Fluorescence Resonance Energy Transfer-Fluorescence Lifetime IMaging) analysis of EDS1 indicated an ability to bind nucleic acid, although this needs to be further verified by ChIP (Chromatin ImmunoPrecipitation) and EMSA (Electrophoretic Mobility Shift Assay) assays (D. Lapin-MPIPZ, personal communication).

The disease susceptibility of the EP domain R493A variant raises the question whether R493A fails to bind nucleic acid. Positively charged amino acids arginine, lysine and histidine bind the negatively charged phosphate moieties in DNA (Atchley & Fitch, 1997; Cherstvy, 2009). A single arginine residue has been implicated in modulating DNA binding specificity of certain bHLH TFs (Kim et al., 1995). I hypothesised that if the delay in R493A immune signalling is due to disturbed DNA association, then an equivalent positive charge should restore function. Indeed, mutating arginine to a positively charged lysine (R493K) but not to a negatively charged glutamic acid (R493E) restored EDS1 immune activity (Figure 2.22). These R493 mutant resistance phenotype are preliminary because they are based on infection assays of heterozygous T<sub>1</sub> transgenic lines (Table 2.2, Figure 2.4) and need to be re-tested in homozygous T<sub>3</sub> material and respective EDS1 protein accumulation measured. FRET-FLIM analysis of the set of resistance phenotyped EDS1 EP domain mutants will allow us to judge whether EDS1 association with DNA is biologically meaningful. FRET-FLIM analysis of EDS1 mutants K478R and R493A showed a loss of

association with nucleic acid (performed with D. Lapin, MPIPZ; L. Deslandes and A. Jauneau, LIPM Toulouse).

Two modes of EDS1 signalling might be envisaged from postulated EDS1-DNA associations. In the first model, the EDS1 EP domain is targeted by effectors such as AvrRps4 or PopP2 leading to modification of EDS1 and disruption of DNA binding. EDS1 released from DNA can form heterodimers with PAD4 or SAG101 to form a signalling complex activating immunity (Figure 4.2). A caveat of this model is that R493A which is not associated with DNA, but maintains association with PAD4 and SAG101, should be autoactive. No autoactive phenotype in the form of elevated SA or expression of immune genes in unchallenged tissue was observed in the R493A mutant lines (Figures 2.13, 2.26).

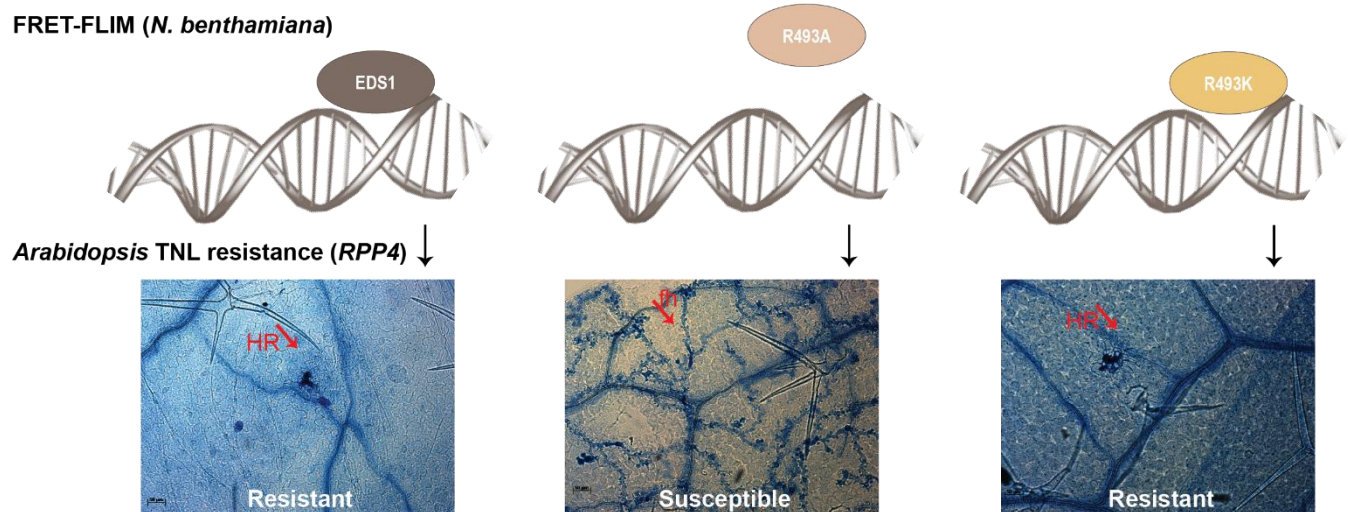


**Figure 4.2: Model for EDS1 association with DNA based on FRET-FLIM and disease resistance assays.** Wild-type EDS1 (cEDS1) associates with DNA and confers TNL (*RPP4*) to *Hpa* EMWA1 shown in T1 transgenic plants; R493A does not associate with DNA and has lost TNL resistance. R493K, which is a positive charge-mimic is anticipated to associate with DNA because it displays resistance like cEDS1.

The second model assumes that EDS1 associates with DNA at specific sites. This association might enable a faster assembly of an EDS1 signalling complex at the chromatin. Disruption of DNA association results in a delay in signalling complex formation and delayed transcriptional

reprogramming resulting in disease susceptibility because EDS1 is not at the optimal place for activation. Neither of these models account for resistance of the EP domain mutants in the absence of COR. Thus, EDS1 is likely to have more than one mode of action in TNL resistance.

#### 4.5 Conclusions and future perspectives

The findings presented in this study highlight the importance of structure-guided studies in identifying critical functions of proteins. The structure-guided functional analysis of the EDS1 EP domain, more specifically, residues lining the interface between EDS1-SAG101 strengthen our model that the EP domain is key to EDS1 resistance signalling.

In this thesis, I established a pipeline for testing the functionality of EDS1 mutants and I identified two key amino acids: K478 and R493 that are important for EDS1 immune signalling but not for EDS1 direct associations with its partners, PAD4 and SAG101. These two mutants resulted in partial and complete loss of EDS1 resistance, respectively. Further work will establish the role of other conserved and variable amino acid residues in the EDS1 EP domain to obtain a more complete picture of EDS1 molecular function(s). Also, analysis of the EP domains of PAD4 and SAG101 should answer whether these EDS1 partners have similar functional residues to facilitate interaction of the EP domains in the heterodimer or present novel interfaces for further interactors such as transcription factors.

I establish through phenotypic and transcriptome studies that EDS1 R493A is delayed in TNL resistance signalling and it is the delay rather than an inability to respond to pathogen attack which causes susceptibility of R493A to *Pst*/AvrRps4. An exhaustive analysis of the transcriptome data of R493A, validation of expression trends in independent transgenic lines and combining the EP domain mutants with key mutants of SA-dependent and SA-independent pathways should allow us to consolidate the model (Figure 4.1) of EDS1 resistance signalling. A complimentary analysis would be to examine the transcriptome data of R493A infected with *Pst*/AvrRps4<sup>COR-</sup>.

Based on my results, I propose that EDS1 is directly or indirectly targeted by the phytotoxin COR which dampens the SA-signalling pathway. The resistance of EP domain variants against *Pst*/AvrRps4<sup>COR-</sup> underscore the notion that EDS1 plays an important role in balancing SA-JA



crosstalk. However, I could not yet ascertain whether COR affects EDS1 specifically or generally by dampening SA responses.

Structural studies highlighting the role of DNA binding in NLR immunity (Fenyk et al., 2015; Le Roux et al., 2015), association of EDS1 with the TNL RPS4 (Bhattacharjee et al., 2011; Heidrich et al., 2011), and knowledge that EDS1 has a nuclear activity in transcriptional defence reprogramming (García et al., 2010) makes it tempting to speculate that EDS1 associates functionally with nuclear DNA (Figure 4.2). The evidence presented so far is rudimentary and further analysis of EP domain and other EDS1 and PAD4 mutants is underway to test the relationship between EDS1-nucleic acid binding and function in TNL resistance (Figure 4.2). Moreover, the restoration of full resistance in R493A to *Pst*/AvrRps4<sup>cor-</sup> suggests that nucleic acid binding is not essential at least for a part of EDS1 signalling activity.

EDS1 and PAD4 orthologues are found in all flowering plants, consistent with a conserved role in defence against biotrophic pathogens (Wagner et al., 2013). Nevertheless, different functions of EDS1 and PAD4 in biotic stress responses of plant species other than *A. thaliana* are emerging (Gao et al., 2010; Gao et al., 2014; Kim et al., 2012; Makandar et al., 2015; Wang et al., 2014). Transferring knowledge assimilated from *A. thaliana* to crop plants will be important to establish the fundamental regulatory role of the EDS1 family. The mutants analysed in this study serve as important tools for dissecting how SA-JA and other hormone pathways are balanced in plant species. Our current attempts at obtaining crystal structures of EDS1 EP domain mutants with/without SAG101 should help to illuminate which EDS1 patches and/or conformational changes are integral to EDS1 molecular function in immunity.



## 5. Materials and Methods

The Materials and Methods section is subdivided into two parts. In the first part (4.1) materials used throughout this study, including plant lines, pathogens, bacterial strains, chemicals, enzymes, media, buffers and solutions are listed. Methods applied in this work are described in the second part (5.2).

### 5.1 Materials

#### 5.1.1 Plant materials

##### 5.1.1.1 *Arabidopsis thaliana*

*Arabidopsis* wild-type and mutant lines use in this study are listed in Table 5.1 and 5.2, respectively.

**Table 5.1.** Wild-type *Arabidopsis* accessions used in this study

Accession	Abbreviation	Original source
Columbia	Col-0	J. Dangel <sup>1</sup>
Landsberg- <i>erecta</i>	<i>Ler</i>	Nottingham Arabidopsis stock centre <sup>2</sup>
Wassilewskija	Ws-0	K. Feldmann <sup>3</sup>

1-University of North Carolina, Chapel Hill, NC, USA 2

2-Nottingham, UK

3-University of Arizona, Tuscon, AZ, USA

**Table 5.2.** Mutant *Arabidopsis* lines used in this study

Gene	Accession	Mutagen	Reference/Source
<i>eds1-2</i> <sup>1</sup>	Col-0	FN	AG- Parker
<i>eds1-2</i>	<i>Ler</i>	FN	AG- Parker
<i>eds1-1</i>	Ws-0	EMS	AG- Parker
<i>pad4-1</i>	Col-0	EMS	AG- Parker
<i>sag101-3</i>	Col-0	T-DNA	AG- Parker
<i>pad4-1/sag101-3</i>	Col-0	EMS/T-DNA	AG- Parker

<i>rpm1-3/rps2 101C</i>	Col-0	T-DNA	AG- Tsuda
<i>npr 1-1</i>	Col-0	T-DNA	AG- Tsuda
<i>NahG</i>	Col-0		AG- Parker

1-*Ler eds1-2* allele introgressed into Col-0 genetic background, 8th backcrossed generation, referred to as “*eds1-2*” in this study

**EMS:** ethylmethane sulfonate; **FN:** fast neutron; **T-DNA:** transfer-DNA; **Ds3(GT):** gene trap insertion

**Table 5.3.** Transgenic *Arabidopsis* lines used in this study

Line	Accession	Construct	Source
YFP-cEDS1	Col-0	<i>pEDS1::YFP-cEDS1</i>	AG- Parker
YFP-cEDS1 <sup>LLIF</sup>	Col-0	<i>pEDS1::YFP-cEDS1</i>	AG- Parker
YFP-cEDS1 <sup>L262P</sup>	Col-0	<i>pEDS1::YFP-cEDS1</i>	AG- Parker
PAD4-SII-3xHA	Col-0	<i>35s::PAD4-Strep-3xHA</i>	AG- Parker
SAG101-SII-3xHA	Col-0	<i>35s::SAG101-Strep-3xHA</i>	AG- Parker
gEDS1-YFP	Col-0	<i>pEDS1::gEDS1-YFP</i>	AG- Parker

#### 5.1.1.2 *Nicotiana benthamiana*

*Nicotiana benthamiana* (310A) plants expressing the *N* resistance gene were obtained from MPIPZ, Cologne and used for transient *Agrobacterium*-mediated transformation of leaf tissues.

#### 5.1.2 Pathogens

*Arabidopsis* plants were infected with isogenic *Pseudomonas syringae* pv. *tomato* strains (DC3000) expressing different *Pseudomonas* effector proteins as specified in section 5.1.2.1.

##### 5.1.2.1 *Pseudomonas syringae* pv. *tomato* (*Pst*)

*Pseudomonas syringae* pv. *tomato* (*Pst*) strain DC3000 harbouring either the empty vector pVSP61 or expressing the *Pseudomonas syringae* pv. *pisi* effector AvrRps4 from the same plasmid (Hinsch and Staskawicz, 1996) were obtained from R. Innes (Indiana University, Bloomington Indiana, USA) and used throughout this study. *Pseudomonas syringae* pv. *tomato* (*Pst*) strain

DC3000 expressing AvrRps4 lacking coronatine was obtained from H. Cui, AG-Parker (MPIPZ-Cologne).

### 5.1.2.2 *Hyaloperonospora arabidopsidis*

**Table 5.4.** *Hyaloperonospora arabidopsidis* isolates used in this study

Isolate	Original source	Reference
<b>Cala2</b>	Oospore infection of a single seedling	(Holub <i>et al.</i> , 1994)
<b>Emwa1</b>	Oospore infection of a single seedling	(Holub <i>et al.</i> , 1994)
<b>Noco2</b>	Conidia isolated from a single seedling	(Parker <i>et al.</i> , 1993)

**Table 5.5.** *Hyaloperonospora arabidopsidis* isolates and their interaction with *Arabidopsis thaliana* ecotypes

<i>Arabidopsis</i> ecotype	<i>Hyaloperonospora arabidopsidis</i> isolate		
	Cala2	Emwa1	Noco2
Col-0	Incompatible ( <i>RPP2</i> )	Incompatible ( <i>RPP4</i> )	compatible
Ler	compatible	Incompatible ( <i>RPP5</i> and <i>RPP8</i> )	Incompatible ( <i>RPP5</i> )
Ws-0	Incompatible ( <i>RPP1A</i> )	compatible	Incompatible ( <i>RPP1</i> )

### 5.1.3 Bacterial strains

#### 5.1.3.1 *Escherichia coli* strains

**Table 5.6.** All *E. coli* strains were obtained from Invitrogen™ (Karlsruhe, Germany).

Strain	Genotype
DH5α	Φ80 <i>lacZ</i> Δ <i>M15</i> Δ( <i>lacZYA-argF</i> ) U169 <i>deoR</i> <i>recA1</i> <i>endA1</i> <i>hsdR17</i> (rk <sup>-</sup> , mk <sup>+</sup> ) <i>phoA</i> <i>supE44</i> λ- <i>thi-1</i> <i>gyrA96</i> <i>relA1</i>
DH10B	<i>mcrA</i> Δ( <i>mrr-hsdRMS-mcrBC</i> ) Φ80 <i>lacZ</i> Δ <i>M15</i> Δ <i>lacX74</i> <i>deoR</i> <i>recA1</i> <i>endA1</i> <i>ara</i> Δ139 Δ( <i>ara</i> , <i>leu</i> )7697 <i>galU</i> <i>galK</i> λ- <i>rpsL</i> (StrR) <i>nupG</i>
DB3.1	<i>gyrA462</i> <i>endA</i> Δ( <i>sr1-recA</i> ) <i>mcrB</i> <i>mrr</i> <i>hsdS20</i> (rB <sup>-</sup> mB <sup>-</sup> ) <i>supE44</i> <i>ara14</i> <i>galK2</i> <i>lacY1</i> <i>proA2</i> <i>rpsL20</i> (StrR) <i>xyl5</i> λ- <i>leu</i> <i>mtl1</i>

### 5.1.3.2 *Agrobacterium tumefaciens* strains

DNA constructs for stable transformation of *Arabidopsis thaliana* plants (2.2.3) and transient expression in *Nicotiana benthamiana* or *Nicotiana tabacum* (2.2.8.1) were transformed in *Agrobacterium tumefaciens* strain GV3101 carrying the helper plasmids.

**Table 5.7.** *Agrobacterium tumefaciens* strains used for stable and transient transformations

Bacteria	Strain	Resistance	Purpose
<i>Agrobacterium tumefaciens</i>	Gv3101 pMP90	Rifampicin, Gentamycin	Competent cells
<i>Agrobacterium tumefaciens</i>	Gv3101 pMP90 RK	Rifampicin, Gentamycin, Kanamycin	Competent cells

**Table 5.8.** Empty plasmids for yeast transformation

Name	Supplier	Used for	Selection	Epitope
pGADT7-Rec	Clontech	GAL4 AD fusion	<i>LEU2</i>	HA
pGBKT7	Clontech	GAL4 BD fusion	<i>TRP1</i>	c-Myc

**Table 5.9.** Untransformed yeast strains

Name	Supplier	Genotype
AH-109	Clontech	MATa, trp1-901, leu2-3, 112, ura3-52, his3-200, gal4Δ, gal80Δ, LYS2::GAL1 <sub>UAS</sub> -GAL1 <sub>TATA</sub> -HIS3, GAL2 <sub>UAS</sub> -GAL2 <sub>TATA</sub> -ADE2, URA3::MEL1 <sub>UAS</sub> -MEL1 <sub>TATA</sub> -lacZ, MEL1

### 5.1.4 Oligonucleotides

Primers used in this study are listed in Table 4.10. Oligonucleotides were purchased from Sigma-Aldrich (Germany). Target nucleotide bases for Mutation are highlighted in red. Lyophilised

primers were resuspended in ddH<sub>2</sub>O to a final concentration of 100 µM. Working solutions were diluted to 10 µM. F- forward; R-reverse primers.

**Table 5.10.** List of primers used for site-directed mutagenesis

Name	Sequence (5'→3')	length
K387A_F	gagggttttaaagGCactagcatggatag	29
K387A_R	ctatccatgctagtGCctttaaaacctc	29
K387R_F	gagggttttaaagaGactagcatggatag	29
K387R_R	ctatccatgctagtCtctttaaaacctc	29
K478A_F	catcgacatttaGCgaacgaagacacagg	29
K478A_R	cctgtgtcttcgttcGCTaaatgtcgatg	29
K478R_F	catcgacatttaGgaacgaagacacagg	29
K478R_R	cctgtgtcttcgttcCTaaatgtcgatg	29
K478Q_F	ctaccatcgacatttaCagaacgaagacac	30
K478Q_R	gtgtcttcgttctGtaaatgtcgatgtag	30
K487R_F	gggccgtacatgaGaagaggaagaccaac	29
K487R_R	ggtgtcttcctcttCtcatgtacggccc	29
K487A_F	gggccgtacatgGCaagaggaagaccaac	29
K487A_R	ggtgtcttcctcttGCcatgtacggccc	29
K478A_K487A_F	ccatcgacatttaGCgaacgaagacacagggccgtacatgGCaagaggaagacc	54
K478A_K487A_R	ggtcttcctcttGCcatgtacggccctgtgtcttcgttcGCTaaatgtcgatgg	54
K478R_K487R_F	ccatcgacatttaGgaacgaagacacagggccgtacatgaGaagaggaagacc	54
K478R_K487R_R	ggtcttcctcttCtcatgtacggccctgtgtcttcgttcCTaaatgtcgatgg	54
R488A_F	ggccgtacatgaaaGCaggaagaccaacc	29
R488A_R	ggttggtcttcctGCtttcatgtacggcc	29
R493A_F	ggaagaccaaccGCctacatatatgctcag	30
R493A_R	ctgagcatatatgtagGCggttggtcttc	30
R493K_F	gaggaagaccaaccAAGtacatatatgctc	30
R493K_R	gagcatatatgtaCTTggttggtcttcctc	30
R493E_F	gaggaagaccaaccGAGtacatatatgctc	30
R493E_R	gagcatatatgtaCTCggttggtcttcctc	30
L477K480AA_F	ccatcgacatGCaagaacgCagacacagggc	32
L477K480AA_R	gccctgtgtctGcggtctttGCatgtcgatgg	32

### 5.1.5 Enzymes

#### 5.1.5.1 Restriction endonucleases

Restriction enzymes were purchased from New England Biolabs (Germany). Enzymes were supplied with 10x reaction buffer which was used for restriction digests.

#### 5.1.5.2 Nucleic acid modifying enzymes

Standard PCR reactions were performed using home made *Taq* DNA polymerase. To achieve high accuracy, *Pfu* polymerases were used when PCR products were generated for cloning.

Modifying enzymes and their suppliers are listed below:

*Taq* DNA polymerase home made

*PfuTurbo*® DNA polymerase Stratagene® (Germany)

SuperScript™ II RNase H- Reverse Transcriptase Invitrogen™ (Germany)

Gateway™ LR Clonase™ Enzyme mix Invitrogen™ (Germany)

### 5.1.6 Chemicals

Laboratory grade chemicals and reagents were purchased from Sigma-Aldrich (Germany), Roth (Germany), Merck (Germany), Invitrogen™ (Germany), Serva (Germany), and Gibco™ BRL® (Germany) unless otherwise stated.

### 5.1.7 Antibiotics (stock solutions)

Ampicillin (Amp) 100 mg/ml in ddH<sub>2</sub>O

Carbenicillin (Carb) 50 mg/ml in ddH<sub>2</sub>O

Gentamycin (Gent) 15 mg/ml in ddH<sub>2</sub>O

Kanamycin (Kan) 50 mg/ml in ddH<sub>2</sub>O

Rifampicin (Rif) 100 mg/ml in DMSO

Tetracycline (Tet) 10 mg/ml in 70 % ethanol

Stock solutions (1000x) stored at -20° C. Aqueous solutions were sterile filtered.



### 5.1.8 Media

Media were sterilised by autoclaving at 121° C for 20 min. For the addition of antibiotics and other heat labile compounds the solution or media were cooled to 55° C. Heat labile compounds were sterilised using filter sterilisation units prior to addition.

**Table 5.11** Media

Name	Components
Luria-Bertani (LB) pH 7	0.5% yeast extract; 1% tryptone; 1% NaCl; 1.5% agar
YEB	0.5% beef extract; 1% yeast extract; 0.5% peptone; 0.5% sucrose; 0.5g/l MgCl <sub>2</sub> ; 1.5% agar
NYGA pH 7	0.5 % bactopectone; 0.3 % yeast extract; 2 % glycerol; 1 % bacto agar
½ Murashige & Skoog (MS) pH 5.8	2.2 g/l Murashige and Skoog medium incl. vitamins and MES buffer 0.8 % sucrose; 0.8 % plant agar

### 5.1.9 Antibodies

Listed below are primary and secondary antibodies used for immunoblot detection.

**Table 5.12** Primary antibodies

Antibody	Source	Dilution	Supplier
α-EDS1	rabbit polyclonal	1:250 and 1:500	AG- Parker
α-PAD4	rabbit polyclonal	1:500	AG- Parker
α-GFP	mouse polyclonal	1:2500	Roche
α-HA	rat polyclonal	1:2500	Roche

**Table 5.13** Secondary antibodies

Antibody	Source	Dilution	Supplier
goat anti-rabbit IgG-HRP	horseradish peroxidase conjugated	1:5000	Santa Cruz (USA)
goat anti-mouse IgG-HRP			
goat anti-rat IgG-HRP			

### 5.1.10 Buffers and solutions

General buffers and solutions are displayed in the following listing. All buffers and solutions were prepared with Milli-Q® water. Buffers and solutions for molecular biological experiments were autoclaved and sterilised using filter sterilisation units, respectively. Buffers and solutions not displayed in this listing are denoted with the corresponding methods.

**Table 5.14** Buffers

	Buffer	Components
DNA electrophoresis	10x running buffer	0.4M Tris, 0.2M acetic acid, 10mM EDTA, pH 8.5
	6x loading buffer	40% (w/v) sucrose, 0.5M EDTA, 0.2%(w/v) bromophenol blue
	DNA ladder	10%(v/v) 6xloading buffer, 5%(v/v) 1 Kb DNA ladder (Roth)
Protein electrophoresis	10x Tris-glycine running buffer	250mM Tris, 1.92M glycine, 1%(w/v) SDS
	2x SDS sample buffer	60mM Tris pH 6.8, 4%(w/v) SDS, 200mM DTT, 20%(v/v) glycerol, 0.2%(w/v) bromophenol blue
	Staining solution	25%(v/v) isopropanol, 10%(v/v) acetic acid, 0.04%(w/v) Coomassie Brilliant Blue G-250
	Destaining solution	25%(v/v) isopropanol, 10%(v/v) acetic acid
Immunoblotting	TBS buffer	10mM Tris, 150mM NaCl, pH 7.5
	TBS-T buffer	10mM Tris, 150mM NaCl, 0.05%(v/v) Tween 20, pH 7.5
	10x transfer buffer	250mM Tris, 1.92M glycine, 1%(w/v) SDS, 10%(v/v) Methanol

	Ponceau S	Dilution of ATX Ponceau concentrate (Fluka) 1:5 in water
Protein purification	IMAC lysis buffer	50mM HEPES, 150mM NaCl, 20mM imidazole, 1mM DTT, 10%(v/v) glycerol, pH 8.0
	IMAC elution buffer	50mM HEPES, 150mM NaCl, 250mM imidazole, 1mM DTT, 10%(v/v) glycerol, pH 8.0
	Lysis- strep buffer	100mM Tris, pH 8.0, 5mM EGTA, 5mM EDTA, 150mM NaCl, 10mM DTT, plant protease inhibitor cocktail (Roche), 0.5% Triton X-100, 100 µg/ml avidin
	Wash- strep buffer	50mM Tris, pH 8.0, 2.5mM EDTA, 150mM NaCl, 2mM DTT, 0.05%(v/v) Triton X-100
	Elution- strep buffer	Elu-Strep buffer 10mM Tris pH 8.0, 10mM desthiobiotin, 2mM DTT, 0.05%(v/v) Triton X-100
	YFP-buffers	50 mM Tris- HCl(pH7.5), 150 mM NaCl, 10% glycerol, 2 mM EDTA, 5 mM DTT, 1 tablet of Roche protease inhibitor, 0.01% Triton x-100 made in 25 ml H <sub>2</sub> O

#### 5.1.11 Software.

**Table 5.15** List of software employed in various analysis

Purpose	Software	source
Preparation of figures	Adobe illustrator	Adobe systems
Preparation of figures	Adobe photoshop	Adobe systems
Protein structure figures	PyMOL	Schrödinger, LLC

Preparation of text	MS word	Microsoft systems
Preparation of tables	MS excel	Microsoft systems
Reference manager	Mendeley	www.mendeley.com
DNA sequence analysis	LASERGENE package	DNASTAR
Sequence alignments	MUSCLE	www.ebi.ac.uk/Tools/msa/muscle/
Confocal images	Image J	http://imagej.nih.gov/ij/
Confocal images	ZEN silver	Carl zeiss
Statistics and alignment	R package for windows	https://cran.r-project.org/

## 5.2 Methods

### 5.2.1 Maintenance and cultivation of *Arabidopsis* plants

*Arabidopsis* seeds were germinated by sowing directly on moist soil (MPIPZ, Cologne). Seeds were covered with a propagator lid and vernalised at 4° C for 48 h in the dark. Subsequently seeds were transferred to a controlled environment growth chamber and maintained under short day conditions (10 h photoperiod, light intensity of approximately 200  $\mu$ Einsteins m<sup>-2</sup> sec<sup>-1</sup>, 22° C and 65 % humidity). Propagator lids were removed 3-5 days post germination. To obtain progeny three-week old plants were transferred to long day conditions (16 h photoperiod) and allowed to flower. To collect seed aerial tissue was enveloped with a paper bag and sealed with tape at its base until siliques shattered.

### 5.2.2 *Agrobacterium*-mediated stable transformation of *Arabidopsis* (floral dip)

This method for *Agrobacterium*-mediated stable transformation of *Arabidopsis* is based on the floral dip protocol described by Clough and Bent (1998). Nine *Arabidopsis* plants were grown in 9 cm square pots (3 pots for each transformation) under short day conditions for 4 weeks. Then the plants were shifted to 16 h photoperiod conditions to induce flowering. First inflorescence shoots were cut off as soon as they emerged to induce the growth of more inflorescences. Plants were used for transformation when they did not have pods but maximum number of young flower heads. *Agrobacterium* was streaked out onto selective YEB plates containing appropriate antibiotics and was grown at 28 °C for 3 days. A 20 ml O/N culture was prepared in selective YEB

medium and cultured at 28 °C in an orbital shaker. The next day 200 ml YEB broth with appropriate antibiotics was inoculated with the entire O/N culture and grown O/N at 28° C in an orbital shaker until OD<sub>600</sub> > 1.6 was achieved. Cultures were spun down at 5000 rpm for 10 min at room temperature and the pellet was resuspended in 5 % sucrose to OD<sub>600</sub> ~ 0.8. Silwet L-77 (Lehle seeds, USA) at 500µl/l was added as surfactant. Plants to be transformed were inverted in the cell-suspension ensuring all flower heads were submerged. Plants were agitated slightly to release air bubbles and left in the solution for approximately 5 sec. Plants were removed and dipping was repeated as before. Excess inoculum was removed by dabbing of inflorescences onto tissue paper. Plants were then placed into plastic bags, sealed with tape and placed overnight into the glasshouse away from direct light. Bags were removed and pots were moved to direct light and left to set seed.

### 5.2.3 Maintenance of *P. syringae* pv. *tomato* cultures

*Pseudomonas syringae* pv. *tomato* strains were streaked onto selective NYGA plates containing Rifampicin (100 µg/ml) and Kanamycin (50 µg/ml) from -80 °C DMSO stocks. Streaked plates were incubated at 28 °C for 72 h before storing at 4° C and restreaked weekly.

#### 5.2.3.1 *P. syringae* pv. *tomato* growth assay

*P. syringae* cultures of the denoted strains were started from bacteria grown on NYGA plates in 20 ml NYG broth with Rifampicin (100 µg/ml) and Kanamycin (50 µg/ml). The 20 ml cultures were incubated overnight at 28 °C and 160 rpm in a rotary shaker. 2.5 ml of the overnight cultures were used to inoculate 50 ml of NYG broth in 300 ml Erlenmeyer flasks supplemented with antibiotics. The flasks were incubated at 28 °C and 160 rpm in a rotary shaker for 3 h. An ideal OD<sub>600</sub> reading at this time point should be 0.2. The bacteria were transferred to sterile 50 ml Falcon tubes and pelleted at 4600 rpm for 10 min at 20° C (Heraeus Multifuge 3S-R). The bacterial pellet was resuspended in 40 ml of sterile 10 mM MgCl<sub>2</sub>, and the culture was centrifuged as above. The supernatant was removed and the bacteria were resuspended in 20 ml of sterile 10 mM MgCl<sub>2</sub>. Concentration of bacteria was adjusted according to the method of infection (spray OD<sub>600</sub>- 0.2; infiltration OD<sub>600</sub>-0.0002).

#### 5.2.3.2 Bacterial spray infection of leaves

For spray-infection, the concentration of bacteria was adjusted to 1 x 10<sup>7</sup> cfu/ml in 10 mM MgCl<sub>2</sub> containing 0.04 % Silwet L-77 (Lehle seeds, USA) if not otherwise stated. For bacterial growth

assays, single pots with five plants grown under short day conditions for 4-5 weeks, were used. Two hours before spray-infection, plants were watered and kept under a dH<sub>2</sub>O-humidified lid to allow opening of stomata. Plants were spray-infected with a dispenser and kept under a dH<sub>2</sub>O-humidified lid for 3 hours. Day zero (d0) samples were taken 3-4 hours after spray-infection by using a cork borer (d= 0.6 cm). 3 parallel samples each with 3 leaf discs were taken from 5 independent plants and transferred to a 1.5 ml centrifuge tube, resulting in a total excised area of ~1 cm<sup>2</sup>. Bacterial titers were determined by shaking leaf discs from infected leaves in 10 mM MgCl<sub>2</sub> supplemented with 0,01% Silwet L-77 at 28°C for 1 h. 20 µl of the resulting bacterial suspension were plated on NYGA plates containing the appropriate antibiotics and incubated at 28°C for 48 h before colonies were counted. Day three (d3) samples were taken in an identical manner to that of d0. For each sample a dilution series ranging between 10<sup>-1</sup> and 10<sup>-7</sup> was made and 20 µl aliquots from each dilution were spotted sequentially onto a single NYGA plate containing the appropriate antibiotics. Bacterial plates were incubated at 28° C for 48 h before colony numbers were determined.

#### 5.2.3.3 Bacterial infiltration into leaves

One day before infection, bacterial strains were re-streaked on NYGA plates containing the appropriate antibiotics and incubated O/N at 28°C. The concentration of bacteria was adjusted to OD<sub>600</sub>- 0.0002 in 10 mM MgCl<sub>2</sub>. Leaves of 4-5 week old plants were infiltrated with a needle-less syringe. Samples were collected at the appropriate time points.

#### 5.2.3.4 *Arabidopsis* T<sub>1</sub> complementation analysis

Transformants in T<sub>1</sub> generation of *Arabidopsis* were selected for resistance to BASTA (Glufosinate ammonium, Bayer), by spraying the BASTA on 2 week old seedlings. Transformants were re-potted in fresh soil and grown in short day condition for one more week. Conidiospores of *Hpa* isolates were spray inoculated onto 3-week-old plants at 4x10<sup>4</sup> spores/ml. Host cell-death and *Hpa* infection structures were visualized in true leaves by Trypan Blue staining at 4–5 dpi. Infected T<sub>1</sub> seedlings were treated with Ridomil (Syngenta) in order to kill *Hpa*, and protein expression was measured in leaf extracts of plants harvested – 2 weeks later.

### 5.2.4 Transient protein expression in *N. benthamiana*

*Agrobacteria* carrying pAM-PAT 35s::*PAD4-SII-3xHA*, 35s::*SAG101-SII-3xHA*, *pEDS1::YFP-cEDS1* and mutant variants were grown for 2 days on selective YEB or LB plates at 28°C and incubated for 3-5h in infiltration medium (10mM MES pH 5.6, 10mM MgCl<sub>2</sub>, 0.15mM acetosyringone) at OD<sub>600</sub>=1. 3-4 week-old *Nicotiana benthamiana* plants were syringe-infiltrated with different v/v mixes of the prepared *Agrobacteria* strains. Leaf samples were taken at 2 dpi.

### 5.2.5 *Arabidopsis* seed surface sterilization

For *Arabidopsis* grown *in vitro*, seeds were sterilized before sowing. Briefly, the bottom of a 1.5 ml microcentrifuge tube was covered with seeds and placed inside a desiccator jar together with a beaker containing 100 ml 6 % NaClO (sodium hypochlorite). To produce Chlorine gas, 10 ml of 37 % HCl was added directly into the hypochlorite solution and the desiccator closed and vacuum was applied. After 4-8 h, the desiccator was opened for 15 min. to allow evaporation of remaining chlorine gas in the laminar flow hood. Microcentrifuge tube caps were closed before removing from the desiccator jar. Alternatively, seeds were sterilized with ethanol using microcentrifuge spin columns from DNA preps. Therefore, seeds were subsequently incubated with 70 % ethanol for 2 min. and 100 % ethanol for 1 minute, followed by 1 min centrifugation at full speed, to remove all ethanol. Afterwards, seeds were dried under a sterile flow hood for 10 min. Sterile seed were spread out on suitable culture media and stratified for 48 h at 4°C in the dark.

### 5.2.6 Exogenous application of salicylic acid

Surface sterilized *Arabidopsis* seeds were sown individually in 200 µl of ½ liquid MS on 48-well culture plates. Plates were stratified at 4 °C for 2 days and shifted to a controlled environment growth chamber with 12 h photoperiod. 2-week old seedlings were drained of the liquid MS and treated with MS+ 200 µM SA or plain MS. Samples were harvested at 24 h post treatment.

### **5.2.7 Biochemical methods**

#### **5.2.7.1 Arabidopsis total protein extraction for immunoblot analysis**

Total protein extracts were prepared from 4-5 week-old plant materials. Liquid nitrogen frozen samples were homogenized 2 x 30 sec to a fine powder using a Mini-Bead-Beater-8™ (Biospec Products) and 1.2 mm stainless steel beads (Roth) in 1.5 ml centrifuge tubes. After the first 15 sec of homogenisation samples were transferred back to liquid nitrogen and the procedure was repeated. 100 µl of 2x SDS-PAGE sample buffer was added to 50 mg sample on ice. Subsequently, samples were boiled for 10 min while shaking at 500 rpm in an appropriate heating block. Samples were stored at -20° C if not directly loaded onto SDS-PAGE gels.

#### **5.2.7.2 Denaturing SDS-polyacrylamide gel electrophoresis (SDS-PAGE)**

Denaturing SDS-polyacrylamide gel electrophoresis (SDS-PAGE) was carried out using the Mini-PROTEAN® 3 system (BioRad) and discontinuous polyacrylamide (PAA) gels. Gels were made fresh on the day of use according to the manufacturer instructions. Resolving gels were poured between to glass plates and overlaid with 500 µl of water-saturated n-butanol or 50 % isopropanol. After gels were polymerised for 30 – 45 min the alcohol overlay was removed and the gel surface was rinsed with dH<sub>2</sub>O. Excess water was removed with a filter paper. A stacking gel was poured onto the top of the resolving gel, a comb was inserted and the gel was allowed to polymerise for 30 - 45 min. In this study, 8%, 10% and 12% resolving gels were used, overlaid by 4 % stacking gels. Gels were 0.75 mm or 1.5 mm in thickness.

If protein samples were not directly extracted in 2x SDS-PAGE sample buffer proteins were denatured by adding 1 volume of 2x SDS-PAGE sample buffer to the protein sample followed by boiling for 5 min. After removing the combs under running water, each gel was placed into the electrophoresis tank and submerged in 1x running buffer. A pre-stained molecular weight marker (Precision plus protein standard dual colour, BioRad) and denatured protein samples were loaded onto the gel and run at 80 - 100 V (stacking gel) and 100 – 150 V (resolving gel) until the marker line suggested the samples had resolved sufficiently.

#### **5.2.7.3 Immunoblot analysis**

Proteins that had been resolved on PAA gels were transferred to Hybond™-ECL™ nitrocellulose membrane (Amersham Biosciences) after gels were released from the glass plates and stacking gels were removed with a scalpel. PAA gels and membranes were pre-equilibrated in 1x transfer

---



buffers for 10 min on a rotary shaker and the blotting apparatus (Mini Trans-Blot® Cell, BioRad) was assembled according to the manufacturer instructions. Transfer was carried out at 110 V for 60 min. The transfer cassette was dismantled and membranes were checked for equal loading by staining with Ponceau S for 5 min before rinsing with deionised water. Ponceau S stained membranes were scanned and thereafter washed for 5 min in TBS-T before membranes were blocked for 1 h at room temperature in TBS-T containing 5% (w/v) non-fat dry milk. The blocking solution was removed and membranes were washed briefly with TBS-T. Incubation with primary antibodies was carried out overnight by slowly shaking on a rotary shaker at 4°C in TBS-T supplemented with 2% (w/v) non-fat dry milk. Next morning the primary antibody solution was removed and membranes were washed 3 x 10 min with TBS-T at room temperature on a rotary shaker. Bound primary antibodies were detected using horseradish peroxidase (HRP)-conjugated secondary antibodies. Membranes were incubated in the secondary antibody solution for 1 h at room temperature at slow rotation. The antibody solution was removed and membranes were washed as described above. This was followed by chemiluminescence detection using the SuperSignal® West Pico Chemiluminescent kit or a 9:1 - 4:1 mixture of the SuperSignal® West Pico Chemiluminescent- and SuperSignal® West Femto Maximum Sensitivity-kits (Pierce) according to the manufacturer instructions. Luminescence was detected by exposing the membrane to photographic film (BioMax light film, Kodak).

#### **5.2.7.4 Salicylic acid measurement**

SA measurements was obtained of leaf material (70 to 200 mg fresh weight) according to Straus et al. (2010), using a chloroform/methanol extraction and analysed by gas chromatography coupled to a mass spectrometer (GC-MS, Agilent, Santa Clare, USA).

#### **5.2.7.5 IP with GFP trap beads (Chromotek)**

All steps were carried out on ice in the cold room (4°C).

One gram of leaf tissue was ground to a fine powder in liquid Nitrogen. The leaf tissue was added to 1 ml of cold extraction buffer and made upto 5 ml. To this 50 µL 50% slurry of GFP trap beads (Chromotek) were added to each sample (~ 5 mL) into a 15 mL Falcon tube. Next, samples were incubated for 2-3 h at 4°C on a roller mixer. Afterwards, samples were spun down at 4°C at 3000 rpm for 1 minute. Supernatant was removed by pipetting. Next, 1 mL wash buffer (i.e. extraction buffer) was added and the suspension of the same sample was pooled together into a 2 mL protein

LoBind Eppendorf tube. To pellet beads, samples were centrifuged for 5 sec. at 500 g. 1 mL fresh extraction buffer was added into the Falcon tubes to capture remaining beads and transfer into the respective tubes. Washing with 1 mL extraction buffer was repeated 3 times. The last wash was removed with a syringe needle (smallest possible) directly into the beads, to suck off all remaining liquid. To concentrate the eluate, 50 µL of SDS buffer (1 x NuPage) were added to beads and samples heated to 70°C for 20 min. Samples were spun down briefly again, transferred to a mini -BioRad chromatography column and spun down for 20 sec at 500 g to separate beads from eluate. The eluate was collected and used for gel electrophoresis of the IP samples.

## 5.2.8 Molecular biology methods

### 5.2.8.1 Isolation of genomic DNA from *Arabidopsis* (Quick prep for PCR)

This procedure yields a small quantity of poorly purified DNA. However, the DNA is of sufficient quality for PCR amplification. If preps are to be used over a long period of time, they should be frozen in aliquots. The aliquot in use should be stored at 4° C. The cap of a 1.5 ml microcentrifuge tube was closed onto a leaf to clip out a section of tissue and 400 µl of DNA extraction buffer were added. A micropestle was used to grind the tissue in the tube until the tissue was well mashed. The solution was centrifuged at maximum speed for 5 min in a bench top microcentrifuge and 300 µl supernatant were transferred to a new tube. 1 volume of isopropanol was added to precipitate DNA and centrifuged at maximum speed for 5 min in a bench top microcentrifuge. The supernatant was discarded carefully. The pellet was washed with 750 µl of 70 % ethanol and dried for 5 min at 45 °C. Finally the pellet was dissolved in 100 µl 10 mM Tris-HCl pH 8.0 and 0.5 - 2 µl of the solution were used for PCR.

### 5.2.8.2 Isolation of total RNA from *Arabidopsis*

Total RNA was prepared from 3-5 week-old plant materials. Liquid nitrogen frozen samples (approximately 50 mg) were homogenized 2 x 30 sec to a fine powder using a Mini- Bead-Beater-8™ (Biospec Products) and 1.2 mm stainless steel beads (Roth) in 2 ml centrifuge tubes. After the first 15 sec of homogenisation samples were transferred back to liquid nitrogen and the procedure was repeated. Thereafter RNA was isolated using RNeasy kit from QIAGEN according to the manufacturer's instruction. Samples were stored at -80° C.

### 5.2.8.3 Polymerase chain reaction (PCR)

Standard PCR reactions were performed using home-made *Taq* DNA polymerase while for cloning of PCR products *Pfu* polymerase was used (see 2.1.6.2) according to the manufacturer instructions. All PCRs were carried out using a PTC-225 Peltier thermal cycler (MJ Research). A typical PCR reaction mix and thermal profile is shown below.

**Table 5.16** PCR mix (20 µl total volume):

Component	Volume
Template DNA	0.2-10 ng
10x PCR buffer	2 µl
dNTP (2.5 mM each) mix	2 µl
Forward primer (10 µM)	1 µl
Reverse primer (10 µM)	1 µl
Taq DNA polymerase (4U/ml)	0.5 µl
Nuclease free water	Make upto 20 µl total volume

**Table 5.17** Thermal cycling

Stage	Temperature (°C)	Time	Cycles
Initial denaturation	94	2 min	1x
Denaturation	94	30 sec	25-35x
Annealing	55-60	30 sec	
Extension	72	1 min/kb	
Final extension	72	3 min	1x

### 5.2.8.4 Site-directed mutagenesis

Site-directed mutagenesis was performed with minor modifications as described in the instruction manual of the QuickChange® site-directed mutagenesis kit of Stratagene®.

**Table 5.18** PCR mix (20 µl total volume):

Component	Volume
Template plasmid (25 ng/μl)	1 μl
10x <i>pfu Turbo</i> reaction buffer	2 μl
dNTP (2.5 mM each) mix	2 μl
Forward primer (10 μM)	1 μl
Reverse primer (10 μM)	1 μl
<i>pfu Turbo</i> DNA polymerase (2.5U/ml)	0.4 μl
Nuclease free water	Make upto 20 μl total volume

**Table 5.19** Thermal cycling

Stage	Temperature (°C)	Time	Cycles
Initial denaturation	94	1 min	1x
Denaturation	94	45 sec	18x
Annealing	55-60	45 sec	
Extension	72	1 min/kb	
Final extension	72	8 min	1x

After the PCR, 1 μl *DpnI* (20 U/μl) were added to the reaction mix to digest methylated, parental DNA and to enable selection of mutation-containing synthesised DNA. The reaction was incubated for 1 h at 37° C before the endonuclease was heat-inactivated at 65° C for 20 min. 3 μl of the reaction mixture, containing the circular, nicked vector DNA with the desired mutations were then transformed into DH10B cells and plated on LB agar containing the appropriate antibiotic.

#### 5.2.8.5 Reverse transcription-polymerase chain reaction (RT-PCR)

RT-PCR was carried out in two steps. SuperScript™ II RNase H- Reverse Transcriptase (Invitrogen) was used for first strand cDNA synthesis by combining 1 μg total RNA, 1 μl oligo dT (0.5 μg/μl), 5 μl dNTP mix (each dNTP 2.5 mM) in a volume of 13.5 μl (made up with H<sub>2</sub>O). The sample was incubated at 65°C for 10 min to destroy secondary structures before cooling on ice. Subsequently the reaction was filled up to a total volume of 20 μl by adding 4 μl of 5x reaction buffer, 2 μl of 0.1 M DTT and 0.5 μl reverse transcriptase. The reaction was incubated at 42°C for 60 min before the enzyme was heat inactivated at 70°C for 15 min. For subsequent PCR, synthesised cDNA was diluted to 50 ng/μl and 2.5 ng of cDNA was used as template.

#### 5.2.8.6 Plasmid DNA isolation from bacteria

Standard alkaline cell lysis minipreps of plasmid DNA were carried out using the Qiagen miniprep plasmid isolation kit according to the manufacturer's instructions. Larger amounts of plasmid DNA were isolated using Qiagen Midi preparation kits.

#### 5.2.8.7 Restriction endonuclease digestion of DNA

Restriction digests were carried out using the recommended manufacturer's conditions. Typically, reactions were carried out in 0.5 ml tubes, using 1 µl of restriction enzyme per 20 µl reaction. All digests were carried out at the appropriate temperature for a minimum of 60 min.

#### 5.2.8.8 Agarose gel electrophoresis of DNA

DNA fragments were separated by agarose gel electrophoresis in gels consisting of 1 – 2 % (w/v) agarose in TAE buffer. Agarose was dissolved in TAE buffer by heating in a microwave. Molten agarose was cooled to 50° C before 2.5 µl of ethidium bromide solution (10 mg/ml) was added. The agarose was poured and allowed to solidify before being placed in TAE in an electrophoresis tank. DNA samples were loaded onto an agarose gel after addition of 2 µl 6x DNA loading buffer to 10 µl PCR- or restriction reaction. Separated DNA fragments were visualised by placing the gel on a 312 nm UV transilluminator and photographed.

#### 5.2.8.9 Isolation of DNA fragments from agarose gels

DNA fragments separated by agarose gel electrophoresis were excised from the gel with a clean razor blade and extracted using the QIAEX®II gel extraction kit (Qiagen) according to the manufacturer's protocol.

#### 5.2.8.10 Site specific recombination of DNA in Gateway®-compatible vectors

In order to create EDS1 entry clones of cEDS1 for the Gateway® system, the pENTR/D vector was used to clone cEDS1 (mutated variants). To transfer the fragment of interest into gene expression construct (*pEDS1::YFP-cEDS1*), an LR reaction between the entry clone and a Gateway® destination vector was performed.

**Table 5.20** Basic LR reaction approach:

Components	Volume
LR reaction buffer (5x)	1 µl
Entry clone (100 ng/µl)	1.5 µl

Destination vector (100 ng/μl)	1 μl
LR clonase enzyme mix	0.5 μl
TE buffer	Make upto 5 μl

Reactions were incubated for 1 h at room temperature before 0.5 μl proteinase K solution was added. Reactions were incubated at 37° C for 10 min. Entire reaction was transformed into *E. coli* strain DH10B.

#### 5.2.8.11 DNA sequencing

DNA sequences were determined by Sanger sequencing at the “Automatische DNA Isolierung und Sequenzierung” (ADIS) service unit at the MPIPZ, Cologne.

#### 5.2.8.12 RNA sequencing

Samples for RNA-Seq and RNA isolation was performed as described above. Here, one biological triplicate is the sum of 9 leaves from 3 biological replicates from one treatment. Three biological replicates were used for deep sequencing. Illumina sequencing libraries were prepared by the Max Planck Genome Center Cologne using an input of 1.5 μg of total RNA. Sequences were generated using the Illumina HiSeq2500 platform, resulting in approximately 25,000,000 million reads per sample with a length of 100 bp. Strand specific sequence mapping was performed with the software Tophat2 to the newest Arabidopsis genome data base (Tair10).

#### 5.2.8.13 DNA sequence analysis

Sequence data were analysed mainly using various packages from DNASTAR and Clone Manager 6 (Scientific and Educational software, USA).

#### 5.2.8.14 Preparation of chemically competent *E. coli* cells

Media and solutions required for preparation of rubidium chloride *E. coli* chemically competent cells

**Table 5.21** preparation of competent cells

ΦB	TFB1	TFB2
Yeast extract 0.5 %	KAc 30 mM	MOPS 10 mM
Tryptone 2 %	MnCl <sub>2</sub> 50 mM	CaCl <sub>2</sub> 75 mM
MgSO <sub>4</sub> 0.4 %	RbCl 100 mM	RbCl 10 mM
KCl 10 mM	CaCl <sub>2</sub> 10 mM	Glycerol 15 %

pH 7.6	Glycerol 15 %	
autoclave	pH 5.8 sterile-filter	sterile-filter

5 ml of an *E. coli* strain DH10B over-night culture grown in  $\Phi$ B was added to 400 ml of  $\Phi$ B and shaken at 37° C until the bacterial growth reached an OD600 0.4 - 0.5. Cells were cooled on ice and all following steps were carried out on ice or in a 4° C cold room. The bacteria were pelleted at 5000 g for 15 min at 4° C. The pellet was gently resuspended in 120 ml icecold TFB1 solution and incubated on ice for 10 min. The cells were pelleted as before and carefully resuspended in 16 ml ice-cold TFB2 solution. 1.5 ml eppendorf reaction tubes containing 50  $\mu$ l aliquots of cells were frozen in liquid nitrogen and stored at -80° C until use.

#### 5.2.8.15 Transformation of chemically competent *E. coli* cells

A 50  $\mu$ l aliquot of chemically competent cells was thawed on ice. 10 to 25 ng of ligated plasmid DNA (or  $\sim$  5  $\mu$ l of ligated mix from 10  $\mu$ l ligation reaction) was mixed with the aliquot and incubated on ice for 30 min. The mixture was heat-shocked for 30 sec at 42° C and immediately put on ice for 1 min. 500  $\mu$ l of SOC medium was added to the microcentrifuge tube and incubated at 37° C for 1 h on a rotary shaker. The transformation mixture was centrifuged for 5 min at 1500 g, resuspended in 50  $\mu$ l LB broth and plated onto selective media plates.

#### 5.2.8.16 Preparation of electro-competent *A. tumefaciens* cells

The desired *Agrobacterium* strain was streaked out onto YEB agar plate containing adequate antibiotics and grown at 28° C for two days. A single colony was picked and a 5 ml YEB culture, containing appropriate antibiotics, was grown overnight at 28° C. The whole overnight culture was added to 200 ml YEB (without antibiotics) and grown to an OD600 of 0.6. Subsequently, the culture was chilled on ice for 15 – 30 min. From this point onwards bacteria were maintained at 4° C. Bacteria were centrifuged at 6000 g for 15 min and 4° C and the pellet was resuspended in 200 ml of ice-cold sterile water. Bacteria were again centrifuged at 6000 g for 15 min and 4° C. Bacteria were resuspended in 100 ml of ice-cold sterile water and centrifuged as described above. The bacterial pellet was resuspended in 4 ml of ice-cold 10 % glycerol and centrifuged as described above. Bacteria were resuspended in 600  $\mu$ l of ice-cold 10 % glycerol. 40  $\mu$ l aliquots were frozen in liquid nitrogen and stored at -80° C.

**5.2.8.17 Transformation of electro-competent *A. tumefaciens* cells**

50 ng of plasmid DNA was mixed with 40 µl of electro-competent *A. tumefaciens* cells, and transferred to an electroporation cuvette on ice (2 mm electrode distance; Eurogentec, Seraing, Belgium). The BioRad Gene Pulse™ apparatus was set to 25 µF, 2.5 kV and 400 Ω. The cells were pulsed once at the above settings for a second, the cuvette was put back on ice and immediately 1 ml of YEB medium was added to the cuvette. Cells were quickly resuspended by slowly pipetting and transferred to a 2 ml microcentrifuge tube. The tube was incubated for 3 h in an Eppendorf thermomixer at 28° C and 600 rpm. A 5 µl fraction of the transformation mixture was plated onto selection YEB agar plates.

**5.2.8.18 Localisation studies using confocal laser scanning microscopy (CLSM)**

Detailed analysis of intracellular fluorescence was performed by confocal laser scanning microscopy using a Zeiss LSM 680 (Zeiss, Germany) equipped with an Argon ion laser as an excitation source. YFP-tagged proteins were excited by a 514 nm laser line. Images were acquired in the multichannel tracking mode and analysed with Zeiss LSM510 software.



## Appendix

Lipase-like domain	EP domain
R16	N422
S19	V423
Y25	K424
H31	R425
E34	G483
A35	P484
G36	M486
V38	<b>K487</b>
Q116	<b>R488</b>
I142	G489
R152	R490
S167	P491
K174	T492
P213	<b>R493</b>
R214	I495
S287	

**Table S1:** DISPLAR results. List of amino acids in EDS1 that are predicted to bind DNA in the EDS1-SAG101 heterodimer. Amino acids mutated and analysed in this study are highlighted in bold.

EDS1 Mutants	EDS1	PAD4	SAG101
WT	Yes	Yes	Yes
K387A	Yes	Yes	Yes
K387R	Yes	Yes	Yes
K487A	Yes	Yes	Yes
K487R	Yes	Yes	Yes
K478A	Yes	Yes	Yes
K478R	Yes	Yes	Yes
R488A	Yes	Yes	Yes
R493A	Yes	Yes	Yes
KK478/487AA	Yes	Yes	Yes
KK478/487RR	Yes	Yes	Yes
3K_A	Yes	Yes	Yes
3K_R	Yes	Yes	Yes
N285A	Yes	Yes	Yes
N285D	Yes	Yes	Yes
D446A	Yes	Yes	Yes

**Table S2:** Y2H analysis. List of mutated EDS1 variants that were tested in Y2H for interaction with full length EDS1, PAD4 and SAG101.

Genotype	time point	total reads sequenced	reads aligned to <i>A.th</i>	aligned [%]
Col-0	0	22988417	22469415	97,7%
		22675474	20789704	91,7%
		28089150	26830087	95,5%
	4	27241413	25692552	94,3%
		26921378	25573582	95,0%
		23197320	22199779	95,7%
	8	22204110	21025906	94,7%
		25500318	23948598	93,9%
		26758004	24937005	93,2%
	24	27313346	26292984	96,3%
		21887947	20129715	92,0%
		28866131	26118208	90,5%
eds1-2	0	21889578	21353447	97,6%
		25835201	24069749	93,2%
		26428233	23965391	90,7%
	4	27752185	26611973	95,9%
		26222293	24937068	95,1%
		25603286	23855401	93,2%
	8	21628537	21011702	97,1%
		26237457	24118535	91,9%
		27230524	24206357	88,9%
	24	21645352	21013913	97,1%
		27382884	25105740	91,7%
		24302316	22783790	93,8%
cEDS1	0	21392107	20847201	97,5%
		25093759	23330952	93,0%
		26013399	24413705	93,9%
	4	23114257	22143882	95,8%
		25787375	24534777	95,1%
		23337041	22363456	95,8%
	8	26751052	25941923	97,0%
		22926551	21413284	93,4%
		27813598	24546515	88,3%
	24	26287080	25434330	96,8%
		26992984	24946245	92,4%
		27074443	25358103	93,7%
R493A	0	23288364	22498572	96,6%
		25686709	23587896	91,8%
		22097675	20807541	94,2%
	4	26705541	25395361	95,1%
		26428356	24737940	93,6%
		22458129	20851337	92,8%
	8	32313829	31366129	97,1%
		26044656	23397043	89,8%
		28739517	26222102	91,2%
	24	24654480	23646166	95,9%
		28354690	23497043	82,9%
		26614046	25033419	94,1%

**Table S3:** Evaluation of RNA-Seq results from different biological replicates.

time point	no. of DEGs
4hpi	13667
8hpi	12389
24hpi	15968

**Table S4:** Number of differentially expressed genes (DEGs) between plants infected with *Pst*/AvrRps4 compared to untreated plants ( $p < 0.05$ ).

Genotype	no. of DEGs
<i>eds1-2</i> /Col-0	7281
R493A/Col-0	1920
cEDS1/Col-0	100
R493A/ <i>eds1-2</i>	773
cEDS1/ <i>eds1-2</i>	5499
R493A/cEDS1	700

**Table S5:** DEGs between genotypes across 0, 4, 8 and 24 hpi with *Pst*/AvrRps4 ( $p < 0.05$ ).

cluster 4		
Genotype	8hpi	24hpi
<b>cEDS1/<i>eds1-2</i></b>	857/1269	1120/1269
<b>R493A/cEDS1</b>	499/1269	30/1269
<b>R493A/<i>eds1-2</i></b>	3/1269	705/1269

cluster 9		
Genotype	8hpi	24hpi
<b>cEDS1/<i>eds1-2</i></b>	297/1446	1444/1446
<b>R493A/cEDS1</b>	197/1446	185/1446
<b>R493A/<i>eds1-2</i></b>	0/1446	463/1446

**Table S6:** Number of DEGs in *Pst*/AvrRps4-ETI. DEGs between indicated genotypes at 8 and 24 hpi with *Pst*/AvrRps4 ( $p < 0.05$ ). Denominator indicates total number of DEGs in the entire cluster.

Mutant	Observed frequency	Expected frequency	X <sup>2</sup>	p-value
R493A #1	72/100	75/100	0.231	0.63
R493A #2	86/111	83/111	0.155	0.69
K478R #1	54/72	54/72	0	1.00
K478R #2	59/71	53/71	0.02	0.88
3K_R #1	66/93	70/93	0.14	0.70
3K_R #2	77/109	82/109	0.54	0.37

**Table S7:** X<sup>2</sup> goodness of fit and p-values for selected transgenic lines used in this thesis.

---

## References

- Aarts, N., Metz, M., Holub, E., Staskawicz, B. J., Daniels, M. J., & Parker, J. E. (1998). Different requirements for EDS1 and NDR1 by disease resistance genes define at least two R gene-mediated signaling pathways in Arabidopsis. *PNAS*, 95(17), 10306–11.
- Andrade, M. A., Perez-Iratxeta, C., & Ponting, C. P. (2001). Protein Repeats: Structures, Functions, and Evolution. *Journal of Structural Biology*, 134(2-3), 117–131. <http://doi.org/10.1006/jsbi.2001.4392>
- Ashkenazy, H., Erez, E., Martz, E., Pupko, T., & Ben-Tal, N. (2010). ConSurf 2010: calculating evolutionary conservation in sequence and structure of proteins and nucleic acids. *Nucleic Acids Research*, 38(Web Server issue), W529–33. <http://doi.org/10.1093/nar/gkq399>
- Atchley, W. R., & Fitch, W. M. (1997). A natural classification of the basic helix-loop-helix class of transcription factors. *PNAS*, 94(10), 5172–5176. <http://doi.org/10.1073/pnas.94.10.5172>
- Austin, M. J., Muskett, P., Kahn, K., Feys, B. J., Jones, J. D. G., & Parker, J. E. (2002). Regulatory role of SGT1 in early R gene-mediated plant defenses. *Science*, 295(5562), 2077–80. <http://doi.org/10.1126/science.1067747>
- Axtell, M. J., & Staskawicz, B. J. (2003). Initiation of RPS2-specified disease resistance in Arabidopsis is coupled to the AvrRpt2-directed elimination of RIN4. *Cell*, 112(3), 369–377. [http://doi.org/10.1016/S0092-8674\(03\)00036-9](http://doi.org/10.1016/S0092-8674(03)00036-9)
- Azevedo, C., Betsuyaku, S., Peart, J., Takahashi, A., Noël, L., Sadanandom, A., Casais, C., Parker, J., Shirasu, K. (2006). Role of SGT1 in resistance protein accumulation in plant immunity. *EMBO J*, 25(9), 2007–16. <http://doi.org/10.1038/sj.emboj.7601084>
- Azevedo, C., Sadanandom, A., Kitagawa, K., Freialdenhoven, A., Shirasu, K., & Schulze-Lefert, P. (2002). The RAR1 interactor SGT1, an essential component of R gene-triggered disease resistance. *Science*, 295(5562), 2073–6. <http://doi.org/10.1126/science.1067554>
- Bai, S., Liu, J., Chang, C., Zhang, L., Maekawa, T., Wang, Q., Xiao, W., Schulze-Lefert, p., Shen, Q.-H. (2012). Structure-Function Analysis of Barley NLR Immune Receptor MLA10 Reveals Its Cell Compartment Specific Activity in Cell Death and Disease Resistance. *PLoS Pathogens*, 8(6), e1002752. <http://doi.org/10.1371/journal.ppat.1002752>
- Bartsch, M., Bautor, J., & Parker, J. E. (2006). Salicylic Acid – Independent ENHANCED DISEASE SUSCEPTIBILITY1 Signaling in Arabidopsis Immunity and Cell Death Is Regulated by the Monooxygenase FMO1 and the Nudix Hydrolase NUDT7. *The Plant Cell*, 18(April), 1038–1051. <http://doi.org/10.1105/tpc.105.039982.1>
- Belkhadir, Y., Nimchuk, Z., Hubert, D. a, Mackey, D., & Dangl, J. L. (2004). Arabidopsis RIN4 Negatively Regulates Disease Resistance Mediated by RPS2 and RPM1 Downstream or Independent of the NDR1 Signal Modulator and Is Not Required for the Virulence Functions of Bacterial Type III Effectors AvrRpt2 or AvrRpm1, 2822–2835. <http://doi.org/10.1105/tpc.104.024117.mammalian>
-

- Bernoux, M., Ve, T., Williams, S., Warren, C., Valkov, E., Zhang, X., Ellis J. G., Kobe, B., Dodds, P. N. (2011). Structural and Functional Analysis of a Plant Resistance Protein TIR Domain Reveals Interfaces for Self-Association, Signaling, and Autoregulation. *Cell Host Microbe*, 9(3), 200–211. <http://doi.org/10.1016/j.chom.2011.02.009>.Bernoux
- Bhattacharjee, S., Halane, M. K., Kim, S. H., & Gassmann, W. (2011). Pathogen Effectors Target Arabidopsis EDS1 and Alter Its Interactions with Immune Regulators. *Science* (334)1405-08
- Birker, D., Heidrich, K., Takahara, H., Narusaka, M., Deslandes, L., Narusaka, Y., Reymond, M., Parker, J., O'Connell, R. (2009). A locus conferring resistance to *Colletotrichum higginsianum* is shared by four geographically distinct Arabidopsis accessions. *The Plant Journal*, 60(4), 602–13. <http://doi.org/10.1111/j.1365-313X.2009.03984.x>
- BLOCK, A., SCHMELZ, E., JONES, J. B., & KLEE, H. J. (2005). Coronatine and salicylic acid: the battle between Arabidopsis and *Pseudomonas* for phytohormone control. *Molecular Plant Pathology*, 6(1), 79–83. <http://doi.org/10.1111/j.1364-3703.2004.00265.x>
- Böhm, H., Albert, I., Fan, L., Reinhard, A., & Nürnberger, T. (2014). Immune receptor complexes at the plant cell surface. *Current Opinion in Plant Biology*, 20C, 47–54. <http://doi.org/10.1016/j.pbi.2014.04.007>
- Boller, T., & Felix, G. (2009). A renaissance of elicitors: perception of microbe-associated molecular patterns and danger signals by pattern-recognition receptors. *Annual Review of Plant Biology*, 60, 379–406. <http://doi.org/10.1146/annurev.arplant.57.032905.105346>
- Boyes, D. C., Nam, J., & Dangl, J. L. (1998). The Arabidopsis thaliana RPM1 disease resistance gene product is a peripheral plasma membrane protein that is degraded coincident with the hypersensitive response. *PNAS*, 95(26), 15849–15854. <http://doi.org/10.1073/pnas.95.26.15849>
- Brodersen, P., Petersen, M., Bjørn Nielsen, H., Zhu, S., Newman, M.-A., Shokat, K. M., Rietz, S., Parker, J., Mundy, J. (2006). Arabidopsis MAP kinase 4 regulates salicylic acid- and jasmonic acid/ethylene-dependent responses via EDS1 and PAD4. *The Plant Journal*, 47(4), 532–46. <http://doi.org/10.1111/j.1365-313X.2006.02806.x>
- Brooks, D. M., Bender, C. L., & Kunkel, B. N. (2005). The *Pseudomonas syringae* phytotoxin coronatine promotes virulence by overcoming salicylic acid-dependent defences in Arabidopsis thaliana. *Molecular Plant Pathology*, 6(6), 629–639. <http://doi.org/10.1111/j.1364-3703.2005.00311.x>
- Buscaill, P., & Rivas, S. (2014). Transcriptional control of plant defence responses. *Current Opinion in Plant Biology*, 20C, 35–46. <http://doi.org/10.1016/j.pbi.2014.04.004>
- Caarls, L., Pieterse, C. M. J., & Van Wees, S. C. M. (2015). How salicylic acid takes transcriptional control over jasmonic acid signaling. *Frontiers in Plant Science*, 6(3), 170. <http://doi.org/10.3389/fpls.2015.00170>
- Caillaud, M.-C., Asai, S., Rallapalli, G., Piquerez, S., Fabro, G., & Jones, J. D. G. (2013). A downy mildew effector attenuates salicylic Acid-triggered immunity in Arabidopsis by interacting with the host mediator complex. *PLoS Biology*, 11(12), e1001732.

- <http://doi.org/10.1371/journal.pbio.1001732>
- Cao, H., Bowling, S. A., & Gordon, A. S. (1994). Characterization of an Arabidopsis Mutant That Is Nonresponsive to Inducers of Systemic Acquired Resistance. *The Plant Cell*, 6(November), 1583–1592.
- Cesari, S., Bernoux, M., Moncuquet, P., Kroj, T., & Dodds, P. N. (2014). A novel conserved mechanism for plant NLR protein pairs: the ‘integrated decoy’ hypothesis. *Frontiers in Plant Science*, 5(November), 606. <http://doi.org/10.3389/fpls.2014.00606>
- Cesari, S., Thilliez, G., Ribot, C., Chalvon, V., Michel, C., Jauneau, A., Rivas, S., Okuyama, Y., Fournier, E., Tharreau, D., Terauchi, R., Kroj, T. (2013). The Rice Resistance Protein Pair RGA4/RGA5 Recognizes the Magnaporthe oryzae Effectors AVR-Pia and AVR1-CO39 by Direct Binding. *The Plant Cell*, 25(4), 1463–1481. <http://doi.org/10.1105/tpc.112.107201>
- Chang, C., Yu, D., Jiao, J., Jing, S., Schulze-Lefert, P., & Shen, Q.-H. (2013). Barley MLA immune receptors directly interfere with antagonistically acting transcription factors to initiate disease resistance signaling. *The Plant Cell*, 25(3), 1158–73. <http://doi.org/10.1105/tpc.113.109942>
- Chen, F., D’Auria, J. C., Tholl, D., Ross, J. R., Gershenzon, J., Noel, J. P., & Pichersky, E. (2003). An Arabidopsis thaliana gene for methylsalicylate biosynthesis, identified by a biochemical genomics approach, has a role in defense. *The Plant Journal*, 36, 577–588. <http://doi.org/10.1046/j.1365-313X.2003.01902.x>
- Chen, R., Jiang, H., Li, L., Zhai, Q., Qi, L., Zhou, W., Liu, X., Li, H., Zheng, W., Li, C. (2012). The Arabidopsis Mediator Subunit MED25 Differentially Regulates Jasmonate and Abscissic Acid Signaling through Interacting with the MYC2 and ABI5 Transcription Factors. *The Plant Cell*, 24(July), 2898–2916. <http://doi.org/10.1105/tpc.112.098277>
- Cherstvy, a G. (2009). Positively charged residues in DNA-binding domains of structural proteins follow sequence-specific positions of DNA phosphate groups. *The Journal of Physical Chemistry. B*, 113(13), 4242–7. <http://doi.org/10.1021/jp810009s>
- Chisholm, S. T., Coaker, G., Day, B., & Staskawicz, B. J. (2006). Host-microbe interactions: shaping the evolution of the plant immune response. *Cell*, 124(4), 803–14. <http://doi.org/10.1016/j.cell.2006.02.008>
- Chung, K., & Tasaka, M. (2011). RPT2a, a 26S proteasome AAA-ATPase, is directly involved in arabidopsis CC-NBS-LRR protein uni-1D-induced signaling pathways. *Plant and Cell Physiology*, 52(9), 1657–1664. <http://doi.org/10.1093/pcp/pcr099>
- Collier, S. M., & Moffett, P. (2009). NB-LRRs work a ‘bait and switch’ on pathogens. *Trends in Plant Science*, 14(10), 521–9. <http://doi.org/10.1016/j.tplants.2009.08.001>
- Cui, H., Tsuda, K., & Parker, J. E. (2015). Effector-triggered immunity: from pathogen perception to robust defense. *Annual Review of Plant Biology*, 66, 487–511. <http://doi.org/10.1146/annurev-arplant-050213-040012>
- D’Andrea, L. (2003). TPR proteins: the versatile helix. *Trends in Biochemical Sciences*, 28(12), 655–662. <http://doi.org/10.1016/j.tibs.2003.10.007>

- Danot, O., Marquenet, E., Vidal-Ingigliardi, D., & Richet, E. (2009). Wheel of Life, Wheel of Death: A Mechanistic Insight into Signaling by STAND Proteins. *Structure*, 17(2), 172–182. <http://doi.org/10.1016/j.str.2009.01.001>
- Deslandes, L., Olivier, J., Theulieres, F., Hirsch, J., Feng, D. X., Bittner-Eddy, P., Beynon, J., Marco, Y. (2002). Resistance to *Ralstonia solanacearum* in *Arabidopsis thaliana* is conferred by the recessive RRS1-R gene, a member of a novel family of resistance genes. *PNAS*, 99(4), 2404–2409. <http://doi.org/10.1073/pnas.032485099>
- Dodds, P. N., & Rathjen, J. P. (2010). Plant immunity: towards an integrated view of plant-pathogen interactions. *Nature Reviews. Genetics*, 11(8), 539–48. <http://doi.org/10.1038/nrg2812>
- Duke, S. O., & Dayan, F. E. (2011). Modes of Action of Microbially-Produced Phytotoxins. *Toxins*, 3(12), 1038–1064. <http://doi.org/10.3390/toxins3081038>
- Durrant, W. E., & Dong, X. (2004). Systemic acquired resistance. *Annual Review of Phytopathology*, 42, 185–209. <http://doi.org/10.1146/annurev.phyto.42.040803.140421>
- Eckardt, N. a. (2009). The Arabidopsis RPW8 Resistance Protein Is Recruited to the Extrahaustorial Membrane of Biotrophic Powdery Mildew Fungi. *The Plant Cell Online*, 21(9), 2543–2543. <http://doi.org/10.1105/tpc.109.210911>
- Edgar, R. C. (2004). MUSCLE: multiple sequence alignment with high accuracy and high throughput. *Nucleic Acids Research*, 32(5), 1792–7. <http://doi.org/10.1093/nar/gkh340>
- Eichmann, R., & Schäfer, P. (2015). Growth versus immunity-a redirection of the cell cycle? *Current Opinion in Plant Biology*, 26, 106–112. <http://doi.org/10.1016/j.pbi.2015.06.006>
- Ellisdon, A. M., & Stewart, M. (2012). Structural biology of the PCI-protein fold. *Bioarchitecture*, 2(4), 118–23. <http://doi.org/10.4161/bioa.21131>
- Falk, a, Feys, B. J., Frost, L. N., Jones, J. D., Daniels, M. J., & Parker, J. E. (1999). EDS1, an essential component of R gene-mediated disease resistance in Arabidopsis has homology to eukaryotic lipases. *PNAS*, 96(6), 3292–7. Retrieved from <http://www.pubmedcentral.nih.gov/articlerender.fcgi?artid=15935&tool=pmcentrez&render type=abstract>
- Fan, M., Bai, M.-Y., Kim, J.-G., Wang, T., Oh, E., Chen, L., Park, C. H., Son, S., Kim, S., Mudgett, M., Wang, Z.-Y. (2014). The bHLH Transcription Factor HBI1 Mediates the Trade-Off between Growth and Pathogen-Associated Molecular Pattern-Triggered Immunity in Arabidopsis. *The Plant Cell*, 26(February), 828–841. <http://doi.org/10.1105/tpc.113.121111>
- Fenyk, S., Townsend, P. D., Dixon, C. H., Spies, G. B., de San Eustaquio Campillo, A., Slootweg, E. J., Westerhof, L., Gawehns, F., Knight, M., Sharples, G., Goverse, A., Takken, F., Cann, M. J. (2015). The Potato Nucleotide-binding Leucine-rich Repeat (NLR) Immune Receptor Rx1 Is a Pathogen-dependent DNA-deforming Protein. *Journal of Biological Chemistry*, 290(41), 24945–24960. <http://doi.org/10.1074/jbc.M115.672121>
- Feys, B. J., Moisan, L. J., Newman, M. a, & Parker, J. E. (2001). Direct interaction between the



- Arabidopsis disease resistance signaling proteins, EDS1 and PAD4. *The EMBO Journal*, 20(19), 5400–11. <http://doi.org/10.1093/emboj/20.19.5400>
- Feys, B. J., Wiermer, M., Bhat, R. a, Moisan, L. J., Medina-Escobar, N., Neu, C., Cabral, A., Parker, J. E. (2005). Arabidopsis SENESCENCE-ASSOCIATED GENE101 stabilizes and signals within an ENHANCED DISEASE SUSCEPTIBILITY1 complex in plant innate immunity. *The Plant Cell*, 17(9), 2601–13. <http://doi.org/10.1105/tpc.105.033910>
- Flor. (1971). Current Status of the Gene-for-Gene. *Annual rev. phytopathol.*, 275–296.
- Gao, F., Dai, R., Pike, S. M., Qiu, W., & Gassmann, W. (2014). Functions of EDS1-like and PAD4 genes in grapevine defenses against powdery mildew. *Plant Molecular Biology*, 86(4-5), 381–393. <http://doi.org/10.1007/s11103-014-0235-4>
- Gao, F., Shu, X., Ali, M. B., Howard, S., Li, N., Winterhagen, P., Qiu, W., Gassmann, W. (2010a). A functional EDS1 ortholog is differentially regulated in powdery mildew resistant and susceptible grapevines and complements an Arabidopsis eds1 mutant. *Planta*, 231, 1037–1047. <http://doi.org/10.1007/s00425-010-1107-z>
- Gao, H., Wu, X., Chai, J., & Han, Z. (2012). Crystal structure of a TALE protein reveals an extended N-terminal DNA binding region. *Cell Research*, 22(12), 1716–20. <http://doi.org/10.1038/cr.2012.156>
- Garces, R. G., & Gillon, W. (2007). Atomic model of human Rcd-1 reveals an armadillo -like-repeat protein with in vitro nucleic acid binding properties, 176–188. <http://doi.org/10.1110/ps.062600507.Schizosaccharomyces>
- García, A. V, Blanvillain-Baufumé, S., Huibers, R. P., Wiermer, M., Li, G., Gobbato, E., ... Parker, J. E. (2010). Balanced nuclear and cytoplasmic activities of EDS1 are required for a complete plant innate immune response. *PLoS Pathogens*, 6(7), e1000970. <http://doi.org/10.1371/journal.ppat.1000970>
- García, A. V, & Parker, J. E. (2009). Heaven's Gate: nuclear accessibility and activities of plant immune regulators. *Trends in Plant Science*, 14(9), 479–87. <http://doi.org/10.1016/j.tplants.2009.07.004>
- Geng, X., Jin, L., Shimada, M., Kim, M. G., & Mackey, D. (2014). The phytotoxin coronatine is a multifunctional component of the virulence armament of Pseudomonas syringae. *Planta*, 240, 1149–1165. <http://doi.org/10.1007/s00425-014-2151-x>
- Ghoorah, A., Devignes, M.-D., Alborzi, S., Smaïl-Tabbone, M., & Ritchie, D. (2015). A Structure-Based Classification and Analysis of Protein Domain Family Binding Sites and Their Interactions. *Biology*, 4(2), 327–343. <http://doi.org/10.3390/biology4020327>
- Gimenez-Ibanez, S., Boter, M., Fernández-Barbero, G., Chini, A., Rathjen, J. P., & Solano, R. (2014). The bacterial effector HopX1 targets JAZ transcriptional repressors to activate jasmonate signaling and promote infection in Arabidopsis. *PLoS Biology*, 12(2), e1001792. <http://doi.org/10.1371/journal.pbio.1001792>
- Gimenez-ibanez, S., Boter, M., & Solano, R. (2015). Novel players fine-tune plant trade-offs, 83–100. <http://doi.org/10.1042/BSE0580083>

- Griebel, T., Maekawa, T., & Parker, J. E. (2014). NOD-like receptor cooperativity in effector-triggered immunity. *Trends in Immunology*, 35(11), 562–570. <http://doi.org/10.1016/j.it.2014.09.005>
- Groves, M. R., & Barford, D. (1999). Topological characteristics of helical repeat proteins. *Current Opinion in Structural Biology*, 9, 383–389. [http://doi.org/10.1016/S0959-440X\(99\)80052-9](http://doi.org/10.1016/S0959-440X(99)80052-9)
- Guharoy, M., & Chakrabarti, P. (2007). Secondary structure based analysis and classification of biological interfaces: Identification of binding motifs in protein-protein interactions. *Bioinformatics*, 23(15), 1909–1918. <http://doi.org/10.1093/bioinformatics/btm274>
- He, Y., & Gan, S. (2002). A Gene Encoding an Acyl Hydrolase Is Involved in Leaf Senescence in Arabidopsis, 14(April), 805–815. <http://doi.org/10.1105/tpc.010422.and>
- Heidrich, K., Wirthmueller, L., Tasset, C., Pouzet, C., Deslandes, L., & Parker, J. E. (2011). Arabidopsis EDS1 connects pathogen effector recognition to cell compartment-specific immune responses. *Science*, 334(6061), 1401–4. <http://doi.org/10.1126/science.1211641>
- Holm, L., & Rosenstrom, P. (2010). Dali server: conservation mapping in 3D. *Nucleic Acids Research*, 38(Web Server), W545–W549. <http://doi.org/10.1093/nar/gkq366>
- Hu, Z., Yan, C., Liu, P., Huang, Z., Ma, R., Zhang, C., Chai, J. (2013). Crystal structure of NLRC4 reveals its autoinhibition mechanism. *Science*, 341(6142), 172–5. <http://doi.org/10.1126/science.1236381>
- Hu, Z., Zhou, Q., Zhang, C., Fan, S., Cheng, W., Zhao, Y., Chai, J. (2015). Structural and biochemical basis for induced self-propagation of NLRC4, 350(October), 1–11. <http://doi.org/10.1126/science.aac5489>
- Huot, B., Yao, J., Montgomery, B. L., & He, S. Y. (2014). Growth-Defense Tradeoffs in Plants: A Balancing Act to Optimize Fitness. *Molecular Plant*, 7(8), 1267–1287. <http://doi.org/10.1093/mp/ssu049>
- Iii, B. F. H., Boyes, D. C., Siefers, N., Wiig, A., Kauffman, S., Grant, M. R., Dangl, J. L. (2002). An Evolutionarily Conserved Mediator of Plant Disease Resistance Gene Function Is Required for Normal Arabidopsis Development Imperial College at Wye Curriculum in Genetics. *Developmental Cell*, 2, 807–817.
- Inoue, H., Hayashi, N., Matsushita, A., Xinqiong, L., Nakayama, A., Sugano, S., Jiang, C-J., Takatsuji, H. (2013). Blast resistance of CC-NB-LRR protein Pb1 is mediated by WRKY45 through protein-protein interaction. *PNAS*, 110(23), 9577–82. <http://doi.org/10.1073/pnas.1222155110>
- Jacob, F., Vernaldi, S., & Maekawa, T. (2013). Evolution and Conservation of Plant NLR Functions. *Frontiers in Immunology*, 4(September), 297. <http://doi.org/10.3389/fimmu.2013.00297>
- Janssen, B. J., & Snowden, K. C. (2012). Strigolactone and karrikin signal perception: receptors, enzymes, or both? *Frontiers in Plant Science*, 3(December), 296. <http://doi.org/10.3389/fpls.2012.00296>

- Jeong, R.-D., Zhu, S., Kachroo, A., & Kachroo, P. (2012). New insights into resistance protein-mediated signaling against turnip crinkle virus in Arabidopsis. *Journal of Plant Biochemistry and Biotechnology*, 21(S1), 48–51. <http://doi.org/10.1007/s13562-012-0138-x>
- Jiang, S., Yao, J., Ma, K.-W., Zhou, H., Song, J., He, S. Y., & Ma, W. (2013). Bacterial Effector Activates Jasmonate Signaling by Directly Targeting JAZ Transcriptional Repressors. *PLoS Pathogens*, 9(10), e1003715. <http://doi.org/10.1371/journal.ppat.1003715>
- Jirage, D., Tootle, T. L., Reuber, T. L., Frost, L. N., Feys, B. J., Parker, J. E., Ausbel, F. M., Glazebrook, J. (1999). Arabidopsis thaliana PAD4 encodes a lipase-like gene that is important for salicylic acid signaling. *PNAS*, 96(23), 13583–8. Retrieved from <http://www.pubmedcentral.nih.gov/articlerender.fcgi?artid=23991&tool=pmcentrez&render type=abstract>
- Johal, G. S., & Briggs, S. P. (1992). Reductase activity encoded by the HM1 disease resistance gene in maize. *Science*, 258(5084), 985–987. <http://doi.org/10.1126/science.1359642>
- Jones, J. D. G., & Dangl, J. L. (2006). The plant immune system. *Nature*, 444(7117), 323–9. <http://doi.org/10.1038/nature05286>
- Karasov, T. L., Horton, M. W., & Bergelson, J. (2014). Genomic variability as a driver of plant-pathogen coevolution? *Current Opinion in Plant Biology*, 18, 24–30. <http://doi.org/10.1016/j.pbi.2013.12.003>
- Katsir, L., Schillmiller, A. L., Staswick, P. E., He, S. Y., & Howe, G. a. (2008). COI1 is a critical component of a receptor for jasmonate and the bacterial virulence factor coronatine. *PNAS*, 105(19), 7100–7105. <http://doi.org/10.1073/pnas.0802332105>
- Kazan, K., & Manners, J. M. (2013). MYC2: The master in action. *Molecular Plant*, 6(3), 686–703. <http://doi.org/10.1093/mp/sss128>
- Ke, Y., Liu, H., Li, X., Xiao, J., & Wang, S. (2014). Rice Os *PAD4* functions differently from Arabidopsis At *PAD4* in host-pathogen interactions. *The Plant Journal*, 78, 619–631. <http://doi.org/10.1111/tpj.12500>
- Kemen, E., & Jones, J. D. G. (2012). Obligate biotroph parasitism: can we link genomes to lifestyles? *Trends in Plant Science*, 17(8), 448–57. <http://doi.org/10.1016/j.tplants.2012.04.005>
- Kemen, E., Kemen, A. C., Rafiqi, M., Hempel, U., Mendgen, K., Hahn, M., & Voegelé, R. T. (2005). Identification of a Protein from Rust Fungi Transferred from Haustoria into Infected Plant Cells. *Molecular Plant-Microbe Interactions*, 18(11), 1130–1139. <http://doi.org/10.1094/MPMI-18-1130>
- Kim, J. B., Spotts, G. D., Halvorsen, Y. D., Shih, H. M., Ellenberger, T., Towle, H. C., & Spiegelman, B. M. (1995). Dual DNA binding specificity of ADD1/SREBP1 controlled by a single amino acid in the basic helix-loop-helix domain. *Molecular and Cellular Biology*, 15(5), 2582–2588.
- Kim, M. G., da Cunha, L., McFall, A. J., Belkhadir, Y., DebRoy, S., Dangl, J. L., & Mackey, D. (2005). Two *Pseudomonas syringae* Type III Effectors Inhibit RIN4-Regulated Basal

- Defense in Arabidopsis. *Cell*, 121(5), 749–759. <http://doi.org/10.1016/j.cell.2005.03.025>
- Kim, T.-H., Kunz, H.-H., Bhattacharjee, S., Hauser, F., Park, J., Engineer, C., Liu, A., Ha, T., Parker, J. E., Gassmann, W., Schroeder, J. I. (2012). Natural variation in small molecule-induced TIR-NB-LRR signaling induces root growth arrest via EDS1- and PAD4-complexed R protein VICTR in Arabidopsis. *The Plant Cell*, 24(12), 5177–92. <http://doi.org/10.1105/tpc.112.107235>
- Kim, Y., Tsuda, K., Igarashi, D., Hillmer, R. A., Sakakibara, H., Myers, C. L., & Katagiri, F. (2014). Mechanisms underlying robustness and tunability in a plant immune signaling network. *Cell Host & Microbe*, 15(1), 84–94. <http://doi.org/10.1016/j.chom.2013.12.002>
- Kunkel, B. N., Bent, A. F., Dahlbeck, D., Innes, R. W., & Staskawicz, B. J. (1993). RPS2, an Arabidopsis disease resistance locus specifying recognition of *Pseudomonas syringae* strains expressing the avirulence gene *avrRpt2*. *The Plant Cell*, 5(8), 865–75. <http://doi.org/10.1105/tpc.5.8.865>
- Kunkel, B. N., & Brooks, D. M. (2002). Cross talk between signaling pathways in pathogen defense. *Current Opinion in Plant Biology*, 5, 325–331. [http://doi.org/10.1016/S1369-5266\(02\)00275-3](http://doi.org/10.1016/S1369-5266(02)00275-3)
- Kwon, S. Il, Kim, S. H., Bhattacharjee, S., Noh, J. J., & Gassmann, W. (2009). SRFR1, a suppressor of effector-triggered immunity, encodes a conserved tetratricopeptide repeat protein with similarity to transcriptional repressors. *Plant Journal*, 57(1), 109–119. <http://doi.org/10.1111/j.1365-313X.2008.03669.x>
- Le Roux, C., Huet, G., Jauneau, A., Camborde, L., Trémousaygue, D., Kraut, A., Zhou, B., Levallant, M., Adachi, H., Yoshioka, H., Raffaele, S., Berthome, R., Coute, Y., Parker, J. E., Deslandes, L. (2015). A Receptor Pair with an Integrated Decoy Converts Pathogen Disabling of Transcription Factors to Immunity. *Cell*, 161, 1074–1088. <http://doi.org/10.1016/j.cell.2015.04.025>
- Lechtenberg, B. C., Mace, P. D., & Riedl, S. J. (2014). Structural mechanisms in NLR inflammasome signaling. *Current Opinion in Structural Biology*, 29C, 17–25. <http://doi.org/10.1016/j.sbi.2014.08.011>
- Lenfant, N., Hotelier, T., Velluet, E., Bourne, Y., Marchot, P., & Chatonnet, A. (2013). ESTHER, the database of the  $\alpha/\beta$ -hydrolase fold superfamily of proteins: tools to explore diversity of functions. *Nucleic Acids Research*, 41(Database issue), D423–9. <http://doi.org/10.1093/nar/gks1154>
- Li, M., Ma, X., Chiang, Y.-H., Yadeta, K. A., Ding, P., Dong, L., Li, X., Yu, Y., Zhang, L., Shen, Q.-H., Xia, B., Coaker, G., Liu, D., Zhou, J.-M. (2014). Proline Isomerization of the Immune Receptor-Interacting Protein RIN4 by a Cyclophilin Inhibits Effector-Triggered Immunity in Arabidopsis. *Cell Host & Microbe*, 16(4), 473–483. <http://doi.org/10.1016/j.chom.2014.09.007>
- Li, X., Clarke, J. D., Zhang, Y., & Dong, X. (2001). Activation of an EDS1-mediated R-gene pathway in the *snc1* mutant leads to constitutive, NPR1-independent pathogen resistance. *Molecular Plant-Microbe Interactions : MPMI*, 14(10), 1131–1139.

- <http://doi.org/10.1094/MPMI.2001.14.10.1131>
- Li, Y., Li, S., Bi, D., Cheng, Y. T., Li, X., & Zhang, Y. (2010). SRFR1 Negatively Regulates Plant NB-LRR Resistance Protein Accumulation to Prevent Autoimmunity. *PLoS Pathogens*, 6(9), e1001111. <http://doi.org/10.1371/journal.ppat.1001111>
- Lingaraju, G. M., Bunker, R. D., Cavadini, S., Hess, D., Hassiepen, U., Renatus, M., Fischer, E., Thomä, N. H. (2014). Crystal structure of the human COP9 signalosome. *Nature*, 512(7513), 161–5. <http://doi.org/10.1038/nature13566>
- Loake, G., & Grant, M. (2007). Salicylic acid in plant defence--the players and protagonists. *Current Opinion in Plant Biology*, 10(5), 466–72. <http://doi.org/10.1016/j.pbi.2007.08.008>
- Macho, A. P., & Zipfel, C. (2014). Plant PRRs and the activation of innate immune signaling. *Molecular Cell*, 54(2), 263–72. <http://doi.org/10.1016/j.molcel.2014.03.028>
- Maekawa, T., Kufer, T. a, & Schulze-Lefert, P. (2011). NLR functions in plant and animal immune systems: so far and yet so close. *Nature Immunology*, 12(9), 817–26. <http://doi.org/10.1038/ni.2083>
- Makandar, R., Nalam, V. J., Chowdhury, Z., Sarowar, S., Klossner, G., Lee, H., Burdan, D., Trick, H., Gobbato, E., Parker, J. E., Shah, J. (2015). The Combined Action of ENHANCED DISEASE SUSCEPTIBILITY1, PHYTOALEXIN DEFICIENT4, and SENESCENCE-ASSOCIATED101 Promotes Salicylic Acid-Mediated Defenses to Limit Fusarium graminearum Infection in Arabidopsis thaliana. *Molecular Plant-Microbe Interactions*, 28(8), 943–953. Retrieved from <http://apsjournals.apsnet.org/doi/full/10.1094/MPMI-04-15-0079-R>
- Maqbool, a, Saitoh, H., Franceschetti, M., Stevenson, C., Uemura, a, Kanzaki, H., Kamoun, S., Terauchi, R., Banfield, M. J. (2015). Structural basis of pathogen recognition by an integrated HMA domain in a plant NLR immune receptor. *eLife*, 4(Cc), 1–24. <http://doi.org/10.7554/eLife.08709>
- Martin, G. B., Brommonschenkel, S. H., Chunwongse, J., Frary, A., Ganai, M. W., Spivey, R., Wu, T., Earle, E., Tanksley, S. D. (1993). Map-Based Cloning of a Protein-Kinase Gene Conferring Disease Resistance in Tomato. *Science*, 262(5138), 1432–1436. Retrieved from <Go to ISI>://A1993MJ04600037\ <http://www.sciencemag.org/content/262/5138/1432>
- Mauch, S., Shen, Q., Peart, J., Devoto, A., & Casais, C. (2004). RAR1 Positively Controls Steady State Levels of Barley MLA Resistance Proteins and Enables Sufficient MLA6 Accumulation for Effective Resistance, 16(December), 3480–3495. <http://doi.org/10.1105/tpc.104.026682.1>
- Meinzer, U., Barreau, F., Esmiol-Welterlin, S., Jung, C., Villard, C., Léger, T., Sanah, B., Berrebi, D., Dussailant, M., ALnabhani, Z., Roy, M., Bonacorsi, S., Watz, H., Perroy, J., Ollendorf, V., Hugot, J. P. (2012). Yersinia pseudotuberculosis effector YopJ subverts the Nod2/RICK/TAK1 pathway and activates caspase-1 to induce intestinal barrier dysfunction. *Cell Host and Microbe*, 11, 337–351. <http://doi.org/10.1016/j.chom.2012.02.009>
- Melotto, M., Underwood, W., Koczan, J., Nomura, K., & He, S. Y. (2006). Plant Stomata Function in Innate Immunity against Bacterial Invasion. *Cell*, 126(5), 969–980.

- <http://doi.org/10.1016/j.cell.2006.06.054>
- Mindrinos, M., Katagiri, F., Yu, G. L., & Ausubel, F. M. (1994). The *A. thaliana* disease resistance gene RPS2 encodes a protein containing a nucleotide-binding site and leucine-rich repeats. *Cell*, 78(6), 1089–1099. [http://doi.org/10.1016/0092-8674\(94\)90282-8](http://doi.org/10.1016/0092-8674(94)90282-8)
- Mittal, S., & Davis, K. R. (1995). Role of the phytotoxin coronatine in the infection of *Arabidopsis thaliana* by *Pseudomonas syringae* pv. tomato. *Molecular Plant-Microbe Interactions : MPMI*.
- Moore, J. W., Loake, G. J., & Spoel, S. H. (2011). Transcription Dynamics in Plant Immunity. *The Plant Cell*, 23(August), 2809–2820. <http://doi.org/10.1105/tpc.111.087346>
- Mukhtar, M. S., Carvunis, A., Dreze, M., Epple, P., Steinbrenner, J., Moore, J., Beynon, J. (2011). Plant Immune System Network, (July), 596–602.
- Murase, K., Hirano, Y., Sun, T., & Hakoshima, T. (2008). Gibberellin-induced DELLA recognition by the gibberellin receptor GID1. *Nature*, 456(November), 459–463. <http://doi.org/10.1038/nature07519>
- Narusaka, M., Shirasu, K., Noutoshi, Y., Kubo, Y., Shiraishi, T., Iwabuchi, M., & Narusaka, Y. (2009). *RRS1* and *RPS4* provide a dual *Resistance*- gene system against fungal and bacterial pathogens. *The Plant Journal*, 60, 218–226. <http://doi.org/10.1111/j.1365-313X.2009.03949.x>
- Naseem, M., Kaltdorf, M., & Dandekar, T. (2015). The nexus between growth and defence signalling: auxin and cytokinin modulate plant immune response pathways. *Journal of Experimental Botany*, 66, 4885–4896. <http://doi.org/10.1093/jxb/erv297>
- Navarro, L., Zipfel, C., Rowland, O., Keller, I., Robatzek, S., Boller, T., & Jones, J. D. G. (2004). The Transcriptional Innate Immune Response to flg22 . Interplay and Overlap with Avr Gene-Dependent Defense Responses and Bacterial Pathogenesis 1 [ w ], 135(June), 1113–1128. <http://doi.org/10.1104/pp.103.036749.1>
- Nawrath, C. (1999). Salicylic Acid Induction Deficient Mutants of *Arabidopsis* Express PR-2 and PR-5 and Accumulate High Levels of Camalexin after Pathogen Inoculation. *The Plant Cell Online*, 11(8), 1393–1404. <http://doi.org/10.1105/tpc.11.8.1393>
- Ng, G., Seabolt, S., Zhang, C., Salimian, S., Watkins, T. a, & Lu, H. (2011). Genetic dissection of salicylic acid-mediated defense signaling networks in *Arabidopsis*. *Genetics*, 189(3), 851–9. <http://doi.org/10.1534/genetics.111.132332>
- Nürnberg, T., Brunner, F., Kemmerling, B., & Piater, L. (2004). Innate immunity in plants and animals: Striking similarities and obvious differences. *Immunological Reviews*, 198, 249–266. <http://doi.org/10.1111/j.0105-2896.2004.0119.x>
- Ollis, D. L., Cheah, E., Cygler, M., Dijkstra, B., Frolova, F., Franken, S. M., Harel, M., Remington, J., Silman, I., Schrag, J., Sussman, J., Verschueren, K., Goldman, A. (1992). The  $\alpha / \beta$  hydrolase fold. *Protein Engineering, Design and Selection*, 5(3), 197–211. <http://doi.org/10.1093/protein/5.3.197>
- Overmyer, K., Brosché, M., & Kangasjärvi, J. (2003). Reactive oxygen species and hormonal

- control of cell death. *Trends in Plant Science*, 8(7), 335–342. [http://doi.org/10.1016/S1360-1385\(03\)00135-3](http://doi.org/10.1016/S1360-1385(03)00135-3)
- Parker, J. E., Holub, E. B., Frost, L. N., Falk, A., Gunn, N. D., & Danielsa, M. J. (1996). Characterization of eds1, a Mutation in Arabidopsis Suppressing Resistance to Peronospora parasitica Specified by Several Different RPP Genes, 8(November), 2033–2046.
- Pathare, G. R., Nagy, I., Bohn, S., Unverdorben, P., Hubert, A., Korner, R., Nickel, S., Lasker, K., Sali, A., Tamura, T., Nishioka, T., Forster, F., Baumeister, W., Bracher, A. (2012). The proteasomal subunit Rpn6 is a molecular clamp holding the core and regulatory subcomplexes together. *PNAS*, 109(1), 149–154. <http://doi.org/10.1073/pnas.1117648108>
- Pegadaraju, V., Louis, J., Singh, V., Reese, J. C., Bautor, J., Feys, B. J., Cook, G., Parker J. E., Shah, J. (2007). Phloem-based resistance to green peach aphid is controlled by Arabidopsis PHYTOALEXIN DEFICIENT4 without its signaling partner ENHANCED DISEASE SUSCEPTIBILITY1. *The Plant Journal*, 52(2), 332–341. <http://doi.org/10.1111/j.1365-3113.2007.03241.x>
- Pieterse, C. M. J., Leon-Reyes, A., Van der Ent, S., & Van Wees, S. C. M. (2009). Networking by small-molecule hormones in plant immunity. *Nature Chemical Biology*, 5(5), 308–316. <http://doi.org/10.1038/nchembio.164>
- Ponting, C. P., & Russell, R. B. (2000). Identification of distant homologues of fibroblast growth factors suggests a common ancestor for all beta-trefoil proteins. *Journal of Molecular Biology*, 302(5), 1041–1047. <http://doi.org/10.1006/jmbi.2000.4087>
- Pré, M., Atallah, M., Champion, A., De Vos, M., Pieterse, C. M. J., & Memelink, J. (2008). The AP2/ERF domain transcription factor ORA59 integrates jasmonic acid and ethylene signals in plant defense. *Plant Physiology*, 147(July), 1347–1357. <http://doi.org/10.1104/pp.108.117523>
- Rietz, S., Stamm, A., Malonek, S., Wagner, S., Becker, D., Medina-Escobar, N., Vlot, A. C., Feys, B. J., Niefind, K., Parker, J. E. (2011). Different roles of Enhanced Disease Susceptibility1 (EDS1) bound to and dissociated from Phytoalexin Deficient4 (PAD4) in Arabidopsis immunity. *The New Phytologist*, 191(1), 107–19. <http://doi.org/10.1111/j.1469-8137.2011.03675.x>
- Rispa, D., Henri, J., Tilbeurgh, H. V. A. N., & Graille, M. (2011). Structural and functional analysis of Nro1 / Ett1 : a protein involved in translation termination in S. cerevisiae and in O<sub>2</sub>-mediated gene control in S. pombe, 1213–1224. <http://doi.org/10.1261/rna.2697111.5>
- Rivas-San Vicente, M., & Plasencia, J. (2011). Salicylic acid beyond defence: its role in plant growth and development. *Journal of Experimental Botany*, 62(10), 3321–38. <http://doi.org/10.1093/jxb/err031>
- Sarris, P. F., Duxbury, Z., Huh, S. U., Ma, Y., Segonzac, C., Sklenar, J., Derbyshire, P., Cevik, V., Rallapalli, G., Saucet, S., Wirthmuller, L., Menke, F., Sohn, K. H., Jones, J. D. G. (2015). A Plant Immune Receptor Detects Pathogen Effectors that Target WRKY Transcription Factors. *Cell*, 161, 1089–1100. <http://doi.org/10.1016/j.cell.2015.04.024>
- Sasaki-Sekimoto, Y., Jikumaru, Y., Obayashi, T., Saito, H., Masuda, S., Kamiya, Y., Ohta, H.,

- Shirasu, K. (2013). *Basic helix-loop-helix transcription factors JASMONATE-ASSOCIATED MYC2-LIKE1 (JAM1), JAM2, and JAM3 are negative regulators of jasmonate responses in Arabidopsis*. *Plant physiology* (Vol. 163). <http://doi.org/10.1104/pp.113.220129>
- Schneider, M., Hellerschmied, D., Schubert, T., Amlacher, S., Vinayachandran, V., Reja, R., Pugh, F., Clausen, T., Köhler, A. (2015). The Nuclear Pore-Associated TREX-2 Complex Employs Mediator to Regulate Gene Expression. *Cell*, 162(5), 1016–1028. <http://doi.org/10.1016/j.cell.2015.07.059>
- Schulze-Lefert, P. (2004). Plant Immunity: The Origami of Receptor Activation. *Current Biology*, 14(1), R22–R24. <http://doi.org/10.1016/j.cub.2003.12.017>
- Schwechheimer, C., Serino, G., & Deng, X.-W. (2002). Multiple ubiquitin ligase-mediated processes require COP9 signalosome and AXR1 function. *The Plant Cell*, 14(10), 2553–2563. <http://doi.org/10.1105/tpc.003434>
- Serino, G., Su, H., Peng, Z., Tsuge, T., Wei, N., Gu, H., & Deng, X. W. (2003). Characterization of the last subunit of the Arabidopsis COP9 signalosome: Implications for the overall structure and origin of the complex. *The Plant Cell Online*, 15(3), 719. <http://doi.org/10.1105/tpc.009092>
- Seyfferth, C., & Tsuda, K. (2014). Salicylic acid signal transduction: the initiation of biosynthesis, perception and transcriptional reprogramming. *Frontiers in Plant Science*, 5(December), 1–10. <http://doi.org/10.3389/fpls.2014.00697>
- Shapiro, A. D., & Zhang, C. (2001). The Role of NDR1 in Avirulence Gene-Directed Signaling and Control of Programmed Cell Death in Arabidopsis 1, 127(November), 1089–1101. <http://doi.org/10.1104/pp.010096.1>
- Shimada, A., Ueguchi-Tanaka, M., Nakatsu, T., Nakajima, M., Naoe, Y., Ohmiya, H., ... Matsuoka, M. (2008). Structural basis for gibberellin recognition by its receptor GID1. *Nature*, 456(7221), 520–3. <http://doi.org/10.1038/nature07546>
- Sinapidou, E., Williams, K., Nott, L., Bahkt, S., Tör, M., Crute, I., Bittner-Eddy, P., Beynon, J. (2004). Two TIR:NB:LRR genes are required to specify resistance to *Peronospora parasitica* isolate Cala2 in Arabidopsis. *The Plant Journal*, 38(6), 898–909. <http://doi.org/10.1111/j.1365-313X.2004.02099.x>
- Singh, I., & Shah, K. (2012). In silico study of interaction between rice proteins enhanced disease susceptibility 1 and phytoalexin deficient 4, the regulators of salicylic acid signalling pathway. *Journal of Biosciences*, 37(3), 563–571. <http://doi.org/10.1007/s12038-012-9208-4>
- Spoel, S. H., & Dong, X. (2012). How do plants achieve immunity? Defence without specialized immune cells. *Nature Reviews. Immunology*, 12(2), 89–100. <http://doi.org/10.1038/nri3141>
- Staskawicz, B. J., Ausubel, F. M., Baker, B. J., Ellis, J. G., & Jones, J. D. G. (1992). Molecular genetics of Plant Disease Resistance. *Science*, 268(6).
- Steinbrenner, A. D., Goritschnig, S., & Staskawicz, B. J. (2015). Recognition and Activation



- Domains Contribute to Allele-Specific Responses of an Arabidopsis NLR Receptor to an Oomycete Effector Protein. *PLOS Pathogens*, 11(2), e1004665.  
<http://doi.org/10.1371/journal.ppat.1004665>
- Takken, F. L., & Goverse, A. (2012). How to build a pathogen detector: structural basis of NB-LRR function. *Current Opinion in Plant Biology*, 15(4), 375–384.  
<http://doi.org/10.1016/j.pbi.2012.05.001>
- Tao, Y., Xie, Z., Chen, W., Glazebrook, J., Chang, H., Han, B., Zhu, T., Zou, G., Katagiri, F. (2003). Quantitative Nature of Arabidopsis Responses during Compatible and Incompatible Interactions with the Bacterial Pathogen *Pseudomonas syringae*, 15(February), 317–330.  
<http://doi.org/10.1105/tpc.007591.can>
- Tasset, C., Bernoux, M., Jauneau, A., Pouzet, C., Brière, C., Kieffer-Jacquino, S., Rivas, S., Marco, Y., Deslandes, L. (2010). Autoacetylation of the *Ralstonia solanacearum* effector PopP2 targets a lysine residue essential for RRS1-R-mediated immunity in Arabidopsis. *PLoS Pathogens*, 6(11), e1001202. <http://doi.org/10.1371/journal.ppat.1001202>
- Thaler, J. S., Humphrey, P. T., & Whiteman, N. K. (2012). Evolution of jasmonate and salicylate signal crosstalk. *Trends in Plant Science*, 17(5), 260–270.  
<http://doi.org/10.1016/j.tplants.2012.02.010>
- Thomma, B. P. H. J., Nurnberger, T., & Joosten, M. H. A. J. (2011). Of PAMPs and Effectors: The Blurred PTI-ETI Dichotomy. *The Plant Cell*, 23(1), 4–15.  
<http://doi.org/10.1105/tpc.110.082602>
- Tjong, H., & Zhou, H.-X. (2007). DISPLAR: an accurate method for predicting DNA-binding sites on protein surfaces. *Nucleic Acids Research*, 35(5), 1465–77.  
<http://doi.org/10.1093/nar/gkm008>
- Tsuda, K., & Katagiri, F. (2010). Comparing signaling mechanisms engaged in pattern-triggered and effector-triggered immunity. *Current Opinion in Plant Biology*, 13(4), 459–465.  
<http://doi.org/10.1016/j.pbi.2010.04.006>
- Tsuda, K., Mine, A., Bethke, G., Igarashi, D., Botanga, C. J., Tsuda, Y., Glazebrook, J., Sato, M., Katagiri, F. (2013). Dual regulation of gene expression mediated by extended MAPK activation and salicylic acid contributes to robust innate immunity in Arabidopsis thaliana. *PLoS Genetics*, 9(12), e1004015. <http://doi.org/10.1371/journal.pgen.1004015>
- Tsuda, K., Sato, M., Glazebrook, J., Cohen, J. D., & Katagiri, F. (2008). Interplay between MAMP-triggered and SA-mediated defense responses. *Plant Journal*, 53(5), 763–775.  
<http://doi.org/10.1111/j.1365-3113X.2007.03369.x>
- Tsuda, K., Sato, M., Stoddard, T., Glazebrook, J., & Katagiri, F. (2009). Network properties of robust immunity in plants. *PLoS Genetics*, 5(12), e1000772.  
<http://doi.org/10.1371/journal.pgen.1000772>
- Tsuda, K., & Somssich, I. E. (2015). Tansley review Transcriptional networks in plant immunity, 2.
- Uppalapati, S. R., Ishiga, Y., Wangdi, T., Kunkel, B. N., Anand, A., Mysore, K. S., & Bender, C.

- L. (2007). The phytotoxin coronatine contributes to pathogen fitness and is required for suppression of salicylic acid accumulation in tomato inoculated with *Pseudomonas syringae* pv. tomato DC3000. *Molecular Plant-Microbe Interactions* : MPMI, 20(8), 955–965. <http://doi.org/10.1094/MPMI-20-8-0955>
- van der Biezen, E. a, Freddie, C. T., Kahn, K., Parker, J. E., & Jones, J. D. G. (2002). Arabidopsis RPP4 is a member of the RPP5 multigene family of TIR-NB-LRR genes and confers downy mildew resistance through multiple signalling components. *The Plant Journal*, 29(4), 439–51. Retrieved from <http://www.ncbi.nlm.nih.gov/pubmed/11846877>
- van der Hoorn, R. a L., & Kamoun, S. (2008). From Guard to Decoy: a new model for perception of plant pathogen effectors. *The Plant Cell*, 20(8), 2009–17. <http://doi.org/10.1105/tpc.108.060194>
- Vance, R. E. (2015). The NAIP/NLRC4 inflammasomes. *Current Opinion in Immunology*, 32, 84–9. <http://doi.org/10.1016/j.coi.2015.01.010>
- Venugopal, S. C., Jeong, R.-D., Mandal, M. K., Zhu, S., Chandra-Shekara, a C., Xia, Y., ... Kachroo, P. (2009). Enhanced disease susceptibility 1 and salicylic acid act redundantly to regulate resistance gene-mediated signaling. *PLoS Genetics*, 5(7), e1000545. <http://doi.org/10.1371/journal.pgen.1000545>
- Vierstra, R. D. (2009). The ubiquitin–26S proteasome system at the nexus of plant biology. *Nature Reviews Molecular Cell Biology*, 10(6), 385–397. <http://doi.org/10.1038/nrm2688>
- Vlot, a C., Dempsey, D. A., & Klessig, D. F. (2009). Salicylic Acid, a multifaceted hormone to combat disease. *Annual Review of Phytopathology*, 47, 177–206. <http://doi.org/10.1146/annurev.phyto.050908.135202>
- Wagner, S. (2013). *Analysing Novel Structures of Protein Complexes Requiring the Central Plant Immune Regulator EDS1*.
- Wagner, S., Rietz, S., Parker, J. E., & Niefind, K. (2011). Crystallization and preliminary crystallographic analysis of Arabidopsis thaliana EDS1, a key component of plant immunity, in complex with its signalling partner SAG101. *Acta Crystallographica Section F Structural Biology and Crystallization Communications*, 67(2), 245–248. <http://doi.org/10.1107/S1744309110051249>
- Wagner, S., Stuttmann, J., Rietz, S., Guerois, R., Brunstein, E., Bautor, J., Niefind, K., Parker, J. E. (2013). Structural Basis for Signaling by Exclusive EDS1 Heteromeric Complexes with SAG101 or PAD4 in Plant Innate Immunity. *Cell Host & Microbe*, 14(6), 619–30. <http://doi.org/10.1016/j.chom.2013.11.006>
- Wang, J., Shine, M. B., Gao, Q.-M., Navarre, D., Jiang, W., Liu, C., Kachroo, P.. (2014). Enhanced Disease Susceptibility1 Mediates Pathogen Resistance and Virulence Function of a Bacterial Effector in Soybean. *Plant Physiology*, 165, 1269–1284. <http://doi.org/10.1104/pp.114.242495>
- Weßling, R., Eppele, P., Altmann, S., He, Y., Yang, L., Henz, S. R., Braun, P. (2014). Convergent Targeting of a Common Host Protein-Network by Pathogen Effectors from Three Kingdoms of Life. *Cell Host & Microbe*, 16(3), 364–375.

- <http://doi.org/10.1016/j.chom.2014.08.004>
- Wiermer, M., Feys, B. J., & Parker, J. E. (2005). Plant immunity: the EDS1 regulatory node. *Current Opinion in Plant Biology*, 8(4), 383–9. <http://doi.org/10.1016/j.pbi.2005.05.010>
- Williams, S. J., Sohn, K. H., Wan, L., Bernoux, M., Sarris, P. F., Segonzac, C., Jones, J. D. G. (2014). Structural basis for assembly and function of a heterodimeric plant immune receptor. *Science (New York, N.Y.)*, 344(6181), 299–303. <http://doi.org/10.1126/science.1247357>
- Wirthmueller, L., Maqbool, A., & Banfield, M. J. (2013). On the front line: structural insights into plant-pathogen interactions. *Nature Reviews. Microbiology*, 11(11), 761–76. <http://doi.org/10.1038/nrmicro3118>
- Wirthmueller, L., Zhang, Y., Jones, J. D. G., & Parker, J. E. (2007). Nuclear Accumulation of the Arabidopsis Immune Receptor RPS4 Is Necessary for Triggering EDS1-Dependent Defense. *Current Biology*, 17(23), 2023–2029. <http://doi.org/10.1016/j.cub.2007.10.042>
- Wu, Y., & Sha, B. (2006). Crystal structure of yeast mitochondrial outer membrane translocon member Tom70p. *Nature Structural & Molecular Biology*, 13(7), 589–93. <http://doi.org/10.1038/nsmb1106>
- Wu, Y., Zhang, D., Chu, J. Y., Boyle, P., Wang, Y., Brindle, I. D., Després, C. (2012). The Arabidopsis NPR1 protein is a receptor for the plant defense hormone salicylic acid. *Cell Reports*, 1(6), 639–47. <http://doi.org/10.1016/j.celrep.2012.05.008>
- Xiao, S., Calis, O., Patrick, E., Zhang, G., Charoenwattana, P., Muskett, P., Turner, J. G. (2005). The atypical resistance gene, RPW8, recruits components of basal defence for powdery mildew resistance in Arabidopsis. *Plant Journal*, 42(1), 95–110. <http://doi.org/10.1111/j.1365-313X.2005.02356.x>
- Xiao, S., Ellwood, S., Calis, O., Patrick, E., Li, T., Coleman, M., & Turner, J. G. (2001). Broad-spectrum mildew resistance in Arabidopsis thaliana mediated by RPW8. *Science (New York, N.Y.)*, 291(January), 118–120. <http://doi.org/10.1126/science.291.5501.118>
- Xue, J.-Y., Wang, Y., Wu, P., Wang, Q., Yang, L.-T., Pan, X.-H., Chen, J.-Q. (2012). A primary survey on bryophyte species reveals two novel classes of nucleotide-binding site (NBS) genes. *PloS One*, 7(5), e36700. <http://doi.org/10.1371/journal.pone.0036700>
- Yalpani, N., Silverman, P., Wilson, T. M., Kleier, D. a., & Raskin, I. (1991). Salicylic acid is a systemic signal and an inducer of pathogenesis-related proteins in virus-infected tobacco. *The Plant Cell*, 3(8), 809–818. <http://doi.org/10.1105/tpc.3.8.809>
- Yan, S., & Dong, X. (2014). Perception of the plant immune signal salicylic acid. *Current Opinion in Plant Biology*, 20C, 64–68. <http://doi.org/10.1016/j.pbi.2014.04.006>
- Yue, J.-X., Meyers, B. C., Chen, J.-Q., Tian, D., & Yang, S. (2012). Tracing the origin and evolutionary history of plant nucleotide-binding site-leucine-rich repeat (NBS-LRR) genes. *The New Phytologist*, 193(4), 1049–63. <http://doi.org/10.1111/j.1469-8137.2011.04006.x>
- Zhang, F., Yao, J., Ke, J., Zhang, L., Lam, V. Q., Xin, X.-F., He, S. Y. (2015). Structural basis of JAZ repression of MYC transcription factors in jasmonate signalling. *Nature*.

<http://doi.org/10.1038/nature14661>

- Zhang, L., Yao, J., Withers, J., Xin, X.-F., Banerjee, R., Fariduddin, Q., He, S. Y. (2015). Host target modification as a strategy to counter pathogen hijacking of the jasmonate hormone receptor. *PNAS*, 201510745. <http://doi.org/10.1073/pnas.1510745112>
- Zheng, X.-Y., Spivey, N. W., Zeng, W., Liu, P.-P., Fu, Z. Q., Klessig, D. F., Dong, X. (2012). Coronatine promotes *Pseudomonas syringae* virulence in plants by activating a signaling cascade that inhibits salicylic acid accumulation. *Cell Host & Microbe*, 11(6), 587–96. <http://doi.org/10.1016/j.chom.2012.04.014>
- Zheng, Z., Mosher, S. L., Fan, B., Klessig, D. F., & Chen, Z. (2007). Functional analysis of Arabidopsis WRKY25 transcription factor in plant defense against *Pseudomonas syringae*. *BMC Plant Biology*, 7, 2. <http://doi.org/10.1186/1471-2229-7-2>
- Zhou, N., Tootle, T. L., Tsui, F., Klessig, D. F., & Glazebrook, J. (1998). PAD4 functions upstream from salicylic acid to control defense responses in Arabidopsis. *The Plant Cell*, 10(6), 1021–30. <http://doi.org/10.2307/3870687>
- Zhu, S., Jeong, R.-D., Venugopal, S. C., Lapchyk, L., Navarre, D., Kachroo, A., Kachroo, P. (2011). SAG101 forms a ternary complex with EDS1 and PAD4 and is required for resistance signaling against turnip crinkle virus. *PLoS Pathogens*, 7(11), e1002318. <http://doi.org/10.1371/journal.ppat.1002318>

## Erklärung

Ich versichere, dass ich die von mir vorgelegte Dissertation selbständig angefertigt, die benutzten Quellen und Hilfsmittel vollständig angegeben und die Stellen der Arbeit – einschließlich Tabellen, Karten und Abbildungen –, die anderen Werken im Wortlaut oder dem Sinn nach entnommen sind, in jedem Einzelfall als Entlehnung kenntlich gemacht habe; dass diese Dissertation noch keiner anderen Fakultät oder Universität zur Prüfung vorgelegen hat; noch nicht veröffentlicht worden ist sowie, dass ich eine solche Veröffentlichung vor Abschluss des Promotionsverfahrens nicht vornehmen werde. Die Bestimmungen dieser Promotionsordnung sind mir bekannt. Die von mir vorgelegte Dissertation ist von Prof. Dr. Paul Schulze-Lefert betreut worden.

Köln,

---

Deepak Bhandari



# Curriculum Vitae

Deepak Bhandari

## Angaben zur

### Person:

---

**geboren am:** 10.10.1985 in Chennai, Indien

**Familienstand:** ledig

**Nationalität:** Indien

### Schulbildung:

---

**06/1991 – 05/2003** G.S.S. Jain Vidyalaya, Chennai

### Studium:

---

**06/2003 – 06/2006** SRM deemed University, Chennai

Bachelor of Sciences in Biotechnology

**08/2006 – 05/2008** D. G. Vaishnav college, University of Madras

Master of Sciences in Biotechnology

**Seit 06/2012** Max Planck Institut für Pflanzenzüchtungsforschung, Köln

Promotion zum Thema ‘Structure-function analysis of the  
*Arabidopsis* EDS1 immune regulatory complex’ unter  
Betreuung von Prof. Dr. Jane E. Parker

Köln, November 2015

